A FINITE ELEMENT MODEL OF OCEAN CIRCULATION

By

RODOLFO BERMEJO-BERMEJO

Naval Archt. and Marine Eng.

The Politechnique University of Madrid, 1977

A THESIS SUBMITTED IN PARTIAL FULFILLMENT OF

THE REQUIREMENTS FOR THE DEGREE OF

MASTER OF SCIENCE

in

THE FACULTY OF GRADUATE STUDIES

Department of Oceanography

We accept this thesis as conforming

to the required standard

THE UNIVERSITY OF BRITISH COLUMBIA

December 1986

In presenting this thesis in partial fulfilment of the requirements for an advanced degree at the University of British Columbia, I agree that the Library shall make it freely available for reference and study. I further agree that permission for extensive copying of this thesis for scholarly purposes may be granted by the head of my department or by his or her representatives. It is understood that copying or publication of this thesis for financial gain shall not be allowed without my written permission.

Department of Oceanography

The University of British Columbia
1956 Main Mall
Vancouver, Canada
V6T 1Y3

Date Jan / 28 / 1987

DE-6(3/81)

ABSTRACT

Preliminary results of a two-layer quasi-geostrophic box model of a wind-driven ocean are presented. The new aspects of this work in relation with conventional eddy models are a finite element formulation of the quasi-geostrophic equations and the use of no-slip boundary condition on the horizontal solid boundaries.

In contrast to eddy resolving models that utilize free-slip boundary conditions our results suggest that the obtention of ocean eddies with the no-slip constraints requires a more restricted range of parameters, in particular much lower horizontal eddy viscosity eddy coefficients A_H and higher Froude numbers F_1 and F_2. We show explicitly that a given range of parameters, which is eddy generating when the free-slip boundary condition is used, leads to a quasi-laminar flow in both, upper and lower, layers. An analytical model to interpret the numerical results is put forth. It is an extension of an earlier model of Ierley and Young (1983) in that the relative vorticity terms are of primary importance for the dynamics. Thus, it is shown that the boundary layer dynamics is active in the interior of the second layer, and it can be concluded from our method that for given F_1 and F_2 such that the lower layer geostrophic

contours are closed, to the existence of the western boundary layer will prevent the homogenization of the potential vorticity so long as A_H is large enough to stabilize the northwestern undulations of the flow.

TABLE OF CONTENTS

LIST OF FIGURES

ACKNOWLEDGEMENTS

I wish to thank my supervisor, Professor L.A. Mysak for his guidance and advice during this study. I am also very grateful for the support and encouragement received from Dr. M. Foreman and Dr. W. Hsieh.

This work was supported by the generosity of Dr. Mysak who appointed me as a Research Assistant under an Office of Naval Research Grant.

CHAPTER 1

INTRODUCTION

During the past fifteen years or so, oceanographers have made great progress in the development and understanding of large-scale oceanic phenomena. This progress is the result of a balanced scientific approach involving better observational techniques as well as more sophisticated theoretical models. The impetus for the development of eddy resolving general circulation models (EGCMs) came from the need to simulate numerically and to understand a posteriori the nature of the eddies which were the most outstanding observational features of field programs such as POLYGON, MODE, and POLYMODE. The EGCMs, which include eddy motions at least on some space-time scales, require much greater horizontal resolution to take into account the instability properties of the larger-scale circulation, which yields mesoscale eddies on the spatial scale of Rossby radius of deformation. Thus, in contrast with the earlier analytical models and numerical models with coarse resolution and high viscosity which produced an inadequate representation of the process involved in the ocean dynamics, EGCMs depict a circulation that is strongly turbulent and time-dependent. The first experiments of this kind were carried out by Holland and Lin (1975) in which they showed that instability

in the swift boundary currents and their intertial return flows led to significant eddy energy production and that the eddies then modified the large-scale flow in a fundamental way. The success of this early work led to further eddy-resolving calculations that continued to explore the details of eddy production and eddy interaction with the mean flow and the effects of the inclusion of thermodynamics (Robinson et al. 1977, Semtner and Mintz, 1977). All these models were designed to simulate the mid-ocean gyre dynamics of the North Atlantic Ocean by using the primitive equations (PE) and as ocean domain an idealized box without bottom topography or with a very simple shelf and slope. The forcing wind stress was a steady sinusoidal signal.

If one thinks that the main dynamical variable of a baroclinic mid-latitutde ocean is the potential vorticity q

$$q = \frac{(2\vec{\Omega} + \vec{\zeta}) \cdot \nabla\rho}{\rho} ,$$

where $\vec{\Omega}$ is the earth's rotation vector, $\vec{\zeta}$ is the relative vorticity and ρ a conservative fluid property, then it seems natural to simulate the eddy dynamics by making use of the quasi-geostrophic approximation. Several modellers working with an EGCM-baroclinic ocean have followed this approach particularly since 1978 when Holland (1978) initiated an extensive set of numerical experiments with a two layer box ocean and the quasi-geostrophic approximation to the PE.

Later on, Holland has extended these 1978 experiments by including more layers (up to 8, 1986 personal communication) and enlarging the geometrical dimensions of the box ocean. The improvement in the resolution of the vertical structure yields such interesting results as the homogenization of potential vorticity in the intermediate layers--a result predicted theoretically by Rhines and Young (1982).

The advantages of a quasi-geostrophic model over a PE model are mainly computational (Semtner and Holland 1978) so long as we assume that the mid-latitutde ocean circulation is within a range of parameters. How representative such a parameter range is of the real ocean is a debatable matter. More accurate observational and numerical results and further theoretical developments show that the quasi-geostrophic approximation is insufficient to display some important features of the ocean dynamics such as the outcropping of the isopycnals allowing the ventilation of subsurface layers. The latter is believed to play a fundamental role in the dynamics of potential vorticity (Luyten et al. 1983).

Any numerical model designed to elucidate the role of certain mechanisms of the dynamics of the ocean circulation requires the adoption of compromises in carrying out the calculations. Two compromises of this kind are the parameterization of the sub-grid scale motion and the choice of the boundary conditions. As for the first one, geostrophic turbulence theory (Charney, 1971) shows a cascade

of energy to larger length scales while the enstrophy cascades towards the smaller ones. This enstrophy cascade, on sub-deformation radius scales, must be represented with a physically motivated parameterization. At present, this is an unsolved problem in ocean dynamics; however, two explicit parameterizations are popular in EGCMs. The first one is the classic Laplacian friction in which the lateral dissipative terms of the relative vorticity equation are represented as $\nabla \cdot (A_H \nabla \zeta)$, where A_H is a diffusion coefficient; the second one is known as biharmonic friction because the explicit dissipation is of the form $B_H \nabla^4 \zeta$, where B_H is a constant coefficient. The physical motivation of both parameterizations or closures has no solid ground. The Laplacian friction is a molecular-type diffusion operator, usual in most subsonic fluid dynamics computations. It has very poor damping selective properties, which necessitate keeping A_H as low as possible in order not to damage severely the energy spectrum of the motion. The biharmonic friction is highly selective so it damps very efficiently the small wavelength scales and, therefore, the enstrophy can be non-intrusively removed (Holland, 1978). A possible inconvenience of this type of closure is that it requires boundary conditions that are somewhat artificial in the sense that vorticity derivatives of order higher than 2 are arbitrarily set to zero in order to close the mathematical problem. Other alternative closures have been suggested

recently (Basdevant et al., 1978 and Sadourny and Basdevant, 1981).

The choice of boundary conditions, particularly on the horizontal solid boundaries, is a matter that is not yet settled. There are several possibilities such as slip, no-slip and other less conventional choices. The latter ones, such as those used by Marshall (1982, 1984), are so mathematically conditioned that it seems unrealistic that the real ocean obeys such conditions. Most of EGCM modellers eager to get an ocean full of eddies (with reasonable computer expenses) have used the slip boundary condition; however, it is not clear whether that condition is more realistic than the non-slip one. If one follows Stewart's (1964) argument that the ocean water is a real fluid and, therefore, adheres to the solid boundaries so that the velocity must be zero on them, then it seems that the non-slip boundary condition is the proper one. Other arguments supporting the choice of this boundary condition are shown in Section 2.1 of this thesis. However, if one looks at the no-slip constraint from a computational point-of-view, the results are somewhat discouraging, because, as the author of this thesis has learned in the course of these preliminary experiments, such a boundary condition implies a larger amount of dissipation of energy by the lateral friction terms than in the case of the free-slip constraint. (Ierley and Young, 1986, personal communication,

have noted that the energy dissipation of a barotropic model with the no-slip condition is 30 percent larger than with the free-slip one.) This means that if a given range of parameters is valid for the obtention of eddies with the free-slip condition, the same range may become laminar by using the no-slip constraint. (This has been our experience in these preliminary experiments with our model.) Therefore, a drastic change in some of the parameters such as A_H (which has to be considerably reduced), is necessary in order to simulate the eddy dynamics of the ocean; such an alteration of the values of the parameters involves a great increase in the computational burden.

One important aspect of any numerical model to which little attention has been paid by many ocean modellers is the accuracy of the method. Most of the GCMs and EGCMs are finite difference models of second order in time and space accuracy. Very few attempts to use higher order methods have been done so far; however, we feel it is time to move to more accurate methods because the present computer technology allows large-scale simulations at reasonable price. The purpose of our work, of which this thesis is a first step, is twofold; first, the development of an eddy model using finite element as a numerical technique because it is well known that for regular grids (see Fix, 1975, Staniforth and Mitchell, 1977, Haidvogel et al., 1980) the accuracy of linear finite element is much higher than that of standard

finite difference methods which are commonly used in the present operational ECGM; secondly, the systematic study of EGCM dynamics, under several parameter regimes, when the no-slip condition is used as a lateral constraint.

We believe that the first stage of our projected task has been fulfilled in the sense that we have developed a finite element model to integrate numerically a set of coupled parabolic-elliptic equations, and we have found a range of parameters which produces eddies with the free-slip boundary condition but which yields a quasi-laminar dynamics with the no-slip one. An analytical boundary layer method to understand the numerical results has also been developed.

The contents of the thesis are divided into chapters, and the latter into sections as follows:

Chapter 2 - In Section 2.1, we obtain the equation of the potential vorticity for mid-ocean gyres based on the relative vorticity equation and the β-plane-quasi-geostrophic paradigm of mid-ocean dynamics. In Section 2.2, it is established that the application of the no-slip condition on the solid boundaries to the potential vorticity equation removes McWilliams' incompatibilities of those equations and the free-slip condition. In Section 2.3, a method is described to discretize the vertical structure of the potential vorticity equation into a finite number of layers.

Chapter 3 - This chapter describes the procedure to construct a finite element version of the potential vorticity

equations in a two layer ocean. After the introduction in Section 3.1 of some notation and basic definitions, standard in finite element literature, we set up the variational formulation of the two-layer potential vorticity equations in Section 3.2. In Section 3.3, we describe the Galerkin technique to discretize the variational equations. Special care has been taken to derive the discrete no-slip boundary condition. Time discretization of the equations of Section 3.3 and their stability analysis is taken up in Section 3.4. We have not presented any error estimate analysis of the discrete equations because such matters will be reported elsewhere.

Chapter 4 - This chapter presents the results of three numerical experiments. We have chosen for this stage of our study the same paramters Holland used in his experiment of 1978 with the addition of linear bottom friction. The reasons of choosing such a range of parameters was to compare consistently our results with those of Holland.

In Section 4.2, we develop an analytical model to interpret the numerical results of the experiment-3. This analytical model is based on boundary layer methods and has as non-linearities the vortex stretching and relative vorticity terms. A non-dimensional analyis reveals that the upper and lower layers dynamics are uncoupled in the western boundary because the stretching terms are much smaller than the other terms of the equations; however, the downward

momentum flux produced by the stretching terms in the Sverdrup interior is the driving mechanism of the motion in the lower layer. Our analytical model is a generalization of Ierley and Young's (1983) model because it includes the important contribution of the relative vorticity at the solid boundaries.

The conclusions and the list of references terminate the thesis.

The obtention of the relative vorticity equation is carried out in the appendix.

CHAPTER 2

2.1 Equation of Potential Vorticity in a Stratified Mid-Ocean Gyre

Let us consider a bounded stratified oceanic domain D centered at a mid-latitude θ_0 The equation of the relative vorcity ζ in such domain is (see Appendix):

$$\frac{D'\zeta}{D't} + \vec{u} \cdot \nabla f = fW_z + A_H \nabla_H^2 \zeta + \frac{\partial}{\partial z} (\nabla \wedge \vec{\tau}), \qquad (2.1)$$

where

$\vec{u}$ $(x,y,z) = (u,v)$ is the horizonal velocity vector,

w is the vertical component of the velocity,

$f = f_0 + \beta y$, $\beta = \dfrac{2\Omega \cos\theta_0}{r_0}$, $f_0 = 2\Omega \sin\theta_0$,

A_H is the lateral eddy viscosity coefficient,

$\vec{\tau}$ is the external forcing function,

$\dfrac{D'}{D't} = \dfrac{\partial}{\partial t} + \vec{u} \cdot \nabla_H$.

Since our main interest is the description of motions which take place at mid-latitudes and such that their metric can be accurately described by the tangent plane approximation, we introduce the standard scaling variables for a mid-latitude β-plane.

The scaling parameters are (Pedlosky 1979)

$$\rho = \rho_s(z)\ (1 + \varepsilon\ F\ \rho'),$$

$$\varepsilon = \frac{U}{f_0 L} = \text{Rossby Number},$$

$$S = \frac{g}{f_s}\frac{\partial \rho_s}{\partial z}\frac{D^2}{f_0^2\ L^2} = \left(\frac{L_D}{L}\right)^2,$$

$$N^2 = \frac{S\ f_0\ L^2}{D^2}$$

$$\beta = \frac{\beta_0\ L^2}{U} \qquad (2.2)$$

where $F = \dfrac{f_0^2 L^2}{SD}$

L is a typical longitude scale of the motion

D is the mean depth of the ocean

U is a typical velocity scale of the floor

$\rho'(x,y)$ is a perburbation density in excess of $\rho_s(z)$

For ocean gyre scales, the following parametric relations hold (Pedlosky, 1979).

$$\beta \gg 1,\ F \approx 0(1),$$

$$\beta S = \frac{\beta_0^2\ L_D^2}{U} \approx 0(1),$$

$$\frac{\beta}{\varepsilon} = \frac{\beta_0 L}{f_0} = \left(\frac{L}{r_0}\right) < 1,$$

$$\frac{S}{\varepsilon} \approx \frac{f_0 L_D^2}{U} \gg 1, \qquad (2.3a,b,c,d)$$

where r_0 is the radius of the earth.

The equation (2.1) is up to order 0(1)

$$v\beta_0 = fw_z, \qquad (2.4)$$

or, equivalently, the advection of planetary vorticity in the interior of the mid-ocean gyres is balanced by vortex-tube stretching. The vertical integral of (2.4) from z = -h, where it is assumed that the velocity is zero, up to the surface, where an Ekman layer type is allowed, gives the classic Sverdrup relation:

$$\beta_0 \int_{-h}^{0} v dz = f[w]_{-h}^{0} = ((\nabla \Lambda)_z \vec{\tau}), \qquad (2.5)$$

where $\vec{\tau}$ is the surface wind stress.

The geostrophic equilibrium allows the introduction of a stream function ψ as a function of the perturbation pressure p' to the hydrostatic pressure P_s. Thus, we define ψ as:

$$\psi = \frac{p'}{\rho_s f_0} \qquad (2.6)$$

The hydrostatic relation is now written as

$$\rho' = -\frac{\rho_s f}{g}\frac{\partial \psi}{\partial z} - \frac{f_0 \psi}{g}\frac{\partial \rho_s}{\partial z} \approx -\frac{\rho_s f_0}{g}\frac{\partial \psi}{\partial z}$$

because $\frac{\partial \rho_s}{\partial z}$ is of the order of $0(10^{-3})$. w_z is given as (see Appendix)

$$w_z = \frac{D'}{D't}\left[\frac{\partial}{\partial z}\left(-\frac{\rho}{\rho_{sz}}\right)\right] + \frac{\partial}{\partial z}\left(\frac{G}{\rho_{sz}}\right)$$

$$= \frac{D'}{D't}\left[\frac{\partial}{\partial z}\left(-\frac{\rho_s f_0}{g\rho_{sz}}\frac{\partial \psi}{\partial z}\right)\right] + \frac{\partial}{\partial z}\left(\frac{G}{\rho_{sz}}\right)$$

$$= -\frac{D'}{D't}\left[\frac{\partial}{\partial z}\left(\frac{f_0}{N^2}\frac{\partial \psi}{\partial z}\right)\right] + \frac{\partial}{\partial z}\left(\frac{G}{\rho_{sz}}\right), \qquad (2.7)$$

where G is defined in (A.12).

Substituting (2.7) into (2.1) and arranging terms yields to the classic equation of the potential vorticity:

$$\frac{D'}{D't}\left[\zeta + f + \frac{\partial}{\partial z}\left(\frac{f_0^2}{N^2}\frac{\partial \psi}{\partial z}\right)\right]$$

$$= f\frac{\partial}{\partial z}\left(\frac{G}{\rho_{sz}}\right) + A_H \nabla^2 \zeta + \frac{\partial}{\partial z}\left((\nabla \Lambda)_z \vec{\tau}\right). \qquad (2.8a)$$

The heat equation (A.12) becomes in terms of $\psi_z = \frac{\partial \psi}{\partial z}$

$$\frac{D'\psi_z}{D't} + \frac{N^2}{f_0} w = K \nabla^2 \psi_z + \frac{\alpha g}{\rho} Q, \qquad (2.8b)$$

where q is now given by

$$q = \zeta + f + \frac{\partial}{\partial z}\left(\frac{f^2}{N^2}\frac{\partial \psi}{\partial z}\right). \qquad (2.9a)$$

At planetary scales (gyre-scales) and outside certain narrow areas attached to the boundaries, the potential vorticity q can be aproximated by

$$q \approx f + \frac{\partial}{\partial z}\left(\frac{f_0^2}{N^2}\frac{\partial \psi}{\partial z}\right) + O(\beta^{-1}), \qquad (2.9b)$$

whereas, for the motions of the mesoscale, q is given by (2.9a). Hence, we can conclude that so long as $\frac{L}{r_0} \ll 1$, no thermocline processes, and $N^2 = N^2(z)$ equations (2.8) are valid either for synoptic scales or gyre-scales.

At this point, it is necessary to stress the fundamental role played by equations (2.4) and (2.5) to explain why there must exist zonal velocities in the ocean or, in other words, why the ocean circulation is composed of gyres. For an homogeneous ocean, it is obvious from the Sverdrup relation that there exists a return flow along the western boundaries of the oceans and, hence, the existence of zonal velocities. In the case of a baroclinic ocean where the thermocline effects as well as the horizontals variations of the isopycnals are neglected, the driving mechanism is the vertical velocity from the divergent Ekman layer at the surface. A scale analysis of (2.4) leads to

$$\left(\frac{v}{w}\right)_1 \approx \frac{f\beta}{D} .$$

If we now assume that the circulation is two-dimensional in meridional planes, that is, that the divergence of the Ekman layer yields to closed cell circulations in meridional planes, the mass conservation equation requires that $v_y + w_z = 0$. A new scale analysis of the latter relation yields to the new ratio

$$\left(\frac{v}{w}\right)_2 \approx \frac{L_y}{D} ,$$

where L_y is the north-south scale of the flow. The ratio of these estimates gives:

$$\left(\frac{v}{w}\right)_1 : \left(\frac{v}{w}\right)_2 = \frac{f}{\beta L_y} = \frac{r_0}{L_y} > 1$$

So, there must be a zonal velocity flowing into the meridional planes.

2.2 Boundary Conditions

This is one of the most conflicting issues of the quasi-geostrophic models, and therefore, one of the shortcomings of the quasi-geostrophic dynamics. The sensitivity of these models to the type of boundary conditions is well known. Blandford (1971) shows how the solutions of the vorticity equation of a barotropic ocean can be altered by changing the boundary conditions. Ierley and

Young ((1986) personal communication) reassert Blandford's conclusions for a baroclinic ocean. McWilliams (1977) shows that the application of freeslip boundary condition on the boundaries of a multiply connected closed domain leads to incompatibilities between the order of the potential vorticity equation and the number of constraints required for the problem to be well-posed. To remove both incompatibilities, McWilliams concludes that neither horizontal diffusion of temperature nor vertical diffusion of momentum are processes to be represented by the quasi-geostrophic dynamics. However, if one considers that the ocean water is a real fluid, then the condition required on the solid boundaries is that the tangential velocity be zero. It is this condition, together with the kinematic condition (that the normal component of the velocity be zero on the solid boundaries) that is required to remove McWilliams' indeterminancies without ruling out any diffusive process from the quasi-geostrophy dynamics. It is worth noting that the imposition of the no-slip boundary condition on the bottom and a slight modification of it at the free surface allows the existence of Ekman boundary layers (Pedlosky, 1979).

The boundary conditions for the velocity are:

a. solid boundaries

$$\left.\begin{aligned} \vec{u} \cdot \vec{n} &= 0 \\ \vec{u} \cdot \vec{t} &= 0 \end{aligned}\right\} \quad \text{on } \Omega_H \cup \Omega_B \tag{2.10}$$

where Ω_H denotes the horizontal solid walls and Ω_B stands for the bottom. $\vec{n}$ and $\vec{t}$ are the outward normal vector and clockwise tangent vector, respectively, on such boundaries.

b. free surface

The rigid lid condition and the continuity of frictional stress across the surface are the constraints used at the free surface.

As for buoyancy, we use Kotchine's theorem (Krauss, 1973) and assume that the solid boundaries are insulated, whereas, at the free surface, there is an atmospheric buoyancy flux which is communicated to the ocean via boundary layer process on ageostrophic scales. Such a flux is given by $\frac{g\alpha\, Q_A}{H_u' \rho_0 C_p}$ where H_u' is the thickness of the uppermost level of penetration of atmospheric heat Q_A. We further assume that there are no internal processes of generation/sinking of buoyancy. Thus, we have

$$K_H \nabla_H \rho \cdot \vec{n} = 0 \text{ on } \Omega_H$$

$$(K_v \frac{\partial}{\partial z} - K_H \nabla H_B \cdot \nabla)\, \rho = 0 \text{ on } \Omega_B$$

$$K_v \frac{\partial \rho}{\partial z} = 0 \text{ at the free surface,} \qquad (2.11)$$

where $H_B(x,y)$ is the bottom profile.
Conditions (2.10) and (2.11) can be written in terms of the

geostrophic stream function, through a leading order in ε, as

$$\psi = C(t), \ \frac{\partial \psi}{\partial n} = 0, \ K_H \frac{\partial}{\partial z} \left(\frac{\partial \psi}{\partial n}\right) = 0 \text{ on } \Omega_H \ ,$$

$$w = \vec{u}_B \cdot \nabla H_B - \gamma \nabla^2 \psi, \ K_v \frac{\partial^2 \psi}{\partial z^2} = 0 \text{ on } \Omega_B \ ,$$

$$w = \frac{(\nabla \Lambda)_z}{f_0} \vec{\tau}^w, \ K_v \frac{\partial^2 \psi}{\partial z^2} = 0 \text{ at } z = 0 \qquad (2.12a,b,c)$$

where $((\nabla \Lambda)_z \ \vec{\tau}^w)$ denotes the z-component of the curl of the wind stress. $C(t)$ is a time dependent constant on the perimeter of the domain. $\vec{u}_B$ is the horizontal velocity at the edge of the bottom Ekman layer. γ is a bottom friction coefficient. Notice that the condition (no-slip) $\frac{\partial \psi}{\partial n} = 0$ implies that there be no fluxes of buoyancy by Newtonian processes through the horizontal solid walls. So, we have just removed one of McWilliams' incompatibilities, that is, we can include Newtonian diffusion of buoyancy in the horizontal direction without demanding any additional boundary condition.

The conditions (2.12b) and (2.12c) can be written with the help of (2.8a) as

$$\frac{D'\psi_z}{D't} + \frac{N^2}{f_0} (\vec{u}_B \cdot \nabla H_B + \gamma \nabla^2 \psi_B) - K_H \nabla^2 \psi_z - K_v \frac{\partial^3 \psi}{\partial z^3} = 0,$$

$$K_v \frac{\partial^2 \psi}{\partial z^2} = 0 \text{ on } \Omega_B \qquad (2.13)$$

and

$$\frac{D'\psi_z}{D't} + \frac{N^2}{f_0}\left(\frac{(\nabla\Lambda)_z}{f_0} \overset{+}{\tau} w\right) - K_H \nabla^2\psi_z - K_v \frac{\partial^3\psi}{\partial z^3} - \frac{gQ_A\alpha}{H' \rho_0 C_p} = 0$$

$$K_v \frac{\partial^2\psi}{\partial z^2} = 0, \qquad (2.14)$$

at $z = 0$.

These boundary conditions are not incompatible with the differential order of (2.8) with respect to the z-coordinate. Hence, the strict application of the no-slip boundary condition to the Q.G.E. allows the inclusion of Newtonian frictional and diffusive mechanisms in both vertical and horizontal directions on the ageostrophic scales. A simple scale analysis shows that for typical values of K_H and K_V ($K_H \approx 10^6 K_V$), the lateral diffusion of buoyancy is dominant with respect to the vertical one, so the latter process is not included in many quasi-geostrophic models.

The usual way of computing the solution of (2.8) is by discretizing the vertical structure of the ocean in a given number of layers of constant density. As we will see in the next section, in doing so, the vertical diffusion of momentum appears as a drag term of the form $A\nabla_H^2(\psi_{i+1} - \psi_i)$, where i denotes the i-th layer, A is a drag coefficient equal to

A_V/H_i and H_i is the thickness of the i-th layer. The drag term is similar to the form of the lateral diffusion of buoyancy. Again, a scale analysis shows that the lateral diffusion of buoyancy is much larger than the drag term. The similarity between both processes goes further than a pure mathematical expression in the context of quasi-geostrophic potential vorticity, for as it has been mentioned in the previous section, the potential vorticity in the interior of mid-latitude ocean gyes is given by $f \frac{\rho_z}{\rho}$, in a layered β-plane ocean by $f + (\psi_{i+1} - \psi_i)$, so the lateral diffusivity of potential vorticity in such an ocean is $\nabla_H^2(\psi_{i+1} - \psi_i)$. This means that the role played by the horizontal diffusion of buoyancy and the vertical diffusion of momentum in the quasi-geostrophic dynamics is equivalent to the lateral diffusion of potential vorticity. Rhines and Young (1982a) and de Szoeke (1985) show that the homogeneization of potential vorticity inside closed geostrophic contours at intermediate layers is only possible if the dominant dissipative mechanism is lateral diffusion of potential vorticity by mesoscale eddies. It turns out that a good parameterization, at least qualitatively, of the diffusive effects of the mesoscale eddies is given by a term of the form $\nabla \cdot (\nabla(\psi_{i+1} - \psi_i)$ (a coefficient) which is similar to the lateral diffusion of momentum in the case that is taken as constant.

The quasi-geostrophic equations (2.8), (2.13) and (2.14) are consistent through leading order in ε, but they are themselves insufficient to assure an asymptotically correct solution to the primitive equations. In particular, some additional constraints are to be imposed to insure correct integral budgets of energy, circulation and mass conservation. As McWilliams (1977) shows, the mass conservation constraint in a closed domain requires that at each level-i

$$\int_S \int w d\Omega = 0. \tag{2.15}$$

This constraint will be used to determine the constant C(t) of the stream function on the perimeter of the domain.

2.3 Equations of a Layered Ocean

Let us consider that the vertical structure of the ocean domain D is composed of N layers of constant density ρ_k and depth $H_k (k = 1,2,\ldots,N)$. We wish to obtain the new form of equations (2.8) for such an ocean.

Since the perturbation density ρ_k is constant within each layer, the vertical variation of the stream function ψ_k is controlled by the upper and lower density jumps of each layer, that is to say, within each layer the Taylor-Proudman theorem applies if the fluids were inviscid, but, it is the presence of density jumps that permits jumps in the velocity.

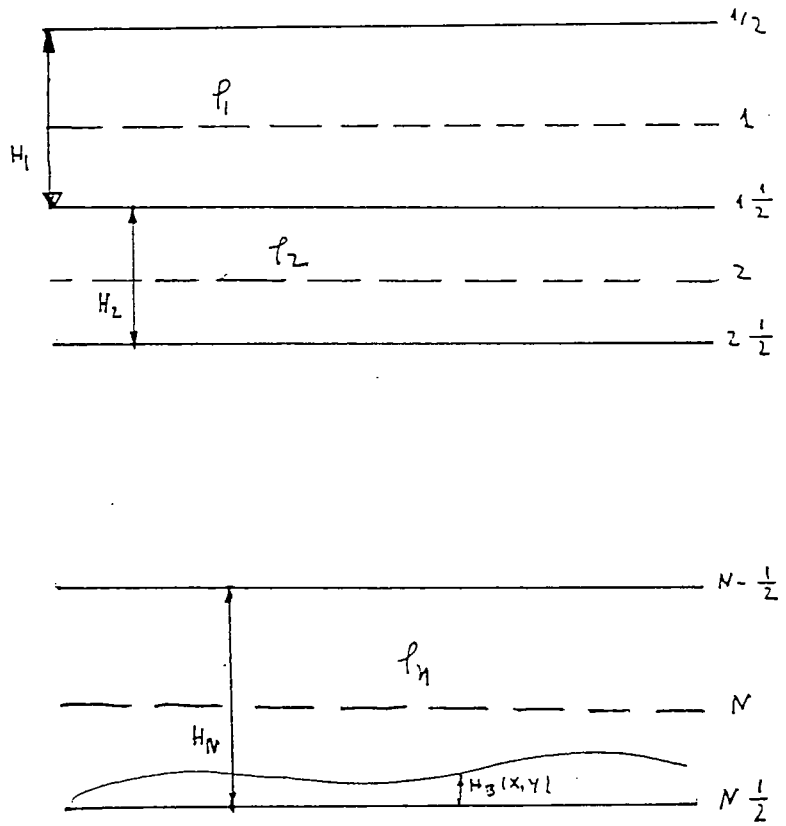

Fig. 1

Vertical finite difference grid.

The derivatives with respect to the z-coordinate in equations (2.8) are computed by using centered differences. Thus, for instance, the z-derivative of a given magnitude A at the level j + 1/2 (see Fig. 1) is:

$$\left(\frac{\partial A}{\partial z}\right)_{j+\frac{1}{2}} = \frac{A_{j+1} - A_j}{z_{j+1} - z_j} \,. \tag{2.16}$$

The value assigned to the potential vorticity in each layer is its value taken at the mid-level. Mid-levels are denoted by integer numbers in Figure 1. The interfaces between adjacent layers are labelled with integer numbers plus 1/2. So, the potential vorticity of the k-th layer is given by

$$q_k = \zeta_k + f + \frac{f_0^2}{H_k}\left[\frac{\psi_{k+1} - \psi_k}{g'_{k+\frac{1}{2}}} - \frac{\psi_k - \psi_{k-1}}{g'_{k-\frac{1}{2}}}\right], \tag{2.17}$$

where

$$g'_{k+\frac{1}{2}} = g\,\frac{\rho_{k+1} - \rho_k}{\rho_{k+1}} \,, \tag{2.18}$$

and (2.16) has been applied twice. Likewise, the vertical derivatives of $f\frac{\partial}{\partial z}\left(\frac{G}{\rho_{sz}}\right)$ and $(\nabla\Lambda)_z \vec{\tau}$ at the k-th layer are given by

$$\{f \frac{\partial}{\partial z} (\frac{G}{\rho_{sz}})\} = \frac{f}{z_{k+\frac{1}{2}} - z_{k-\frac{1}{2}}} \{(\frac{G}{\rho_{sz}})_{k+\frac{1}{2}} - (\frac{G}{\rho_{sz}})_{k-\frac{1}{2}}\}. \quad (2.19a)$$

Neglecting the vertical diffusion of buoyancy

$$G = K_H \nabla_H^2 \psi_z + \frac{\alpha}{C_p} g Q,$$

(2.19a) becomes

$$K_H \nabla_H^2 [\frac{f_0^2}{H_k} (\frac{\psi_{k+1} - \psi_k}{g'_{k+\frac{1}{2}}} - \frac{\psi_k - \psi_{k-1}}{g'_{k-\frac{1}{2}}})] + f_0 \frac{Q^{(k)}}{H_k}, \quad (2.19b)$$

where

$$Q^{(k)} = Q^*_{k+\frac{1}{2}} - Q^*_{k-\frac{1}{2}},$$

$$Q^*_{k+\frac{1}{2}} = \frac{\alpha}{C_p} \frac{H_k + H_{k+1/2}}{2} \frac{Q_{k+1/2}}{g'_{k+\frac{1}{2}}}, \quad (2.19c,d)$$

$$(\nabla\Lambda)_z \vec{\tau} = \begin{cases} \frac{(\nabla\Lambda\vec{\tau})_{k+1/2} - (\nabla\Lambda\vec{\tau})_{k-1/2}}{z_{k+1/2} - z_{k-1/2}} = T^{(k)}, & k \neq 1, N \\ \frac{(\nabla\Lambda\vec{\tau})_{1+1/2}}{z_{k+1/2}} = T^{(1)} \\ -\frac{(\nabla\Lambda\vec{\tau})_{N-1/2}}{z_{N+1/2} - z_{N-1/2}} = T^{(N-1/2)} \end{cases} \quad (2.20)$$

A standard parameterization of $(\nabla\Lambda)_z \vec{\tau}$ is

$$(\nabla\Lambda)_z \vec{\tau} = A_v \frac{\partial \zeta}{\partial z} . \tag{2.21}$$

By using (2.21) and (2.16), the formulae (2.20) become

$$T^{(1)} = \frac{A_v}{H_1} \frac{\zeta_2 - \zeta_1}{\frac{H_1 + H_2}{2}} , \tag{2.22}$$

$$T^{(k)} = \frac{A_v}{H_k} \left[2 \frac{\zeta_{k+1} - \zeta_k}{H_{k+1} + H_k} - 2 \frac{\zeta_k - \zeta_{k-1}}{H_k + H_{k-1}} \right],$$

$$T^{(N)} = - 2 \frac{A_v}{H_N + H_{N+1}} \left[\frac{\zeta_N - \zeta_{N-1}}{H_N} \right].$$

This parameterization is equivalent to a drag interface friction. This form of coupling between layers has been used by Rhines and Young (1982) to parameterize the vertical transfer of momentum by eddy activity. Particularly interesting is the fact that (2.22) is the only drag friction formulation which allows the homogenization of potential vorticity in the intermediate layers because in the quasi-geostrophic approximation $\zeta_k = \nabla_H^2 \psi_k$ so that (2.22) is equivalent to a lateral diffusion of potential vorticity. When lateral diffusion of buoyancy is included and parameterized according to (2.19b) a comparison between (2.22) and (2.19b) reveals that lateral diffusion of potential vorticity by buoyancy diffusive processes is

$\frac{H_k K_H f_0^2}{A_v g'_{k+1/2}} \approx 0(10^2)$ times greater than the interfacial drag friction, so in this case it is justified to neglect interfacial stress as a way of parameterizing the vertical transfer of momentum by eddies. Typical values of the coefficients, K_H and A_V, in mid-latitude ocean are $K_H \approx 10^2$ m^2 s^{-1}, $A_V \approx 10^{-3}$ m^2 s^{-1} for an Ekman layer depth $\delta_\varepsilon = (2A_v/f_0)^{1/2}$ of the order 5-10 m.

Substituting (2.17), (2.19) and (2.22) into (2.8a) yields:

$$\frac{D'_k}{D'_t} q_k = K_H \nabla^2 [\frac{f_0^2}{H_k} (\frac{\psi_{k+1} - \psi_k}{g_{k+1/2}} - \frac{\psi_k - \psi_{k-1}}{g_{k-1/2}}] + A_H \nabla_H^2 \zeta_K + \frac{f_0}{H_k} Q^{(k)} + T^{(k)}, \quad (2.23)$$

where

$$\frac{D'_k}{D'_t} = \frac{\partial}{\partial t} + u_k \frac{\partial}{\partial x} + v_k \frac{\partial}{\partial y}$$

$$u_k = - \frac{\partial \psi_k}{\partial y}, \quad v_k = \frac{\partial \psi_k}{\partial x} \quad (2.24)$$

Thus, equation (2.23) is the equation of potential vorticity for an ocean whose vertical structure is composed of N-layers of constant density. To solve (2.23), it is necessary to apply the boundary constraints (2.12a), (2.13) and (2.14) in a form suitable for a layered ocean. In doing so, one can

obtain another version of (2.23), which is more convenient for numerical implementation by incorporating the surface and bottom constraints into the potential vorticity equation and thus leaving as boundary conditions to be imposed the lateral conditions (2.12).

The vertical velocity of the K-th layer is given by the difference between the vertical velocities of the upper and lower interfaces. Thus,

$$w_k = w_{k-1/2} - w_{k+1/2}. \tag{2.25a}$$

From (2.8b) one obtains

$$w_k = \{\frac{D'}{D't}\ (\frac{f_0}{N^2}\ \psi_z) - \frac{f_0\ K_H}{N^2}\ \nabla_H^2\psi_z - \frac{\alpha g}{C_p}\ \frac{f_0}{N^2}\ Q\}_{k+1/2}$$

$$- \{\frac{D}{D't}\ (\frac{f_0}{N^2}\ \psi_z) - \frac{f_0\ K_H}{N^2}\ \nabla_H^2\psi_z - \frac{\alpha g}{C_p}\ \frac{f_0}{N^2}\ Q\}_{k-1/2}. \tag{2.25b}$$

It is now clear, by using (2.16) and taking

$$(\frac{D'}{D't})_{k\pm1/2} = \frac{\partial}{\partial t} - \frac{\partial\psi_{k\ \pm\ 1/2}}{\partial y}\ \frac{\partial}{\partial x} + \frac{\partial\psi_{k\pm1/2}}{\partial x}\ \frac{\partial}{\partial y}\ ,$$

that (2.25b) becomes:

$$w_k = \frac{\partial}{\partial t}\ \{\frac{f_0}{H_k}\ [\frac{\psi_{k+1} - \psi_k}{g'_{k\ +\ \frac{1}{2}}} - \frac{\psi_k - \psi_{k-1}}{g'_{k\ -\ \frac{1}{2}}}]\}$$

$$+ \frac{f_0}{g'_{k+\frac{1}{2}}} J(\psi_{k+1} - \psi_k, \psi_{k+1/2}) - \frac{f_0}{g'_{k-\frac{1}{2}}} J(\psi_k - \psi_{k-1}, \psi_{k-1/2})$$

$$- K_H \nabla_H^2 \{ \frac{f_0}{H_K} [\frac{\psi_{k+1} - \psi_k}{g'_{k+1/2}} - \frac{\psi_k - \psi_{k-1}}{g'_{k-1/2}}] \} + \frac{f_0}{H_k} Q^{(k)}, \quad (2.25c)$$

where

$J(A,B) = \frac{\partial A}{\partial x}\frac{\partial B}{\partial y} - \frac{\partial A}{\partial y}\frac{\partial B}{\partial x}$ is the Jacobian. The stream functions $\psi_{k\pm1/2}$ are taken as the interpolation values of ψ_{k+1}, ψ_k and ψ_{k-1}. Thus, for example,

$$\psi_{k\pm1/2} = C_{k\pm1/2}\, \psi_{k+1} - (1 - C_{k+1/2})\, \psi_k. \quad (2.26a,b)$$

$$C_{k+1/2} = \frac{H_k}{H_k + H_{k+1}}.$$

It is a simple exercise to show, by using (2.26), that

$$\frac{f_0}{g'_{k+\frac{1}{2}}} J(\psi_{k+1} - \psi_k, \psi_{k+1}) - \frac{f_0}{g'_{k-\frac{1}{2}}} J(\psi_k - \psi_{k-1}, \psi_{k-1/2})$$

$$= J[f_0 (\frac{\psi_{k+1} - \psi_k}{g'_{k+\frac{1}{2}}} - \frac{\psi_k - \psi_{k-1}}{g'_{k-\frac{1}{2}}}), \psi_k]. \quad (2.27)$$

Hence, (2.25c) becomes:

$$w_k = \frac{D'_k}{D'_t}\left[f_0\left(\frac{\psi_{k+1} - \psi_k}{g'_{k+\frac{1}{2}}} - \frac{\psi_k - \psi_{k-1}}{g'_{k-\frac{1}{2}}}\right)\right]$$

$$- K_H \nabla_H^2 \left[f_0\left(\frac{\psi_{k+1} - \psi_k}{g'_{k+\frac{1}{2}}} - \frac{\psi_k - \psi_{k-1}}{g'_{k-\frac{1}{2}}}\right)\right] + \frac{f_0 Q^{(k)}}{H_k}. \quad (2.28)$$

After combining the last equation and (2.25) we can write (2.23) as:

$$\frac{D'_1}{D'_t}(\zeta_1 + f) = A_H \nabla_H^2 \zeta_1 - \frac{f_0}{H_1} w_{1+1/2} + \tau^{(1)},$$

$$\frac{D'_k}{D'_t}(\zeta_k + f) = A_H \nabla_H^2 \zeta_k + \frac{f_0}{H_k}(w_{k-1/2} - w_{k+1/2}) + T^{(k)},$$

$$1 < k < N$$

$$\frac{D'_N}{D'_t}(\zeta_N + f) = A_H \nabla_H^2 \zeta_N + \frac{f_0}{H_N} w_{N-1/2} + \tau^{(N)}, \quad (2.29)$$

where $\tau^{(1)}$ and $\tau^{(N)}$ are given by the following expressions:

$$\tau^{(1)} = \frac{f_0}{H_1} w_{1/2} + T^{(1)},$$

$$\tau^{(N)} = \frac{f_0}{H_N} w_{N+1/2} + T^{(N)}. \quad (2.30a,b)$$

$T^{(1)}$ and $T^{(N)}$ are the interface stress at the upper and bottom layers, respectively, and their formulations in terms of the relative vorticity are given by (2.28). $w_1 + 1/2$

and $w_N + 1/2$ are the vertical velocities at the surface and on the bottom, respectively, that enter the problem as the boundary conditions (2.12b,c). So, with the help of (2.22) and (2.12b,c) $\tau(1)$ and $\tau(N)$ can be written as

$$\tau(1) = \frac{(\nabla \Lambda \vec{\tau}^{w})_z}{H_1} + \frac{A_v}{H_1} \frac{\zeta_2 - \zeta_1}{\frac{H_1 + H_2}{2}},$$

$$\tau(N) = -\frac{f_0}{H_N} (\vec{u}_N \cdot \nabla H_B + \gamma \zeta_N) + 2\frac{A_v}{H_N} (\frac{\zeta_{N-1} - \zeta_N}{H_1 + H_{N+1}}). \quad (2.31a,b)$$

$T^{(k)}$, the interface stress at the K-th layer, is given by (2.12b).

The coefficient γ in (2.31b) is expressed in terms of the eddy viscosity coefficient A_v and the parameter f_0 as (Pedlosky, 1979):

$$\gamma = \frac{1}{2} (\frac{2A_v}{f_0})^{1/2} .$$

The vertical velocity at the level $j + 1/2$ ($j = 1,2...N-1$) in (2.29) are computed from (2.8b) by using (2.16) as

$$w_{j+1/2} = \frac{f_0}{g'_{j+\frac{1}{2}}} \{\frac{\partial}{\partial t} (\psi_{j+1} - \psi_j) - J(\psi_{j+1} - \psi_j, \psi_{j+\frac{1}{2}})$$

$$+ K_H \nabla_H^2 (\psi_{j+1} - \psi_j)\} + \frac{f_0}{H_j} Q^{(j)}. \quad (2.32)$$

In general, $Q^{(j)}$ is taken to be zero for $j > 1$. For $j = 1$

$$\frac{f_0}{H_1} Q^{(1)} = \frac{\alpha g \, Q_s}{\rho_0 \, C_p \, H_1} , \qquad (2.33)$$

where Q_s is the amplitude of the surface heat flux.

Now, the boundary conditions of the problem (2.29) and (2.32) are the lateral boundary conditions and the mass conservation constraint (2.31). As for the lateral constraints, we have carried out experiments with the free-slip and non-slip boundary conditions, i.e.,

Free-slip

$$\psi_k(x,y) = C_k(t), \quad (x,y) \in \Omega_B$$

$$\zeta_k(x,y) = 0, \qquad k=L,2...N \qquad (2.34a,b)$$

Non-slip

$$\psi_k(x,y) = C_k(t), \qquad (x,y) \in \Omega_B$$

$$\frac{\zeta \psi_k}{\partial n} = 0 \text{ or } \zeta_k \neq 0, \quad k = L,2...N \qquad (2.35a,b)$$

As already discussed in the previous paragraph, the free-slip condition leads to incompatibilities in equations (2.29) unless the buoyancy diffusive processes are neglected. Such

incompatibilities do not exist when non-slip constraints are used. Other more sophisticated forms of boundary conditions have been used by Marshall (1982) and Ierley and Young ((1986), personal communication). The equations for a two-layer ocean with no thermal processes, no stress at the interface and constant depth H are readily obtained from (2.29 - 2.32) as

$$\frac{\partial \zeta_1}{\partial t} = J(\zeta_1, \psi_1) - \beta \frac{\partial \psi_1}{\partial x} + A_H \nabla_H^2 \zeta_1 - \frac{f_0}{H_1} W_{1\frac{1}{2}} + \frac{(\nabla \Lambda \vec{\tau}^W)_z}{H_1} ,$$

(2.36a,b)

$$\frac{\partial \zeta_2}{\partial t} = J(\zeta_2, \psi_2) - \beta \frac{\partial \psi_2}{\partial x} + A_H \nabla_H^2 \zeta_2 - \frac{f_0}{H_2} W_{1\frac{1}{2}} - \varepsilon \zeta_2,$$

$$W_{1\frac{1}{2}} = \frac{f_0}{g'_{1\frac{1}{2}}} \left(- \frac{\partial}{\partial t} (\psi_2 - \psi_1) - J(\psi_2 - \psi_1, \psi_{1\frac{1}{2}})\right),$$

(2.36c)

where $\varepsilon = \frac{f_0 \gamma}{H_2}$ is the linear bottom friction coefficient.

Equations (2.36a,b) are the relative vorticity equations which are closed with the relations $\zeta_1 = \nabla_H^2 \psi_1$, $\zeta_2 = \nabla_H^2 \psi_2$. In solving (2.36) the difficulties arise from the term $w_{1\frac{1}{2}}$. A way of overcoming such a problem, particularly when a time explicit scheme is used, is by forming the modal equations.

The equation for the baroclinic mode $\Psi = \psi_1 - \psi_2$ is determined by subtracting (2.36b) from (2.36a) and using (2.36c). Thus

$$(\nabla_H^2 - \lambda^2) \frac{\partial}{\partial t} \Psi = \gamma_a, \text{ in } D, \tag{2.37a}$$

where

$$\gamma_a = J(\zeta_1, \psi_1) - J(\zeta_2, \psi_2) - \beta \frac{\partial}{\partial x} (\psi_1 - \psi_2)$$

$$- \lambda^2 J(\psi_1 - \psi_2, \psi_{1\frac{1}{2}}) + \frac{(\nabla \Lambda \vec{\tau}^w)_z}{H_1} + A_H \nabla_H^2 (\zeta_1 - \zeta_2) + \varepsilon \zeta_2.$$

$\lambda^2 = Hf_0^2/H_1 H_2 g'$. (Note that λ^{-1} is the internal radius of deformation).

The mass conservation constraint (2.15) together with (2.36c) yield

$$\iint_D \frac{\partial}{\partial t} (\Psi) \, dx \, dy = 0. \tag{2.37b}$$

From the boundary conditions either (2.34a) or (2.35b) we have that

$$\frac{\partial}{\partial t} (\Psi) = C(t) \text{ on } \Omega_H. \tag{2.38}$$

To solve (2.37a) and (2.37b) we let

$$\frac{\partial \Psi}{\partial t} = \frac{\partial \Psi_a}{\partial t} + C(t) \frac{\partial \Psi_b}{\partial t} , \tag{2.39}$$

where

$$(\nabla_H^2 - \lambda^2) \frac{\partial \Psi_a}{\partial t} = \gamma_a \text{ in } D,$$

$$\frac{\partial}{\partial t} \Psi_a = 0, \text{ on } \Omega_B$$

$$\frac{\partial}{\partial h} \left(\frac{\partial}{\partial t} \Psi_a\right) = \begin{matrix} 0 \text{ if N.S.C.} \\ \text{free if F.S.C.,} \end{matrix} \text{ on } \Omega_H. \tag{2.40a}$$

and

$$(\nabla_H^2 - \lambda^2) \frac{\partial \Psi_b}{\partial t} = 0,$$

$$\frac{\partial}{\partial t} \Psi_b = 1, \quad \text{on } \Omega_H,$$

$$\frac{\partial}{\partial n} \left(\frac{\partial}{\partial t} \psi_a\right) = \begin{matrix} 0 \text{ if N-S.C.} \\ \text{free if F-S.C.,} \end{matrix} \text{ on } \Omega_H. \tag{2.40b}$$

The constant C(t) is determined by using (2.37b) and (2.39) as

$$C(t) = - \frac{\iint_D \frac{\partial \Psi_a}{\partial t} \, dx \, dy}{\iint_D \frac{\partial \Psi_b}{\partial t} \, dx \, dy} . \tag{2.41}$$

The equation for the barotropic mode $\phi = \frac{H_1 \psi_1 + H_2 \psi_2}{H}$ is

$$\nabla_H \left(\frac{\partial \phi}{\partial t}\right) = \gamma_b, \tag{2.42a}$$

where

$$\gamma_b = [H_1\ J(\zeta_1,\psi_1) + H_2\ J(\zeta_2,\psi_2)]\frac{1}{H} + \frac{(\nabla\Lambda\overset{+}{\tau}^W)_z}{H}$$

$$+ [A_H\nabla_H^2\ (H_1\psi_1 + H_2\psi_2)]\ \frac{1}{H} - \frac{\varepsilon}{H}\ \zeta_2 .$$

The boundary conditions of (2.41a) are

$$\frac{\partial\phi}{\partial t} = 0, \quad \text{on } \Omega_H,$$

$$\frac{\partial}{\partial n}\left(\frac{\partial}{\partial t}\ \phi\right) = \begin{matrix}0 \text{ is N-S.C.} \\ \text{free if F-S.C.}\end{matrix}, \text{ on } \Omega_H. \qquad (2.42b)$$

CHAPTER 3

NUMERICAL FORMULATION

In this chapter, we described the numerical formulation of the quasi-geostrophic equations of a two-layer ocean by finite element. Extension to a n-layer ocean is only a matter of adding more equations to be solved; however, the numerical basis remains unaltered. Our numerical formulation uses finite element to discretize the continuum equations in space and finite differences to step forward in time the computations. We first begin introducing some notations and definitions, which are standard in the context of finite element theory. Then we transform the equations into an integral form which permits obtaining the weak solution of such equations. The next step consists of passing from a continuum formulation of the equations to a discrete one which is suitable for numerical computation. This is carried out by Galerkin's method and the finite element technique of partitioning the domain D into a finite number E of almost disjoint subdomains T_e and interpolating any function defined in D. A key role in our method is played by the boundary space M_h which allows the correct imposition of the no-slip boundary condition. To construct such a space, we define our solution space in the form suggested by Glowinski et al. (1985) to study the steady state stream

function-vorticity formulation of the Navier-Stokes equations.

3.1 Basic Notations and Definitions

Before embarking in the construction of the variational formulation of the equations to compute their weak solution, it is useful to write down the definitions of mathematical spaces on which we are operating and some notations that we use throughout this chapter.

Q denotes an open bounded domain in the n-dimensional Euclidean space R^n with boundary Γ. We always assume that Q is "well-behaved" and that Γ is at least Lipschitzian. Γ is Lipschitzian if in a neighborhood of a given point $\vec{x}' \in \Gamma$, $|\vec{x} - \vec{x}'| < \xi$, Γ can be represented as $x_3 = F(x_1, x_2)$, F being continuous mapping and ξ sufficiently small. $Q_T = QU[0,T]$ where $[0,T]$ is a time interval. Points in Q or R^n are denoted by $\vec{x} = (x_1, x_2, \ldots, x_n)$ whereas points belonging to Q_T are written as $(\vec{x},t)$. An element of surface of either Q or Q_T is denoted by dx and an element of arc by ds.

Let u be a smooth function defined in Q_T. We sometimes use multi-index notation to represent the derivatives of u; that is, let $\alpha = (\alpha_1, \alpha_2, \ldots, \alpha_n)$ be an n-tuple of non-negative integers and denote

$|\alpha| = \alpha_1+\alpha_2+\ldots+\alpha_N$. Then by $D^\alpha u$, we shall mean the α-th derivative of u defined by

$$D^\alpha u = \frac{\partial^{|\alpha|} u}{\partial x_1^{\alpha_1} \partial_2^{\alpha_2} \ldots \partial x_N^{\alpha_N}}$$

$C^m (Q_T)$ = the linear space consisting of all functions u with partial derivatives $D^\alpha u$, $0 \leq |\alpha| \leq m$ continuous on Q_T.

$C^\infty (Q_T)$ = the linear space of functions infinitely differentiable in Q_T.

$C_0^m (Q_T)$, $C_0^\infty (Q_T)$ = linear subspaces of $C^m (Q_T)$ and $C^\infty (Q_T)$, respectively, such that if $u \in C_0^m (Q_T)$, $C_0^\infty (Q_T)$ then $u(\vec{x},t) = 0$ $\forall (\vec{x},t) \in C^m (Q_T)$, $C^\infty (Q_T)$.

$C^m (\overline{Q}_T)$ = linear subspace of $C^m (Q_T)$ such that if $u \quad C^m (\overline{Q}_T)$ then $D^{|\alpha|} u$ is bounded and uniformly continuous in Q_T.

$L^P (Q_T)$ = space of functions u defined on Q_T such that

$$\int_Q |u|^P dx < \infty, \quad 0 \leq t \leq T$$

The norm of $L^P (Q_T)$ is defined as

$$\|u\|_p = \left(\int_Q |u|^P dx\right)^{1/P}, \quad 1 \leq P \leq \infty .$$

For $p = 2$, $L^2(Q_T)$ is a Hilbert space with inner product:

$$(u,v)_2 = \int_Q u\, v\, dx.$$

Let m be a non-negative integer and let p satisfy $1 \leq p \leq \infty$. The Sobolev space $W_m^p(Q_T)$ of order (m,p) is defined as:

$$W_m^p = \{u \mid D^\alpha u \in L^p(Q_T),\ 0 \leq \alpha \leq m\}.$$

The spaces W_m^p are generally endowed with the norm

$$\|u\|_{m,p,Q_T} = \left(\int_Q \sum_{0 \leq |\alpha| \leq m} |D^\alpha u|^p\right)^{1/p}, \quad \begin{matrix} 1 < p < \infty \\ t \in [0,T] \end{matrix}$$

$$\overset{0}{W}{}_m^p(Q_T) \subset W_m^p(Q_T) = \{u \in W_m^p \mid u|_\Gamma = 0\}$$

for $p = 2$. $W_m^2 = H^m$ and $\overset{0}{W}{}_m^2 = H_0^m$

H^m and H_0^m are separable Hilbert spaces with inner product

$$(u,v) = \int_Q \sum_{0 \leq |\alpha| \leq m} D^\alpha u\, D^\alpha v\, dx$$

and with the associated norm

$$\|u\|_{m,Q_T} = \|u\|_{m,2,Q_T}$$

(See Adams, 1975).

3.2 Variational Formulation

For the sake of completeness, we write down again the equations (2.37) and (2.41) whose weak solutions we wish to compute. Since the vorticity and modal equations are linked together by the corresponding (ψ,ζ) Poisson equations, we need to set up an associated variational formulation of (2.37) and (2.41) of mixed type in order to use linear finite elements. Actually, we could compute the weak solutions from the modal equations alone, but in this case, we should use finite elements of class C^1 (Q_T) which are expensive from a computational point of view, although the solution is more accurate; hence, a mixed type variational formulation represents a compromise between computational burden and numerical accuracy. An associated variational formulation (or more properly a finite element method) is of mixed type whenever independent approximations are used for both the dependent variable and its derivatives. In our particular problem, the independent variable is the stream function ψ_i $(i=1,2)$; however, we chose to substitute $\nabla^2\psi_i = \zeta_i$ and the result is two new equations (vorticity and modal equations) of lower order which are approximated independently.

Let us consider the vorticity-modal equations for the two-layer ocean

$$\frac{\partial \zeta_i}{\partial t} = J(\zeta_i, \psi_i) - \beta \frac{\partial \psi_i}{\partial x} + (-1)^i \frac{f_0}{H_1} w_2 + A_H \nabla_H^2 \zeta_i$$

$$+ \frac{1}{2} (1 + (-1)^i) \varepsilon \zeta_i + \frac{1}{2} (1 - (-1)^i) \frac{F}{H_1}, \qquad (3.1)$$

in $Q_T \cap Z_i$, $Z_i = \{(x,y, H_i(x,y)) \in R^3\}$, $i=1,2$

where

$$w_2 = \frac{f_0}{g'} \{- \frac{\partial(\psi_1 - \psi_2)}{\partial t} + J(\psi_1 - \psi_2, \psi_{1\ 1/2})\}$$

$$\zeta_i|_\Gamma = \sigma_i(x,y,t), \quad \zeta_i|_{t=0} = 0. \qquad (3.2)$$

σ_i can be zero (free-slip boundary condition) or non-zero (non-slip boundary condition), or zero on some $\Gamma_1 \subset \Gamma$ and distinct from zero on $\Gamma_2 \subset \Gamma$ such that $\Gamma_1 \cup \Gamma_2 = \Gamma$.

$$(\nabla_H^2 - \lambda^2) \psi'_a = \gamma_a \text{ in } Q_T, \qquad (3.3)$$

$$\psi'_a|_\Gamma = 0, \ \psi'_a|_{t=0} = 0, \qquad (3.4)$$

$$(\nabla_H^2 - \lambda^2) \psi'_b = 0 \text{ in } Q_T, \qquad (3.5)$$

$$\psi'_b|_\Gamma = 1, \qquad (3.6)$$

$$\psi' = \psi'_a + C(t) \psi'_b, \qquad (3.7)$$

$$C(t) = - \frac{\int_Q \psi'_a \, dx}{\int_Q \psi'_b \, dx}, \qquad (3.8)$$

where

$$\Psi' = \frac{\partial}{\partial t} (\psi_1 - \psi_2),$$

$$\gamma_a = J(\zeta_1, \Psi_1) - J(\zeta_2, \psi_2) - \beta(\frac{\partial \psi_1}{\partial x} - \frac{\partial \psi_2}{\partial x})$$

$$- \lambda^2 J(\psi_1 - \psi_2, \psi_{1\frac{1}{2}}) + A_H \nabla_H^2 (\zeta_1 - \zeta_2) - \varepsilon\zeta_2 + \frac{F}{H_1} .$$

$$\nabla_H^2 \phi' = \gamma_b \text{ in } Q_T \tag{3.9}$$

$$\phi'\big|_\Gamma = 0 \quad \phi'\big|_{t=0} = 0, \tag{3.10}$$

where

$$\phi' = \frac{\partial}{\partial t} (\frac{H_1\psi_1 + H_2\psi_2}{H}),$$

$$\gamma_b = \frac{1}{H} (H_1 J(\zeta_1, \psi_1) + H_2 J(\zeta_1, \psi_2)) - \beta \frac{\partial}{\partial x} (\frac{H_1\psi_1 + H_2\psi_2}{H})$$

$$+ A_H \nabla_H^2 (\frac{H_1\zeta_1 + H_2\zeta_2}{H_1}) - \varepsilon \frac{H_2}{H} \zeta_2 + \frac{F}{H} .$$

Following Glowinski et al. (1985), we define two new spaces W_σ^{NS} and W_σ^{FS} as follows:

$$W_\sigma^{NS} = \{(\theta, \Phi) \in H^1(Q_T) \times H^1(Q_T), \quad \Phi\big|_\Gamma = C(t)$$

$$- \int_{Q_T} \nabla_H \Phi \cdot \nabla_H q \, dx = \int_{Q_T} \theta q \, dx$$

$$- \int_\Gamma \frac{\partial \Phi}{\partial n} ds, \forall q \in H^1(Q_T)\}$$

$$W_\sigma^{FS} = \{(\theta,\Phi) \in H_0^1(Q_T) \times H^1(Q_T),\quad \Phi|_\Gamma = C(t)$$

$$- \int_{Q_T} \nabla_H \Phi \cdot \nabla_H q \, dx = \int_{Q_T} \theta q \, dx$$

$$- \int_\Gamma \frac{\partial \Phi}{\partial n} ds,\ \forall q \in H^1(Q_T)\}$$

W_σ^{NS} is the space of solutions for the non-slip boundary condition while W_σ^{FS} is for the free-slip condition.

An associated mixed variational formulation of equations (3.1 - 3.10) is:

Find $\{(\zeta_i,\psi_i)\} \in W_\sigma^K$, $(K = NS,\ FS)$

such that $\forall (\theta,\Phi) \in H_0^1 \times H_0^1$,

$$(\frac{\partial \zeta_i}{\partial t},\ \theta) = (J(\zeta_i,\psi_i),\ \theta) - (\beta \frac{\partial \psi_i}{\partial x},\ \theta) + ((-1)^i \frac{f_0 w_2}{H_1},\ \theta)$$

$$+ (A_H \nabla_H^2 \zeta_i,\ \theta) + \frac{1}{2}(1 + (-1)^i)(\zeta_i,\theta)$$

$$+ (\frac{1-(-1)^i}{2})(\frac{F}{H_1},\ \theta) \qquad \text{in } Q_T \cap Z_i \ (i=1,2)$$

$$\zeta_i|_\Gamma = \sigma_i$$

$$(\nabla_H^2 \psi_a' - \lambda^2 \psi_a',\ \Phi) = (\gamma_a,\ \Phi), \qquad \text{in } Q_\Gamma \cap Z_i$$

$$\psi_a'|_\Gamma = 0,$$

$$(\nabla_H^2 \psi_b' - \lambda^2 \psi_b',\ \Phi) = 0, \qquad \text{in } Q_\Gamma \cap Z_i$$

$$\psi_b'|_\Gamma = 1,$$

$$(\nabla_H^2 \phi',\ \Phi) = (\gamma_b,\ \Phi), \qquad \text{in } Q_T \cap Z_i$$

$$\phi'|_\Gamma = 0,$$

where $(u,v) = \int_Q u \cdot v \, dx$.

Integrating by parts those terms operated by ∇_H^2 yields

$$\left(\frac{\partial \zeta_i}{\partial t}, \theta\right) = \left(J(\zeta_i, \psi_i), \theta\right) - \left(\beta \frac{\partial \psi_i}{\partial x}, \theta\right) + \left((-1)^i \frac{f_0}{H_1} w_2, \theta\right)$$
$$- \left(A_H \nabla_H \zeta_i, \nabla_H \theta\right) + \frac{1}{2}\left(1 + (-1)^i\right)(\zeta_i, \theta)$$
$$+ \frac{(1-(-1)^i}{2}\left(\frac{F}{H_1}, \theta\right), \qquad (3.11)$$

$$\zeta_i\big|_\Gamma = \sigma_i,$$
$$- \left(\nabla_H \psi_a', \nabla_H \Phi\right) - \left(\lambda^2 \psi_a', \Phi\right) = \left(\gamma_a, \Phi\right),$$
$$\psi_a'\big|_\Gamma = 0, \qquad (3.12a)$$

$$- \left(\nabla_H \psi_b', \nabla_H \Phi\right) - \left(\lambda^2 \psi_a', \Phi\right) = 0,$$
$$\psi_b'\big|_\Gamma = 0, \qquad (3.12b)$$

$$- \left(\nabla_H \phi', \nabla_H \Phi\right) = \left(\gamma_b, \Phi\right),$$
$$\phi'\big|_\Gamma = 0, \qquad (3.13)$$

Notice that the largest order of the derivatives in (3.11) - (3.13) is first order in contrast with the second order derivatives of the original equations (3.1) - (3.10); this means that we can relax the smoothness requirements of the solutions of (3.11) - (3.13) with respect to those requirements of the classical solutions of (3.1) - (3.10). Thus, whereas the classical solutions are to be of class

$C^2(Q_T)$, the solution of the variational formulation belongs to $H^1(Q_T)$, but $C^2(Q_T) \subset H^1(Q_T)$, so we have expanded the space of functions that can be solution of (3.1) - (3.10). It is clear that if an initial boundary value problem of elliptical and parabolic type has a classic solution it also has a weak solution because every classic solution is also a weak solution; however, there may be weak solutions which are not classical solutions, although equation (3.11), which is parabolic, and equations (3.12) and (3.13), both of which are elliptic, have unique weak solutions which, under certain regularity requirements for the coefficients and forcing function F, coincide with the classic solutions. (See V.P. Mijailov, 1977). Bennet and Kloeden (1981) have shown the existence and uniqueness of the classical solution of the dissipative quasi-geostrophic equations with periodic boundry conditions.

3.3 Galerkin-Finite Element Method

Galerkin's method consists of approximating the solutions of the equations (3.11) - (3.13) through the solutions ζ_{ih}, ψ_{ih} of the projections of (3.11) - (3.13) onto the finite dimensional space $W^K_{\sigma h}$. We assign a subscript h to the finite dimensional subspaces and discrete variables to imply that their properties generally depend on some real parameter h (such as mesh size) such that, as h decreases,

the finite dimensional spaces tend to fill up the corresponding infinite spaces. To be more specific, assume that $\{\theta_i(\vec{x},t)\}_{i=1,2} \in C^0(Q_T)$ is a complete set of linearly independent functions in $H^1(Q_T)$ that generate a finite dimensional subspace, say $V_h(Q_T) \subset L^2(Q_T)$, Galerkin's method is to seek a function $w_h(x,t) \in V_h(Q_T)$, which is the orthogonal projection of $u \in H^1(Q_T)$ on V_h, such that $w_h(x,t)$ satisfies the original partial differential equation in V_h as well as the initial and boundary conditions projected from $H^1(Q_T)$ onto V_h. This procedure cannot be a general method for constructing the finite dimensional subspaces. It is at this juncture that the finite element method (f.e.m.) plays its role as an approximation method, first by partitioning the domain Q into a finite number E of almost disjoint subdomains Te, and secondly, by approximating any function define on Q from its values at the vertices of the subdomains, Te.

Thus, consider that the bounded domain $\overline{Q}$ has been divided into a finite number of almost disjoint subdomains Te. These subdomains form for a given h (the mesh size) a finite family $\{\mathcal{T}_h\}$ such that

(i) $\tilde{Q}$ = connected model of $\overline{Q} = \bigcup_{e}^{E} Te$,

$\tilde{Q}_T = \tilde{Q} \cup [0,T]$;

(ii) $\forall$ Te, Te' $\in \mathcal{T}_h$, Te # Te' , we have either

$$Te \cap Te' = \text{(empty set)},$$

or Te, Te' have only one vertex in common,

or Te, Te' have only a whole edge in common.

Once the continuum domain $\overline{Q} = Q \cup \Gamma$ has been partitioned, we approximate the spaces $H^1(Q_T)$, $H_0^1(Q_T)$, W_σ^{NS}, W_σ^{FS} by the finite dimensional spaces.

$$H_h^1 = \{v_h \mid v_h \in C^0(\tilde{Q}_T),\ v_n\big|_{Te} \in P_K,\ \forall\ Te \in \mathcal{T}_n\},$$

$$H_{0h}^1 = H_h^1 \cap H_0^1(Q_T) = \{v_h \mid v_h \in H_h^1,\ v_h\big|_\Gamma = 0\},$$

$$W_{\sigma h}^{NS} = \{(\theta_h, \Phi_h) \in H_{0h}^1 \times H_h^1,\ \Phi_h\big|_\Gamma = C_h(t)$$

$$- \int_{\tilde{Q}_T} \nabla_H \Phi_h \cdot \nabla_H q_h = \int_{\tilde{Q}_T} \theta_h q_h - \int_\Gamma \frac{\partial \Phi_h}{\partial n}\, ds\ ,$$

$$\forall\ q_h \in H_h'\}.$$

P_k is the space of polynomials in (x,y) of degree $\leq K$, so $v_h\big|_T \in P_k$ means that the functions of the discrete spaces are polynomials in (x,y) of degree $\leq K$ on the subdomains Te. It follows that N_{oh} = number of vertices of $\mathcal{T}_h$ which are interior to $\tilde{Q}_T$, is the dimension of H_{0h}^1 while the dimension of H_h^1 is equal to the number of N_h of vertices of $\mathcal{T}_n$ which belong to $\tilde{Q}_T$.

$C_h(t)$ is a convenient approximation to $C(t)$ in $H_h^1(Q_T)$.

Inspired by Glowinski and Pironneau (1979), we build up an additional finite dimensional space M_h in order to impose properly the no-slip boundary condition on the vorticity equation. M_h is the complementary space of

H_{oh}^1 in $H_h^1(Q_T)$, i.e.,

$$M_h \subset H_h^1(\tilde{Q}_T),$$

$$H_h^1 = H_{0h}^1 \oplus M_h.$$

Hence, $\forall\ \zeta_{ih} \in H_h^1(\tilde{Q}_T)$, $(i = 1,2)$, which verifies that

$$\zeta_{ih} = (\zeta_{ih} - \zeta_{ih}^*) + \zeta_{ih}^*,$$

where

$$\zeta_{ih}^* \in M_h,\ \zeta_{ih} - \zeta_{ih}^* \in H_{oh}^1.$$

So ζ_{ih}^* is the component of the relative vorticities ζ_{ih} in M_h. The restriction of the integrability property of $W_{\sigma h}^{NS}$ in M_h is

$$\forall\ (\theta_{ih}, \psi_{ih}) \in H_h^1 \times H_h^1,\ \forall\ \mu_h \in M_h$$

$$-\int_{\tilde{Q}} \nabla_H \psi_{ih} \cdot \nabla_H \mu_h = \int_{\tilde{Q}_T} \theta_{ih}\, \mu_h - \int_\Gamma \frac{\partial \psi_{ih}}{\partial n}\, \mu_h\, ds \quad (i=1,2). \tag{3.14}$$

Confining ourselves to Lagrange-type elements of order (K=1 in P_k) we generate the global basis functions $v_h \in H_h^1 (Q_T)$ from local approximation via the formula

$$v_{hj} = \bigcup_{e=1}^{E} \sum_{N=1}^{Ne} {}^{(e)}_{\Omega_j} N \; \nu_N^{(e)} (\vec{x})$$

where

$j = 1,2 \ldots N_h$

Ne is the number of vertices of a given Te

${}^{(e)}_{\Omega_j} N$ is the Boolean transformation matrix for the element Te,

$\nu_N^{(e)}$ is the local interpolation function corresponding to the element Te.

The Galerkin approximations, ζ_{ih}, ψ_{ih} are written as

$$\zeta_{ih} (\vec{x},t) = \sum_{\ell=1}^{N_h} \zeta_{in\ell}(t) \; v_{h\ell}(\vec{x}), \qquad x \in H_h^1$$

$$\psi_{ih} (\vec{x},t) = \sum_{\ell=1}^{N_h} \psi_{in\ell}(t) \; v_{h\ell}(\vec{x}). \qquad (i=1,2) \qquad (3.15)$$

Recalling the relationships among barotropic and baroclinic modes and stream functions, ψ_1 and ψ_2, as well as relationships among ψ_1 and ψ_2 and $\psi_{1\frac{1}{2}}$ we can write

$$\psi'_{ah}(\vec{x},t) = \sum_{\ell=1}^{N_h} \psi'_{ah\ell}(t)\, v_{h\ell}(\vec{x}),$$

$$\psi'_{bh}(\vec{x},t) = \sum_{\ell=1}^{N_h} \psi'_{bh\ell}(t)\, v_{h\ell}(\vec{x}),$$

$$\Phi'_{h}(\vec{x},t) = \sum_{\ell=1}^{N_h} \psi'_{h\ell}(t)\, v_{h\ell}(\vec{x}),$$

$$\psi_{1\frac{1}{2}\,h} = \frac{H_2\ \psi_{1h} + H_1\ \psi_{2h}}{H_1 + H_2}\ . \qquad (3.16)$$

The variational formulation (3.11) - (3.13) is now approximated as:

Find $\{\zeta_{ih},\ \psi_{ih}\} \in W_{\sigma h}$

such that

$$\forall\ \Phi_h \in H^1_h,\ \zeta_{ih} - \zeta^*_{ih} \in H^1_{0h},\ \zeta^*_{ih} \in M_h,$$

$$\left(\frac{\partial \zeta_{ih}}{\partial t},\ \Phi_h\right) = \left(J\ (\zeta_{ih},\ \psi_{ih}),\ \Phi_h\right) - \left(\beta\ \frac{\partial \psi_{ih}}{\partial x}\ ,\ \Phi_h\right)$$

$$+\left((-1)^i\ \frac{f_0}{H_1}\ w_{2h},\ \Phi_h\right) - \left(A_H\ \nabla_H \zeta_{ih},\ \nabla_H \Phi_h\right)$$

$$+\ \frac{1}{2}\ (1 + (-1)^i)\ (\varepsilon\ \zeta_{1h},\ \Phi_h)$$

$$+\ \left(\frac{1-(-1)^i}{2}\right)\ \left(\frac{F}{H_1}\ ,\ \Phi_h\right)\ \text{in}\ \tilde{Q}_{Th} \cap Z_i, \qquad (3.17a)$$

$$- \int_{\tilde{Q}_{Th}} \nabla_H \psi_{ih} \cdot \nabla_H \mu_h = \int_{\tilde{Q}_{Th}} \zeta_{ih} \mu_n + \int_\Gamma \frac{\partial \psi_{ih}}{\partial n} \mu_h \, ds, \tag{3.17b}$$

$$- (\nabla_H \Psi'_{ah}, \nabla_H \Phi_h) - (\lambda^2 \Psi'_{ah}, \Phi_h) = (\gamma_{ah}, \Phi_h) \text{ in } \hat{Q}_{Th} \cap Z_i,$$

$$\Psi_{ah}\big|_{\Gamma_h} = 0, \qquad \Psi'_{ah}\big|_{t=0} = 0, \tag{3.18a}$$

$$- (\nabla_H \Psi'_{bh}, \nabla_H \Phi_h) - (\lambda^2 \Psi'_{bh}, \Phi_h) = 0 \text{ in } Q_{0h} \cap Z_i,$$

$$\Psi_{bh}\big|_{\Gamma_h} = 1, \tag{3.18b}$$

$$- (\nabla_H \phi'_h, \nabla_H \Phi_h) = (\gamma_{bh}, \Phi_h) \text{ in } Q_{Th} \cap Z_i,$$

$$\phi_h\big|_{ih} = 0, \qquad \phi'_h\big|_{t=0} = 0. \tag{3.19}$$

Upon substituting (3.15) and (3.16) into (3.17) - (3.19), we obtain the following implicit systems of ordinary differential equations for the weight functions:

$$\vec{\zeta}_{ih} = \{\zeta_{ih\ell}\}, \ \vec{\psi}_{ih} = \{\psi_{ih\ell}\}, \ (i=1,2), \ (\ell=1,2,\ldots N_h).$$

(i) Relative vorticity equations:

$$M \dot{\vec{\zeta}}_{ih} = J_h(\vec{\zeta}_{ih}, \vec{\psi}_{ih}, \beta) - A_H K \vec{\zeta}_{ih}$$

$$+ \frac{1}{2} (1 + (-1)^i) \varepsilon M \vec{\zeta}_{ih} + \vec{\mathcal{F}}_h \text{ in } \hat{Q}_{Th} \cap Z_i,$$

$$\vec{\zeta}_{ih}\big|_{\Gamma h} = \vec{\sigma}_{ih}. \tag{3.20}$$

(ii) Baroclinic mode equations:

$$- K \dot{\vec{\psi}}_{ah} - \lambda^2 M \dot{\vec{\psi}}_{ah} = \vec{\gamma}_{ah} \text{ in } \tilde{Q}_{Th} \cap Z_i,$$

$$\vec{\psi}_{ah}\big|_{\Gamma h} = 0. \tag{3.21a}$$

$$- K \dot{\vec{\psi}}_{bh} - \lambda^2 M \dot{\vec{\psi}}_{bh} = 0 \quad \text{in } \hat{Q}_{0h} \cap Z_i,$$

$$\psi_{bh}\big|_{\Gamma h} = 1. \tag{3.21b}$$

(iii) Barotropic mode equations:

$$- K \vec{\phi}_h = \vec{\gamma}_{bh} \text{ in } \tilde{Q}_{Th} \cap Z_i$$

$$\vec{\phi}_h\big|_{\Gamma} = 0 \tag{3.22}$$

An upper dot on the variables stands for time-derivative, the "mass matrix" M has the entries

$$\int_Q v_{hk}\, v_{hj}\, dx \qquad (k,j=1,1\ldots N_h),$$

and the entries of the "stiffness matrix" K are given by

$$\int_Q \nabla_H v_{hk} \cdot \nabla_H v_{hj}\, dx, \quad (k,j=1,2,\ldots N_h).$$

M is symmetric and positive definite, whereas K is symmetric only.

$J(\vec{\xi}_{ih}, \vec{\psi}_{ih}, \beta)$ in (3.20) is the matrix which includes the contributions of the Jacobian and β terms of the equations. Depending on the time scheme used to step forward in time the equations J can be either a column vector matrix

or a skew symmetric square matrix. $\vec{\mathcal{F}}_h$ is a (2 x N_h) column vector whose entries are:

$$\int_Q \left[(-1)^i \frac{f_0}{H_1} w_{2h} + \frac{\vec{F}}{H_1} \left(\frac{1-(-1)^i}{2}\right)\right] v_{hj} \, dx$$

$$= \vec{w}_h + \frac{1}{H_1} \vec{F}_{h1}, \quad (j=1,2,\ldots N_h).$$

The right-hand sides $\vec{\gamma}_{ah}$ and $\gamma_{bh}\vec{}$ of the equations (3.21a) and (3.21b), respectively, are matrices which came from the terms (γ_{ah}, Φ_h) in (3.18a) and (γ_{bh}, Φ_h) in (3.19).

An important aspect that still remains to be elucidated is the computation of $\vec{\sigma}_{ih}$ in (3.20). If we assume, a priori, the validity of the free-slip boundary condition on the solid boundaries then we take $\vec{\sigma}_{ih}$ equal to zero at the points of such boundaries and we go on with the computation of the solutions of (3.20); however, if we wish to impose on the solid boundaries the no-slip condition, then $\vec{\sigma}_{ih}$ are unknown values at the points situated on the solid boundaries that have to be computed from the relation (3.17b) which is highly dependent on the properties of the space M_h, so we should chose M_h such that the values of ζ^*_{ih} on the solid boundaries were easy to compute from (3.17b). Let us first define general properties that we wish M_h to have:

(i) Since M_h is a complementary space of H^1_{0h}, then we take

dim $(M_h) = N_h^B$ = No. boundary points.

(ii) We wish that the support of M_h be as small as possible. A convenient support would be

$$\mu_h \in M_h \Rightarrow \mu_h|_{Te} = 0 \quad \forall\, Te \in \mathcal{T}_h \text{ such that } Te \cap \Gamma_h = \text{(empty set)}.$$

(iii) The above properties (i) and (ii) suggest how to define a canonical basis B_{M_h} of the space M_h.

$$B_{M_h} = \{W_\ell\} \quad (\ell = 1,2,\ldots,N_h^B) \text{ such that}$$

(iii-1) $W_\ell \in H_h^1$

(iii-2) $W_\ell(\vec{x}_j) = \delta_{\ell j}$ if $(\vec{x}_j) \quad \Gamma$,

$$W_\ell(\vec{x}_j) = 0 \text{ if } \vec{x}_j \notin \Gamma.$$

Properties (i) to (iii) are quite general and do not depend on how the boundary and an interior narrow strip of $\tilde{Q}_h$ adjacent to the boundary are discretized. They are also independent of the existence of tangential velocity on the boundary. In our particular problem, the tangential velocity is zero on the solid boundaries, so if we require that

$$\forall\, Te \in \mathcal{T}_h \ni Te \cap \Gamma \neq \text{(empty set)},$$

either

one side of Te is normal to the boundary with a vertex on it,

or

two vertices of Te, one on the boundary another in the interior, can be connected along the outward normal to the boundary.

We can define another property such as

$$\text{(iv)} \quad \frac{\partial w_i(\vec{x})}{\partial t} = 0 \quad \forall \vec{x} \in \Gamma,$$

where $\vec{t}$ is the clockwise tangent vector on the boundary.

Notice that (iv) is a particular property in the sense that it depends, first, on the topology of the discrete space $\tilde{Q}_h$ close to the boundary and, secondly, on the vanishing of the tangential velocity on the boundary.

The support of M_h is then composed of the segments $\overline{P_j^B \; P_j^i}$ normal to the boundaries. See Fig. 2.

In that figure $\{P^B\}_j$ denotes boundary points and $\{P^i\}_j$ are the interior points closest to the boundaries along the normal direction. It is clear that (3.14) becomes

$$- \int_{\Omega_N} \frac{\partial \psi_{ih}}{\partial n} \frac{\partial \mu_h}{\partial n} \, d\ell_h = \int_{\Omega_N} \zeta_{ih} \; \mu_h \; d\ell_h,$$

where $\Omega_N = \{P_j^B \; P_j^i\}_{j=1}^{N_h^B}$.

By using Lagrangian linear basis functions, the above integral becomes

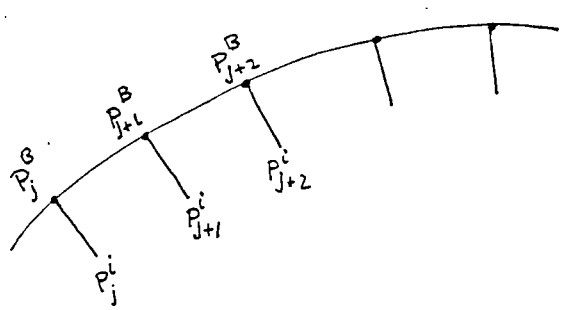

Fig. 2

Support of the space Mn
discussed in Section 3.3

$$\zeta_{i,w} = -\frac{3}{\ell_h^2}(\psi_{i,w} - \psi_{i,I}) - \frac{\zeta_{i,1}}{2}, \qquad (3.23)$$

where $\zeta_{i,w}$ and ψ_{iw} are the vorticity and stream function values, respectively, at a given boundary points;

$\zeta_{i,I}$ and $\psi_{i,I}$ are the same quantities but taken at the corresponding interior points;

ℓ_h is the distance along the normal direction between a boundary point and its corresponding interior point.

Equation (3.23) is Woods' formulation for wall vorticity, a commonly used second order accuracy approximation. Roache (1972) has pointed out that such formulation for the wall vorticity can yield instabilities at high Reynolds numbers (Re $\geq$ 300). This is not our case because as we will see later our Reynolds number is Re = 50. The same formula has been derived by Barret (1978) using a variational principle of Bateman's type for the stream function vorticity formulation of the Navier-Stokes equations with no-slip conditions in conjunction with finite element.

3.4 Time Discretization

In order to carry out the time integration of equations (3.20) - (3.22), we use the leapfrog scheme with the

Laplacian frictional terms lagged by one time step and the bottom friction terms taken as the average of the forward and backward time steps to avoid linear numerical instability. Richtmyer (1967). The reasons for using such a scheme are:

(i) It is explicit so it is easy to implement.

(ii) It is second order accuracy in time.

(iii) It is non-dissipative.

The latter reason is more theoretical rather than practical, because the existence of numerical phase dispersion, which is unavoidable, is equivalent to a damping mechanism (Roache (1972, pp. 56-60 and 80-81).

A disadvantage of the leapfrog scheme is its computational mode (Arakawa-Messinger, 1976) which leads, on one side, to the splitting of the solutions and, on the other side, it acts as a trigger mechanism for the appearance of non-linear instability, Briggs et al. (1983). All these troubles can be mitigated by using every 50 time steps a restart consisting of taking

$$u^{(n+1/2)} = \frac{u^{(n+1)} + u^{(n)}}{2} ,$$

$$u^{(n-1/2)} = \frac{u^{(n)} + u^{(n-1)}}{2} ,$$

where n is the number of time step, and then to continue the computation in the usual way. Sadourny (1975) reports very good results with such a restart, as for the non-linear instability concerns, in the integration of the

quasi-geostrophic equations with finite difference potential vorticity quasi-conservative schemes in space and leapfrog scheme in time. Killworth (1985) showed the good characteristics of the above restart when it is compared, in terms of an equivalent filter, with other standard restarts in geophysics.

For every time step, the equations that have to be solved are:

$$M\,(\vec{\zeta}_{ih}^{(n+1)} - \vec{\zeta}_{ih}^{(n-1)}) = 2\Delta t\ \vec{R}^{(n)}$$

$$\zeta_{ih}^{(n+1)}\Big|_{\Gamma} = \sigma_{ih}^{(n+1)}, \tag{3.24}$$

$$-K\ \dot{\vec{\Psi}}_{ah}^{(n)} - \lambda^2\ M\ \dot{\vec{\psi}}_{ah}^{(n)} = \vec{\gamma}_{ah}^{(n)},$$

$$\dot{\vec{\psi}}_{ah}^{(n)}\Big|_{\Gamma} = 0. \tag{3.25}$$

If n=1 we solve (3.21b).

$$-K\ \dot{\vec{\phi}}_{h}^{(n)} = \vec{\gamma}_{bh}^{(n)},$$

$$\dot{\vec{\phi}}_{h}^{(n)}\Big|_{\Gamma} = 0. \tag{3.26}$$

$$\dot{\vec{\psi}}_{h}^{(n)} = \vec{\Psi}_{bh}^{(n)} + \dot{\vec{\psi}}_{ah}^{(n)}$$

$$= \frac{(\vec{\Psi}_{1h} - \vec{\Psi}_{2h})^{(n+1)} - (\vec{\Psi}_{1h} - \vec{\Psi}_{2h})^{(n-1)}}{2\Delta t},$$

$$\dot{\vec{\phi}}_{h}^{(n)} = \frac{(H_1\vec{\Psi}_{1h} + H_2\vec{\Psi}_{2h})^{(n+1)} - (H_1\vec{\Psi}_{1h} + H_2\vec{\Psi}_{2h})^{(n-1)}}{2\Delta t} \tag{3.27}$$

$$\vec{\psi}^{(n+1)}_{1\frac{1}{2}\,h} = \frac{H_2\ \vec{\psi}^{(n+1)}_{1h} + H_2\ \vec{\psi}^{(n+1)}_{1h}}{H},$$

$$w^{(n)}_{2h} = -\,[\dot{\vec{\psi}}^{(n)}_{h} - J(\vec{\psi}^{(n)}_{1h} - \vec{\psi}^{(n)}_{2h},\ \vec{\psi}^{(n)}_{1\frac{1}{2}\,h})], \tag{3.28}$$

where

$$\vec{R}^{(n)} = J(\vec{\zeta}^{(n)}_{ih},\ \vec{\psi}^{(n)}_{ih},\ \beta) - A_H\ K\ \vec{\zeta}^{(n-1)}_{ih}$$

$$+ \frac{1}{2}\,(1 + (-1)^i)\ \varepsilon\ M\ (\frac{\vec{\zeta}^{(n+1)}_{ih} + \vec{\zeta}^{(n-1)}_{ih}}{2}) + \vec{\mathcal{F}}^{(n)}_{h}. \tag{3.29}$$

Since the leapfrog scheme is a three-level one, we cannot start the computations with it, so we need another scheme, say, a two-level one. The most common scheme used for this purpose is the Euler forward scheme given by

$$u^{(n+1)} = u^{(n)} + \Delta t\ R^{(n)},$$

which is highy unstable if it were used to carry out the time integration of the equations for many time steps. The initial values of all variables are equal to zero.

As we see from (3.24) - (3.26), we have to solve four systems of equations every time step. Two systems for the

vorticity equations and other two for both the baroclinic and barotropic modes. This is a disadvantage of f.e compared to second order finite differences where only the modal equations are to be solved. One form of remedying this is to lump the mass matrix M by adding all the elements of a given row onto the diagonal of the row and then set the off-diagonal terms to zero. That is

$$M_{ij} = \sum_{j} M_{ij} \qquad i = j$$

$$M_{ij} = 0 \qquad i \neq j$$

Later on, we will give the main reason to lump the matrix M.

An algorithm of the computations is as follows:

(1) Compute the element components of the matrices M and K and store them into one dimensional compact vectors. This compact form of storing the matrices is particularly convenient for the Conjugate Gradient Method and for solving the algebraic equations, because rather than operating with matrices and vectors, we only operate with one-dimensional vectors that represent faster computations even on scalar computers as the one we have used. Another remarkable feature of the compact storing is the substantial saving of computer memory (up to 60 percent) in relation with more standard techniques used in finite element codes which solve the system of equations by direct methods. The computations of M and K are done once for all.

(2) If n = 1 set $\vec{\zeta}_1^{(0)} = \vec{\psi}_1^{(0)}$ and $\vec{\psi}^{(0)}_{1\frac{1}{2}} = 0 \quad (i=1,2)$

and

(i) solve (3.25), (3.21b) and (3.26);

(ii) compute $\vec{\psi}_1^{(1)}$, $\vec{\psi}_2^{(1)}$ and $\psi^{(1)}_{1\frac{1}{2}}$ from (3.22) by using the Euler forward scheme rather than the leapfrog one;

(iii) compute $\vec{w}_2^{(1)}$ from (3.28) and $\vec{R}^{(1)}$ from (3.29);

(iv) if the non-slip conditions are applied on the vorticity equations and the matrix M is retained, then compute the boundary conditions; otherwise, go on to solve (3.24);

(v) solve equations (3.24) and impose the boundary conditions; if the matrix M is lumped and the non-slip constraints imposed, then the computation and impositions of the boundary conditions are made together.

For $n \geq 2$, steps (2-i) to (2-v) are repeated successively, but using the leapfrog scheme instead of the Euler forward one.

Observe that we have to solve one Helmholtz equation for the baroclinic mode (two equations when n=1) and one Poisson equation for the barotropic mode. The numerical experiments have shown that for the values of λ^2 and the grid spacing

used in our computations, the Helmholtz matrix is well-conditioned while the Poisson one is only fair-conditioned resulting, therefore, in a computation of the baroclinic mode which is relatively cheap and fast, whereas the barotropic mode is expensive and lengthy of computing. The matrix M is very well conditioned, so the solution of (3.24) is obtained relatively fast (few iterations); however, if the experiments are to be carried out for a large number of time steps, then the process of solving two additional systems can become burdensome. This is an argument that many analysts used to justify the lumping of the matrix M so long as the loss of accuracy is not badly damaged.

3.5 Stability Analysis

It is customary to choose the grid spacing from the beginning based on the physics of the phenomena one wants to simulate numerically, unless a moving mesh or automatic refinement mesh method be used. Once the grid spacing has been fixed, the time interval is determined by the stability condition of the discretized equations. The study of the stability criterion of the discretized equations is relevant because as the Lax equivalence theorem states: if a linear differential problem which is well posed is approximated by a consistent difference scheme, then the resultant

approximation converges to the true solution for all initial data as the space-time mesh is refined if and only if the difference scheme is stable for this refinement (Richtmyer, R.D. and K.W. Morton, 1967). A consequence of this theorem is the closed relationship between the well-posedness of the continuum problem and the stability of the discretized one; actually, for any continuum (even non-linear) partial differential equation, the common way of determining the uniqueness of the solution is via energy norm. The solution of the discrete approximation of an initial boundary value problem (either linear or non-linear) is stable if and only if

$$\forall\ \varepsilon > 0,\quad \delta > 0 \text{ such that}$$

$$\|\vec{u}_h^{(0)}\|_2^2 < \delta \Rightarrow \sup_M \|\vec{u}^{(n)}\|_2^2 < \varepsilon.$$

The above definition of stability is the L^2 norm stability. For linear problems, and assuming that the domain $\tilde{Q}_T$ is infinite or the problem has periodic boundary conditions, Fourier analysis is the technique which gives stability criteria that most of the times are equivalent to the L^2-norm stability criterion (see Kreiss, 1978). If the equations are of variable coefficients it is still possible to apply Fourier analysis by "freezing" coefficients and the local stability criterion obtained in this form can give an

estimate of the overall stability in cases of dissipative systems (Kreiss, 1978); otherwise, the estimate is only indicative of how things can transpire. If the equations are non-linear, as the q.g.e. are, the properties of the linearized equations are not at all sufficient for determining numerical stability because the L^2-norm of the latter does not imply the L^2-norm of the full non-linear equations (Phillips, 1959). The boundedness of the L^2-norm implies that certain quadratic quantities are to be bounded (if there is no dissipation, they are to be conserved); therefore, the first condition we have to require from our discretized scheme is to keep bounded (or to conserve) such quadratic quantities. In quasi-geostrophic dynamics, it turns out that the quadratic quantities, which are bounded or conserved if dissipation is neglected, are the kinetic energy and the enstrophy. The conservation of such quantities implies the conservation of the average wave number and specifies the direction of the non-linear energy transfers. The energy is transferred towards lower wave numbers while the potential enstrophy is in the opposite direction (Charney, 1971). Therefore, it is clear that the discrete schemes of the q.g.e. which are able to conserve the kinetic energy and the potential enstrophy can reproduce the exchanges of energy among the modes better than those which are not. A first success in this direction was achieved by

Arkava in 1966 when he produced a particular form of the convective terms of the vorticity equation which in terms of enstrophy is quadratically semi-conservative. Fix (1975) shows that f.e. discretization of the barotropic quasi-geostrophic equations are potential vorticity semi-conservative and kinetic energy and potential entrophy quadratically semi-conservative. See Appendix B for definitions. In fact, Jespersen (1979) shows that Arakawa's scheme is a finite element scheme. The trouble is that neither finite element nor Arakawa's scheme are able to generate schemes that in the absence of dissipation are kinetic energy and potential enstrophy quadratically conservative; at most, they can yield

$$\sum_{m=1}^{M} \vec{\zeta}_m^{(n+1)} \; \vec{\zeta}_m^{(n)} = \text{Cte}$$

if leap frog scheme is used.

where $\vec{\zeta}$ is potential vorticity,

n is the number of time step,

m denotes the number of the grid points.

The loss of the strict conservation of the quadratic properties when the complete discretization of the equations has been carried out, can make the numerical solution go unstable. Basdevant and Sadourny (1975) show that in addition to the kinetic energy and potential enstrophy, higher order moments have to be conserved by any complete

scheme of the non-linear equations if one wants to avoid the onset of non-linear instability. At present, it seems difficult to devise higher order moment conservative schemes which may be computationally feasible, so we will have to live with the threat of the non-linear instability and to combat it by using recipes as the one we use in our computations. The main mechanism in provoking non-linear instability in those schemes which are neither quadratically semi-conservtive nor quadratically conservative is aliasing (Phillips, 1959). However, with schemes such as the Arakawa scheme or finite element method, in which the alisaing problem is almost ruled out, very little is known about the subtle mechanisms responsible for the onset of the non-linear instability. This instability is very different from the one present in linear equations when the stability criterion is violated. Its peculiar features in those schemes which are quadratically semi-conservative are:

(i) It shows up after several hundred time steps of successful computations.

(ii) As a threshold is reached, it starts locating at a few points of the grid, then focuses and later on, after a few steps of integration, extends very fast all over the domain. At this point, the computations blow up.

(iii) Possible trigger mechanisms are (Briggs et al., 1983) the computational mode if the leapfrog scheme

is used, the spurious oscillations produced either at boundary points which are not well-resolved, or at discontinuity interfaces and others.

At this point, it seems obvious to ask about the relevance of carrying out a linear stability analysis by "freezing" the coefficients of the non-linear partial differential equation. The answer may be given by assuming that the first stages of the non-linear numerical instability are very similar to those of the non-linear hydrodynamic stability. In doing so, we can determine which are the most unstable modes on one side, and an assessment of the non-linear instability threshold in terms of the values of the linear stability criterion on the other side (Briggs et al. 1983).

As is common practice in the theory of the hydrodynamic stability (Pedlosky, 1970, 1971), we start by decomposing the stream functions ψ_i as

$$\psi_i(x,y,t) = \psi_i^{(0)} + \psi_i', \qquad (i = 1,2)$$

such that

$$-\frac{\partial \psi_i^{(0)}}{\partial y} = u_i^{(0)}, \quad \frac{\partial \psi_i^{(0)}}{\partial x} = v_i^{(0)},$$

where $u_i^{(0)}$ and $v_i^{(0)}$ are the basic flow velocities. In our

context, they can be interpreted as the Sverdrupean velocities (in the first layer) in the interior of the ocean and the jet stream velocities in the western boundary layer. ψ_i' (x,y,t) represents the perturbation to the basic flow. With such a decomposition, the Jacobian terms of the vorticity and modal equations (3.1 - 3.10) become, upon linearization,

$$J(\zeta_i, \psi_i) \rightarrow - V_i^{(0)} \cdot \nabla \zeta_i, \quad i = 1,2,$$

where $V_i^{(0)} = (u_i^{(0)}, v_i^{(0)})$. The (') sign has been dropped from the vorticity of the right-hand side. The stability of the linearized equations (3.24) - (3.29) will be dictated by the stability of the first layer vorticity equation because it is in this layer where the velocities $(U_i^{(0)}, V_i^{(0)})$ attain the highest values. It is well known that the stability of the homogeneous equation implies the stability of the inhomogeneous one provided the forcing term is bounded (Kreiss, 1978). Therefore, we have to study the linear stability of the following equation:

$$M\left(\frac{\overset{+}{\zeta}_{1h}^{(n+1)} - \overset{+}{\zeta}_{1h}^{(n-1)}}{2\Delta t}\right) = - V_{ih}^{(0)} \cdot \nabla_H \overset{+}{\zeta}_{1h}^{(n)} - \beta \frac{\partial \overset{+}{\psi}_{1h}^{(n)}}{\partial x} - A_H K \overset{+}{\zeta}_{1h}^{(n-1)}, \tag{3.30}$$

The equation equivalent to (3.30) at the node (pΔx, qΔy) is

$$\frac{1}{36}\{16\dot{\zeta}_{p,q} + 4(\dot{\zeta}_{p,q+1} + \dot{\zeta}_{p,q-1} + \dot{\zeta}_{p+1,q} + \dot{\zeta}_{p-1,q}) + (\dot{\zeta}_{p+1,q+1} + \dot{\zeta}_{p+1,q-1} + \dot{\zeta}_{p-1,q+1} + \dot{\zeta}_{p-1,q-1})\}$$

$$= -\frac{1}{12}\{\frac{u_1^{(0)}}{\Delta x}(\zeta_{p+1,q+1} - \zeta_{p-1,q+1} + \zeta_{p+1,q-1} - \zeta_{p-1,q-1} + 4(\zeta_{p+1,q} - \zeta_{p-1,q}))$$

$$+ \frac{1}{12}\{\frac{v_1^{(0)}}{\Delta x}(\zeta_{p+1,q+1} - \zeta_{p+1,q-1} + \zeta_{p-1,q+1} - \zeta_{p-1,q-1} + 4(\zeta_{p,q+1} - \zeta_{p,q-1}))\}^{(n)}$$

$$- \frac{A_H}{3}\{\zeta_{p+1,q+1} - \zeta_{p,q+1} + \zeta_{p-1,q+1} + \zeta_{p+1,q} - 8\zeta_{p,q} + \zeta_{p-1,q} + \zeta_{p+1,q-1} + \zeta_{p,q-1} + \zeta_{p-1,q-1}\}^{(n-1)}, \qquad (3.31)$$

where:

$u_1^{(0)}$ and $v_1^{(0)}$ are assumed to be constants.

$$\dot{\zeta} = \frac{(\zeta^{(n+1)} - \zeta^{(n-1)})}{(2\Delta t)}.$$

Assume that

$$\zeta_{p,q}^{(n)} = \lambda_1^n \exp[i(kx_p + \ell y_q)]$$

$$x_p = p\Delta x,\ y_q = q\Delta y,\ 0 \leq p \leq P,\ 0 \leq q \leq Q$$

$$P\Delta x = L_x,\ Q\Delta y = Ly$$

λ_1 is an amplification factor

Equation (3.31) gives

$$\lambda_1^2 + i\ 6\ \lambda_1\ \Delta t\{\frac{u_1^{(0)}}{\Delta x}\ \frac{\sqrt{1 - x^2}}{4 + 2\ (x+y) + xy}\ (y + 2)$$

$$+ \frac{v_1^{(0)}}{\Delta x}\ \frac{\sqrt{1 - y^2}}{4 + 2\ (x+y) + xy}\ (x + 2)\}$$

$$- \{1 - \frac{A_H\ 48\ \Delta t}{\Delta x\ \Delta y}\ (\frac{4 - (x+y) - 2xy}{4 + 2\ (x+y) + xy})\} = 0, \qquad (3.33)$$

where

$$x = \cos k\Delta x,\ y = \cos \ell \Delta y,\ -1 \leq x,y \leq 1.$$

Equation (3.31) is stable if and only if

$$|\lambda_1| \leq 1. \qquad (3.34)$$

From (3.33) we obtain that

$$\lambda_1 = i\ 3\Delta t B \pm (-\ 9\Delta t^2 B^2 + 1 - A)^{1/2}, \qquad (3.35a)$$

where

$$B = \frac{u_1^{(0)}}{\Delta x}\ \frac{\sqrt{1 - x^2}}{2 + x} + \frac{v_1^{(0)}}{\Delta y}\ \frac{\sqrt{1 - y^2}}{2 + y},$$

$$A = \frac{48\ A_H\ \Delta t}{\Delta x\ \Delta y}\ (\frac{4 - (x + y) - 2xy}{(2 + x)\ (2 + y)}). \qquad (3.35b)$$

Then

$$|\lambda_1|^2 = 1 - A,$$

$$\text{for } 3\Delta t B \leq (1 - A)^{1/2}. \tag{3.36}$$

Taking into account that $-1 \leq x, y \leq 1$ then

$$\max A = \frac{192 A_H \Delta t}{\Delta x \, \Delta y},$$

$$A \geq 0,$$

$$\max B = \frac{1}{\sqrt{3}} \left(\frac{u_1^{(0)}}{\Delta x} + \frac{v_1^{(0)}}{\Delta y}\right). \tag{3.37a}$$

If $\Delta x = \Delta y$ and $u_1^{(0)} = v_1^{(0)} = \frac{\overline{V}}{\sqrt{2}}$, this gives

$$\max A = \frac{192 A_H \Delta t}{h^2},$$

$$A \geq 0, \tag{3.37b}$$

$$\max B = \sqrt{\frac{2}{3}} \frac{\overline{V}}{h}.$$

By using (3.37b) the stability criterion (3.36) becomes

$$1 - \frac{192 A_H \Delta t}{h^2} \leq |\lambda_1|^2 \leq 1,$$

for

$$\frac{192A_H\Delta t}{h^2} < 1,$$

and

$$\sqrt{6}\,\frac{\Delta t}{h}\,\overline{V} \leq \left(1 - \frac{192A_H\Delta t}{h^2}\right)^{1/2}, \qquad (3.38a,b,c)$$

where h is the smallest value of the grid spacing, and $\overline{V}$ is the highest possible velocity.

Conditions (3.38a) and (3.38b) are quite a severe stability criterion for the grid size and A_H that we have to use in order to make feasible the computations. Notice that (3.35b) is the stability criterion for the hyperbolic part of the equations. From (3.36a) we can show (see Appendix C) that the scheme is dissipative of order 2 according to Kreiss' definition. (See Kreiss (1978)). The term responsible of the harshness of (3.38) is the consistent mass matrix M that makes implicit in space the time derivative operator. A standard technique for converting the implicit discretization into an explicit one is the lumping of the mass matrix M. Thomée (1985) shows that the approximation error of the lumped scheme is of the same order as the consistent scheme; however, the evolutionary error of the lumped scheme is of second order in contrast with the fourth order error that can be achieved by using the consistent scheme. The most standard finite difference models used in oceanography, such

as Holland (1978) and Bryan-Cox's models are second order accuracy too. Since it is not the purpose of this thesis to discuss the positive properties of consistent Galerkin-finite element method in relation to the evolutionary error, we do not go further on such topic. Results on evolutionary error, phase propagation and group velocity of the finite element, applied to the quasi-geostrophic equations, will be reported elsewhere.

As we have already explained, the way of lumping the matrix M is by adding all the elements of a given row onto the diagonal of the row and then set the off-diagonal terms to zero. In doing so, the term on the left-hand side of (3.31) becomes

$$\frac{\zeta_{p,q}^{(n+1)} - \zeta_{p,q}^{(n-1)}}{2\Delta t}$$

whereas the terms on the right-hand side remain unaltered. The equation for the amplification factors λ_1 is

$$\lambda_1^2 + i\,\frac{2}{3}\,\lambda_1\,\Delta t\left[\frac{u_1^{(0)}}{\Delta x}\,\sqrt{1-x^2}\,(2+y) + \frac{v_1^{(0)}}{\Delta y}\,\sqrt{1-y^2}\,(2+x)\right]$$

$$- \left\{1 - \frac{4}{3}\,\frac{\Delta t\, A_H}{\Delta x\,\Delta y}\,(4 - (x+1)\,(y+1)\right\} = 0. \qquad (3.39)$$

Hence

$$\lambda_1 = i \frac{\Delta t}{3} B_1 \pm (- \frac{\Delta t^2}{q} B_1^2 + 1 - A_1)^{1/2}, \qquad (3.39)$$

where

$$A_1 = \frac{4}{3} \frac{A_H \Delta t}{\Delta x \Delta y} (4 - (x + y) - 2xy),$$

$$B_1 = \frac{u_i^{(0)}}{\Delta x} \sqrt{1 - x^2} (2 + y) + \frac{v_1^{(0)}}{\Delta y} \sqrt{1 - y^2} (2 + x). \qquad (3.40a,b)$$

The stability criterion is

$$|\lambda_1|^2 = 1 - A_1,$$

for

$$\frac{\Delta t B_1}{3} \leq (1 - A_1)^{1/2}, \quad (-1 \leq x, y, \leq 1), \qquad (3.41)$$

and

$$A_1 \geq 0.$$

At $(x,y) = - (1/2, 1/2)$ A_1 has a relative maximum in the interval $-1 \leq x, y < 1$.

$$\max A_1 = 18 \frac{A_H \Delta t}{\Delta x \Delta y},$$

$$\max B_1 = 3(\frac{u_1^{(0)}}{\Delta x} + \frac{v_1^{(0)}}{\Delta y}).$$

If $\Delta x = \Delta y^h$ and $u_1^{(0)} = v_1^{(0)} = \frac{\overline{V}}{\sqrt{2}}$, then

$$\max B_1 = 3\sqrt{2} \frac{\overline{V}}{\sqrt{2}} ,$$

and

$$\max A_1 = 18 \frac{A_H \Delta t}{h^2}$$

Thus (3.41) becomes

$$1 - 18 \frac{A_H \Delta t}{h^2} \leq |\lambda_1|^2 \leq 1,$$

for

$$\frac{18 A_H \Delta t}{h^2} < 1,$$

and

$$\sqrt{2} \frac{\Delta t \overline{V}}{h} \leq (1 - \frac{18 A_H \Delta t}{h^2}),$$

where h and $\overline{V}$ represents, as before, the smallest value of the grid spacing and the highest possible velocity, respectively.

By comparing (3.38) and (3.42) two obvious conclusions emerge: (i) The constraint imposed by the diffusive terms is much less severe in (3.42) than in (3.38) because max A ≈ 10 max A_1. On the other hand, for the smallest values Δx, Δy, A_H (3.42b) gives

$$\frac{\Delta t A_H}{h^2} \leq 0.55$$

which is not difficult to satisfy for the usual parameters, A_H, Δt, h used in eddy models.
(ii) The condition (3.43c) to be satisfied by the hyperbolic terms is practically the same as that of the f.d. formulation and is, of course, less severe than (3.38c) because for given values of A_H, Δt and h^2 the right-hand side of the inequalities is much larger in (3.43c) than in (3.38c). The scheme is again dissipative of second order. Conclusions (i) and (ii) have been the main reasons for the lumping of the mass matrix.

From this simple study of the stability properties exhibited by two standard discretizations of the mass matrix M of the finite element--leapfrog scheme applied to the quasi-geostrophic equations, it is clear that to exploit the full advantages of the implicitness of the finite element, it is better to use implicit schemes to time-discretize the equations. The main problem with such schemes is that the

algebraic sysems are not symmetric any more and are time-dependent also, so special care has to be taken to compute the solution in these cases. Work in this direction is currently under way to solve the non-linear quasi-geostrophic equation by using a more powerful version of the Conjugate Gradient Method in conjunction with least squares techniques.

CHAPTER 4

THE EXPERIMENTS

4.1 The Model and Its Parameters

We have carried out three experiments. Two single gyre experiments denoted as Exp. 1 (free-slip boundary condition) and Exp. 2 (no-slip boundary condition). The symmetric double gyre experiment with no-slip boundary condition is denoted as Exp. 3.

Two model basins are used. The single gyre model basin is a square of $L_x = L_y = 1{,}000$ km as horizontal dimensions, a uniform depth $H = 5$ km and is centered at 35°N. The double gyre model basin has $L_x = 1{,}000$ km, $L_y = 2{,}000$ km and $H = 5$ km and is centered at 40°N. Subgrid-scale horizontal diffusion of momentum is parameterized by a constant eddy diffusion coefficient $A_H = 330\ m^2\ s^{-1}$. No thermal forcing nor thermal diffusion are allowed in these preliminary experiments.

The model is forced by a sinusoidal wind stress

$$\tau = - \tau_0 \cos (\pi y / L_y).$$

The numerical grid is composed of either squares or rectangles with variable Δx and Δy. The range of values of Δx and Δy is from 20 km up to 40 km. Adjacent to the

boundaries there are strips with $\Delta x = \Delta y = 20$ km. Thus for instance, the western strip is 200 km wide, then the grid size increases progressively with the sequence (25 km, 30 km, 35 km) up to $\Delta x = \Delta y = 40$ km at approximately 350 km from the western coast; this size is kept from this point up to $x = 880$ km where again the grid is decreased progressively. A similar pattern is repeated along the north and south boundaries. See Figure 3. The vertical resolution consists of two layers with depths $H_1 = 1000$ m and $H_2 = 4000$ m, respectively. The choice of these conditions and quantities deserves explanation. The time step Δt is, according to (3.36b), equal to 4 hours, $|\vec{v}^{(0)}| = 1\ ms^{-1}$ and $h = \Delta x = 20$ km. Notice that in order to calculate Δt we have used the smallest value of Δx and multiply the result by a factor of 0.8 which is an empirical criterion in dealing with non-linear or variable coefficient equations. The physical parameters A_H, τ_0 and the vertical resolution are the same as those of Holland (1978) so that we can compare the results of our model with those of Holland's model. On the other hand, A_H cannot be smaller than 200 $m^2\ s^{-1}$ because, otherwise, the western boundary layer width, as we will see later, is not resolved properly by a grid with $\Delta x = 20$ km and, therefore, the solution exhibits oscillations at the boundary which propagate to the interior (see Gresho and Lee

1981). The horizontal grid distribution was determined by the need of keeping as low as possible the computer storage requirements compatible with the resolution needed at the western boundary and possible eddy areas. The largest value of Δx, Δy is smaller than the internal deformation radius, so even in the central region we still keep a resolution high enough to resolve the eddies.

It is, of course, the non-dimensional statement of the model and its parameters which are physically meaningful. The standard non-dimensionalization scheme is (Holland, 1978):

$$(x,y) = L(x^*, y^*), \quad t = (\beta L)^{-1} t^*,$$

$$(u,v) = U(u^*, v^*), \quad w = \left(\frac{\pi H_2 \tau_0}{f_0 H L}\right) w^*,$$

where the star quantities are dimensional ones,

$U = \left(\frac{\pi \tau_0}{\beta H_1 L}\right)$ is a typical horizontal velocity.

Using such a scheme, we define the following non-dimensional parameters:

$$R_0 = \frac{\pi \tau_0}{H_1 \beta^2 L^3} \text{ (Rossby number)},$$

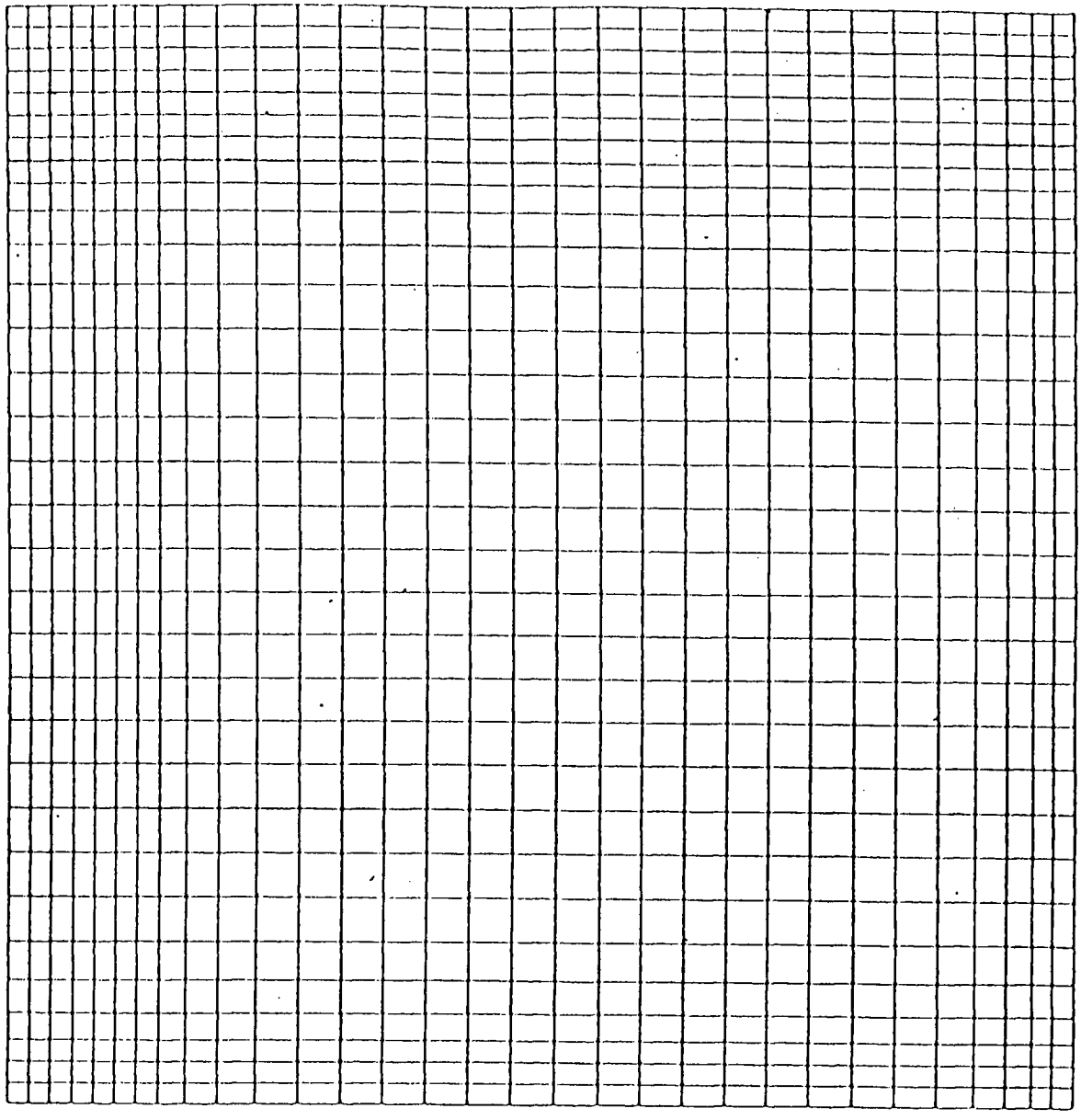

Fig. 3 Lower Basin grid. Exp.3.

$$Re^{-1} = \frac{A_H}{UL} \text{ (Reynolds number)}^{-1},$$

$$\varepsilon^* = \frac{\varepsilon}{L\beta} \frac{H_2}{H} .$$

These non-dimensional parameters can be used to relate the various boundry layer widths to L:

$$W_S = \frac{\varepsilon}{\beta} = \varepsilon^* L \qquad \text{Stommel Layer;}$$

$$W_M = \left(\frac{A_H}{\beta}\right)^{1/3} = \left(\frac{R_0}{R_e}\right)^{1/3} L \qquad \text{Munk Layer;}$$

$$W_I = \left(\frac{U}{\beta}\right)^{1/2} = R^{1/2} L \qquad \text{Intertial Layer.}$$

The values of the non-dimensional parameters and the boundary widths in all of our experiments are:

$$U = 0.0157 \text{ m s}^{-1}$$

$$R_0 = 8 \times 10^{-4}, \qquad R_e = 50, \qquad \varepsilon^* = 4 \times 10^{-3}$$

$$W_S = 5 \text{ km}, \qquad W_M = 25 \text{ km}, \qquad W_I = 28 \text{ km}$$

Notice that according to the values of W_I and W_M, the model is a compromise between a non-linear and a frictional model.

4.2 Results

The main objective of Exp. 1 was to check the internal logic of our model by comparing the finite element results with those given by finite difference models with the same parameters as Holland (1978). The only difference between our experiment and Holland's experiment No. 1 is the inclusion of bottom friction. Exp. 1 was carried out for 200 days. Figure 4 shows the upper layer stream function pattern at T = 200 d. The dominant features are:

(i) a western boundary current;

(ii) a northern wall boundary current flowing to the east;

(iii) a recirculation system flowing predominantly to the west;

(iv) a mid-ocean circulation dominated by closed circulation systems which, at this stage, is qualitatively similar to the traditional Svendrup interior.

Although there are no eddies yet, the ocean should start shedding them from about 400th day; according to Holland (1978). The features of our solution agree well with the average pattern of Holland's results. Therefore, we assume that the logic of our model is correct.

The next computation, Exp. 2, differs from the previous one in that no-slip boundary conditions are used on the solid

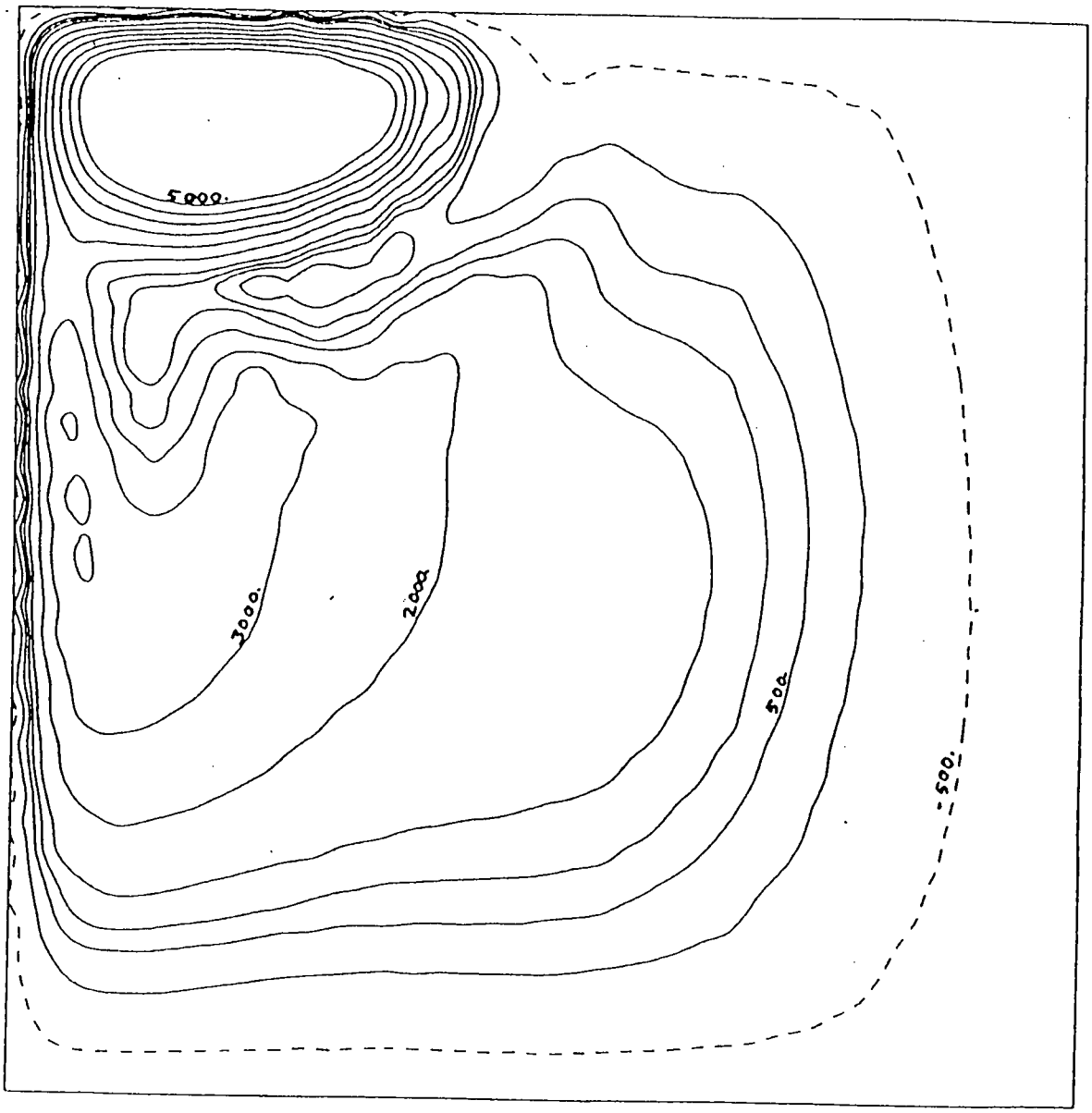

Fig.4.

Stream Function Distribution 1st Layer
(CI 500 $m^2 s^{-1}$)

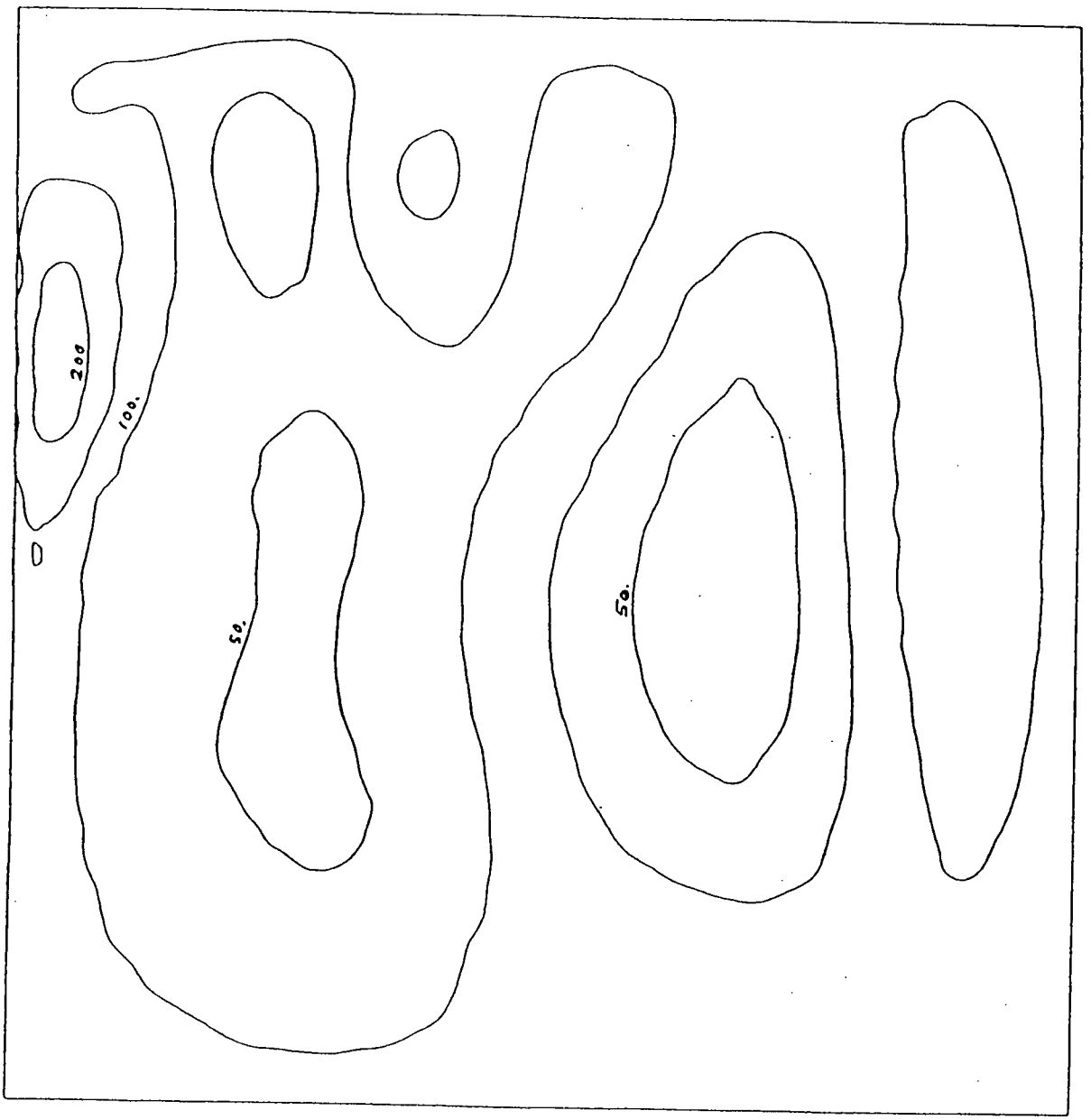

Fig. 5
Stream Function Distribution 2nd Layer
(CI 50 $m^2 s^{-1}$)

boundaries. Insofar as the author's knowledge is concerned, no experiment with a baroclinic ocean and such boundary condition has been reported. Figures 6 and 7 show the upper and lower layer stream function patterns after 200 days of integration. The dominant features of Figure 6 are:

(i) a western boundary;

(ii) a separation of the flow from the western boundary past the point of maximum amplitude of wind stress;

(iii) the entry of the flow to the interior via undulations;

(iv) a mid-ocean circulation dominated by a circulation system in Sverdrup balance.

The differences between this pattern and that of Exp. 1 are the absence of the northwest recirculation and the separation of the flow from the westen boundary.

The flow pattern of the first layer in Exp. 2 is very similar to that of the Bryan (1963) barotropic ocean with comparable Re and Ro and no-slip boundary condition on the West and East boundaries.

The undulations of the stream function in the north-western part of the basin are more conspicuous in the vorticity plots shown in Figure 8.

Results of the symmetric two-gyre experiment with no-slip boundary condition are shown in Figures 9 to 11; they represent upper and lower layers stream function distributions at instants T = 130 days, 300 days and 400

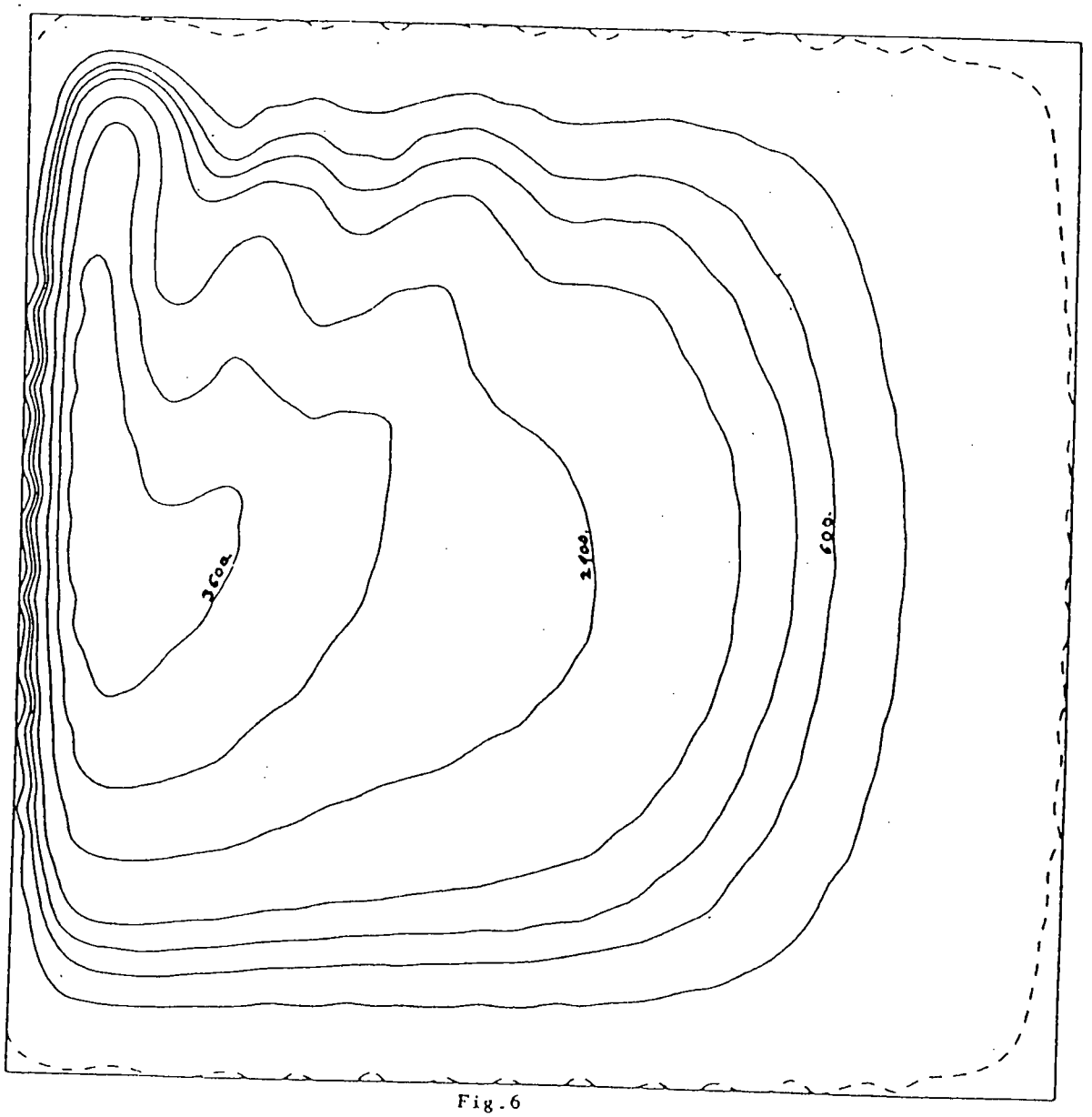

Fig.6

Stream Function Distribution 1st Layer
(CI 600 m' s^{-1})

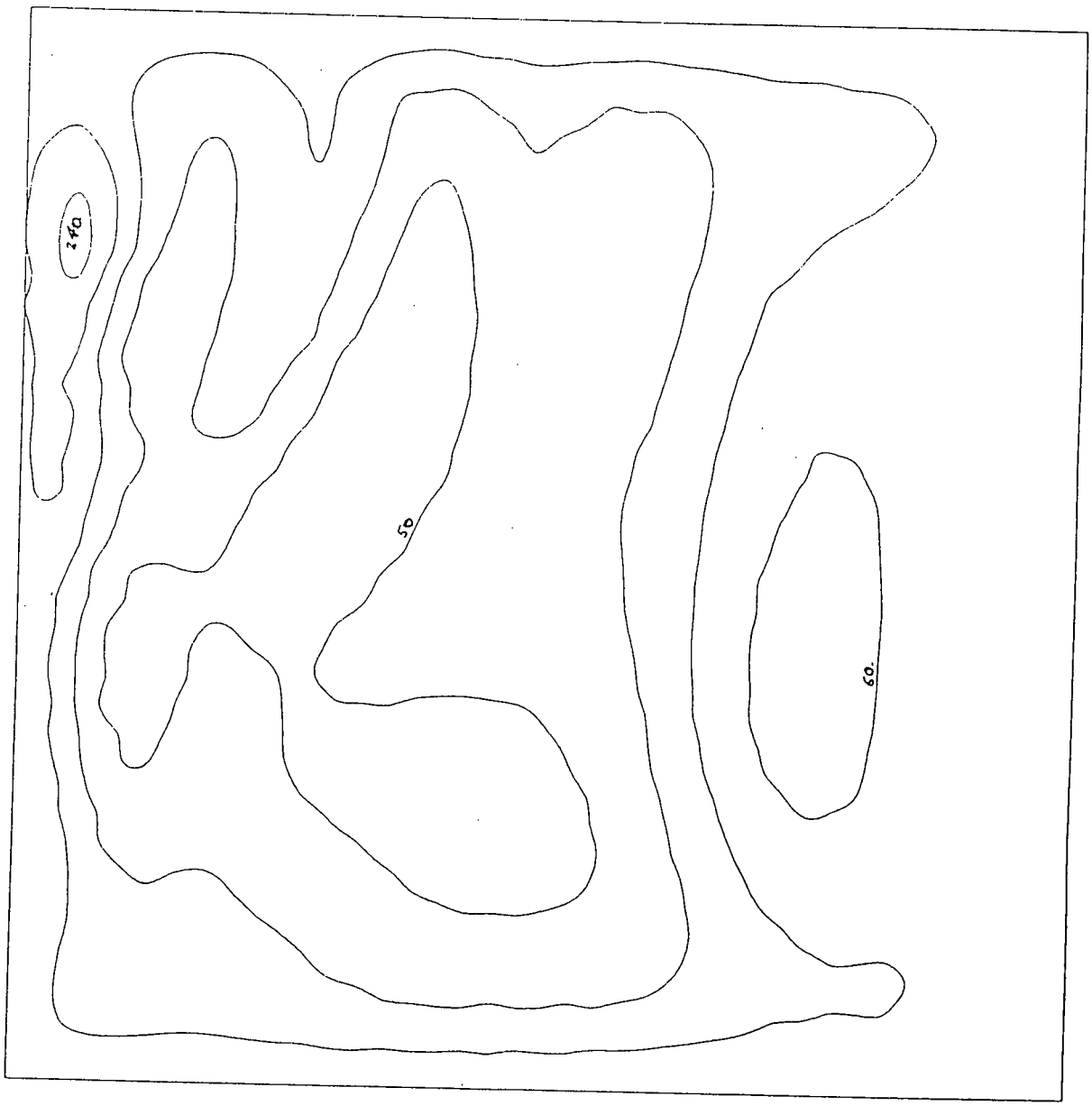

Fig. 7

Stream Function Distribution 2nd Layer
(CI 60 $m^2 s^{-1}$)

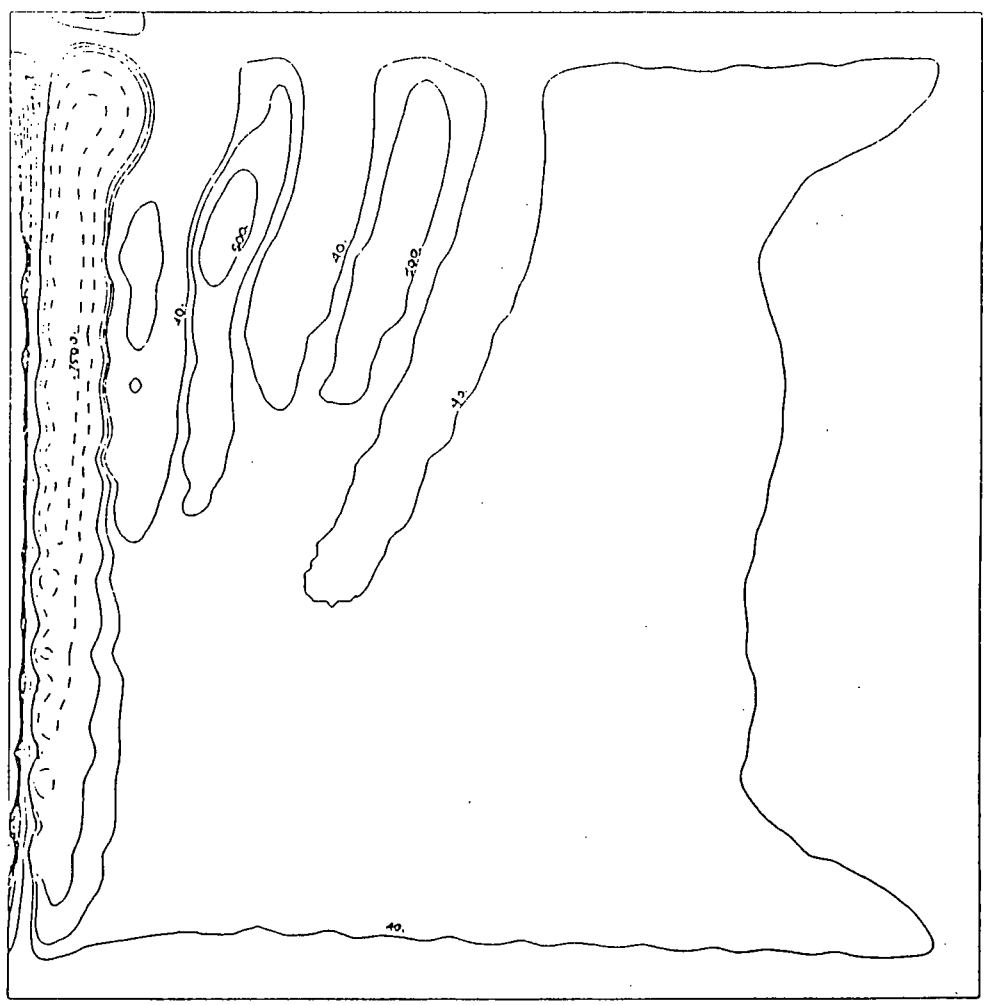

Fig.8

Vorticity Distribution 1st Layer (CI x $10^{-8} S^{-1}$)

days, respectively. We observe the absence of the upper layer free jet at mid-latitude which is a characteristic feature when free-slip boundary condition is applied with the same A_H and wind stress distribution (Holland and Lin (1975). This fact is due to the separation of the flow from the western boundary.

The circulation of the upper layer is established at T = 130 days and from that instant on there exists a balanced boundary layer-interior Sverdrup pattern even when the ocean is being spun up as Figs. 15 (kinetic energy per unit of area of the upper layer) and 16 (stream function at x = 700 km, y = 390 km) show. This circulation pattern is indicative of the barotropicity of the regime of the first layer. As for the lower layer, it takes longer to reach a regular pattern, which is similar to that of the upper layer out of the lower southern/upper northern corners of the channel where an eddy is setting up. This eddy, which matches with the upper/lower interior dynamics, stays at the same location and increases its intensity at the same rate of the boundary layer circulation. The eddy region is just below the region of the upper layer where the western boundary is more inertial. We have not attempted to provide a theoretical analysis of the eddy dynamics because our analytical approach is able to explain the boundary layer-Sverdrup interior of the lower layer as well as the upper layer dynamics.

The lower layer gyres are displaced poleward in agreement with empirical observations, Rhines and Young(1980).

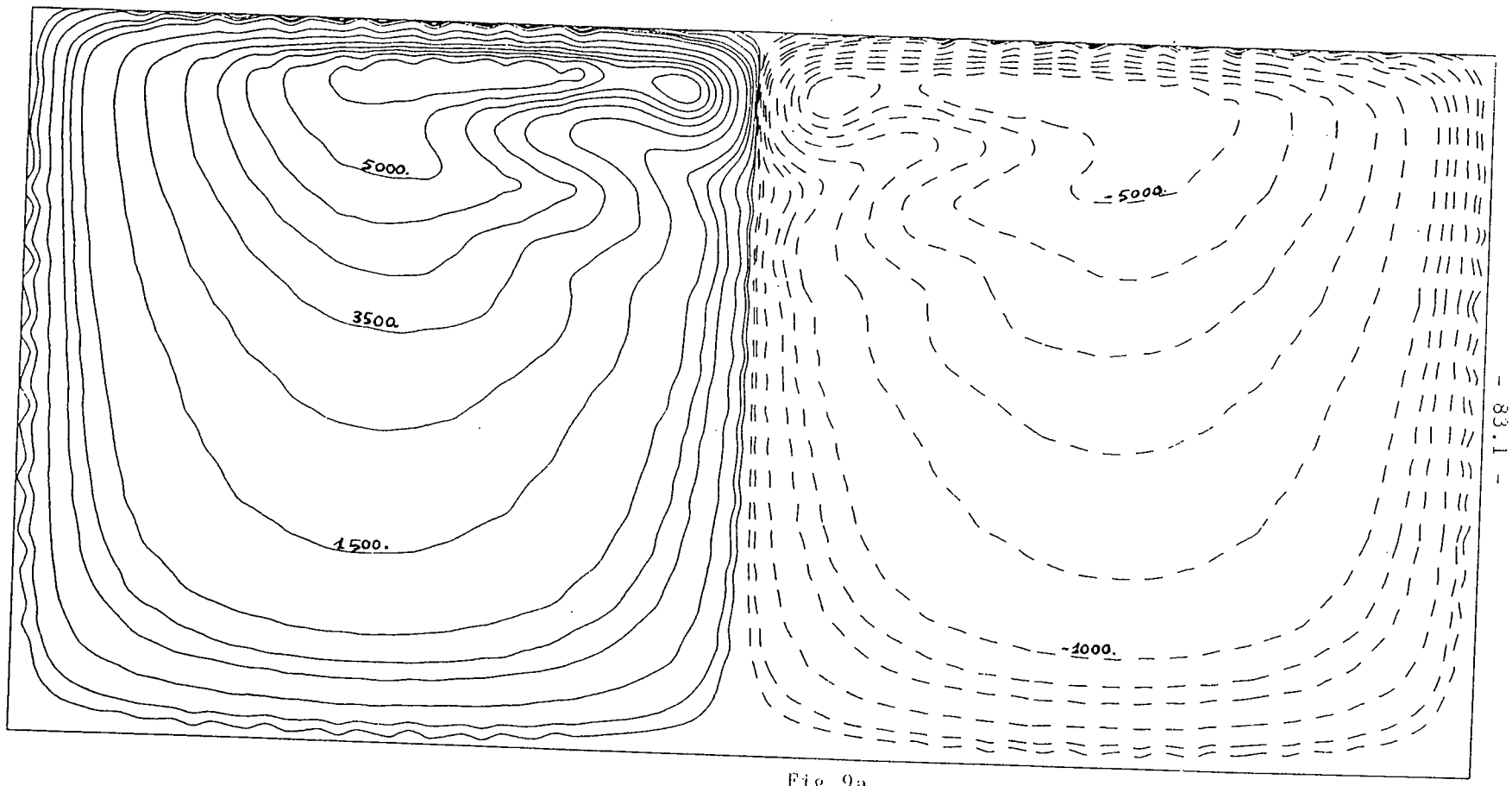

Fig 9a

Stream Function Distribution 1st Layer
(C.I. ± 500 $m^2 s^{-1}$, ± 100 $m^2 s^{-1}$). T = 130 days

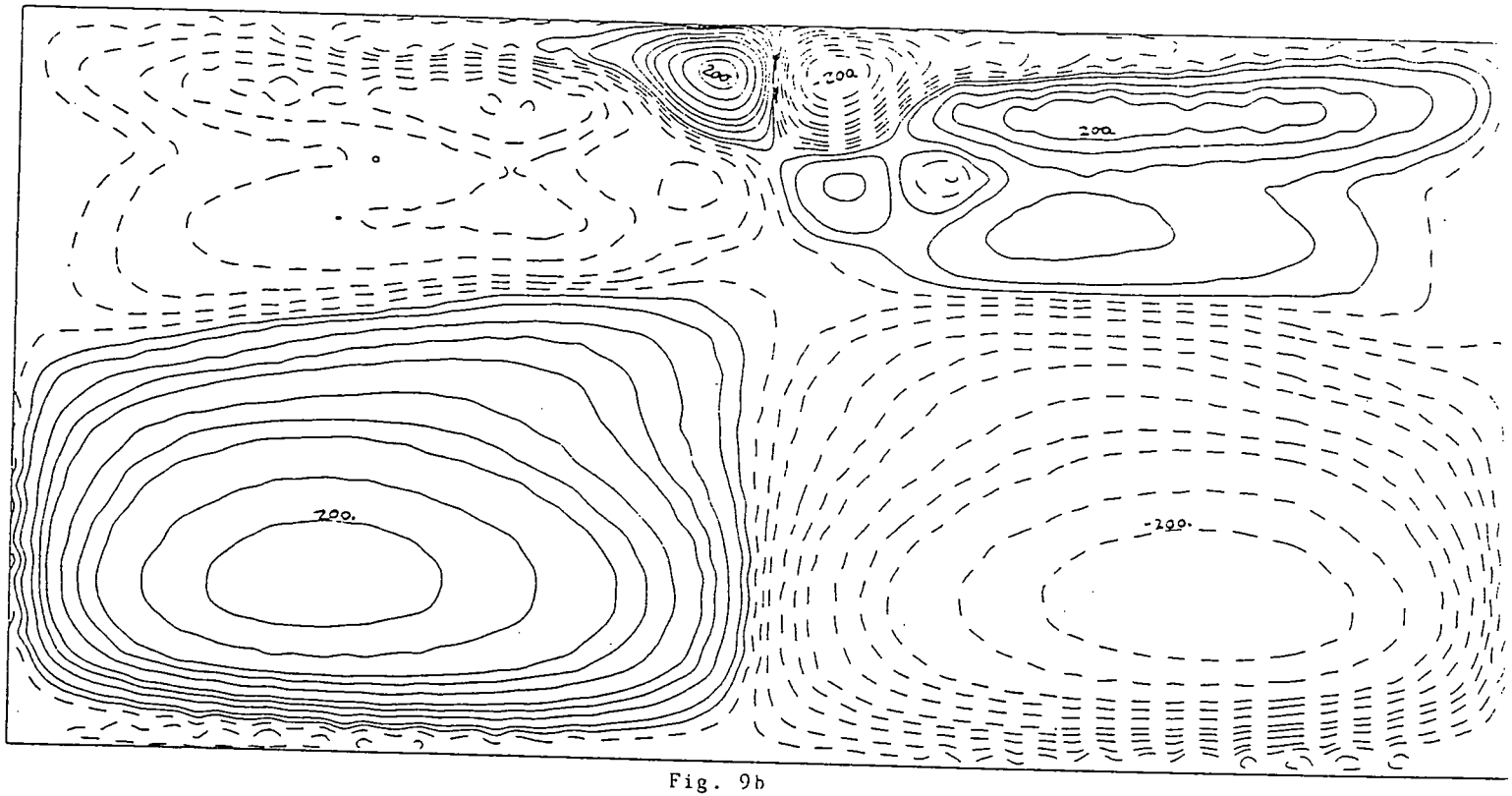

Fig. 9b

Stream Function Distribution 2nd Layer
C.I.± 50 m^2 s^{-1}, ± 10 m^2 s^{-1} T=130 days

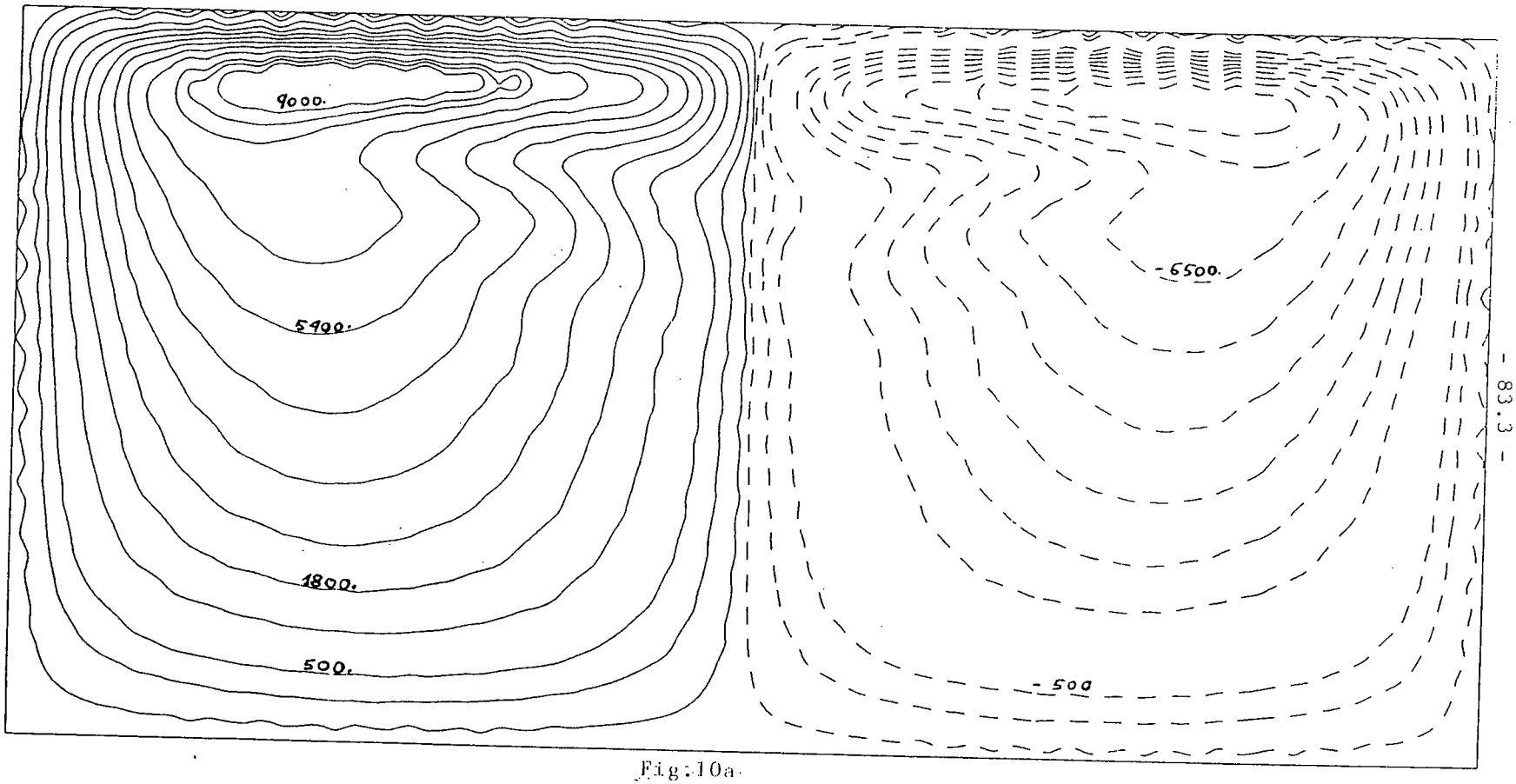

Fig.10a

Stream Function Distribution 1st Layer

(C.I. ± 900 $m^2 s^{-1}$) T = 300 days

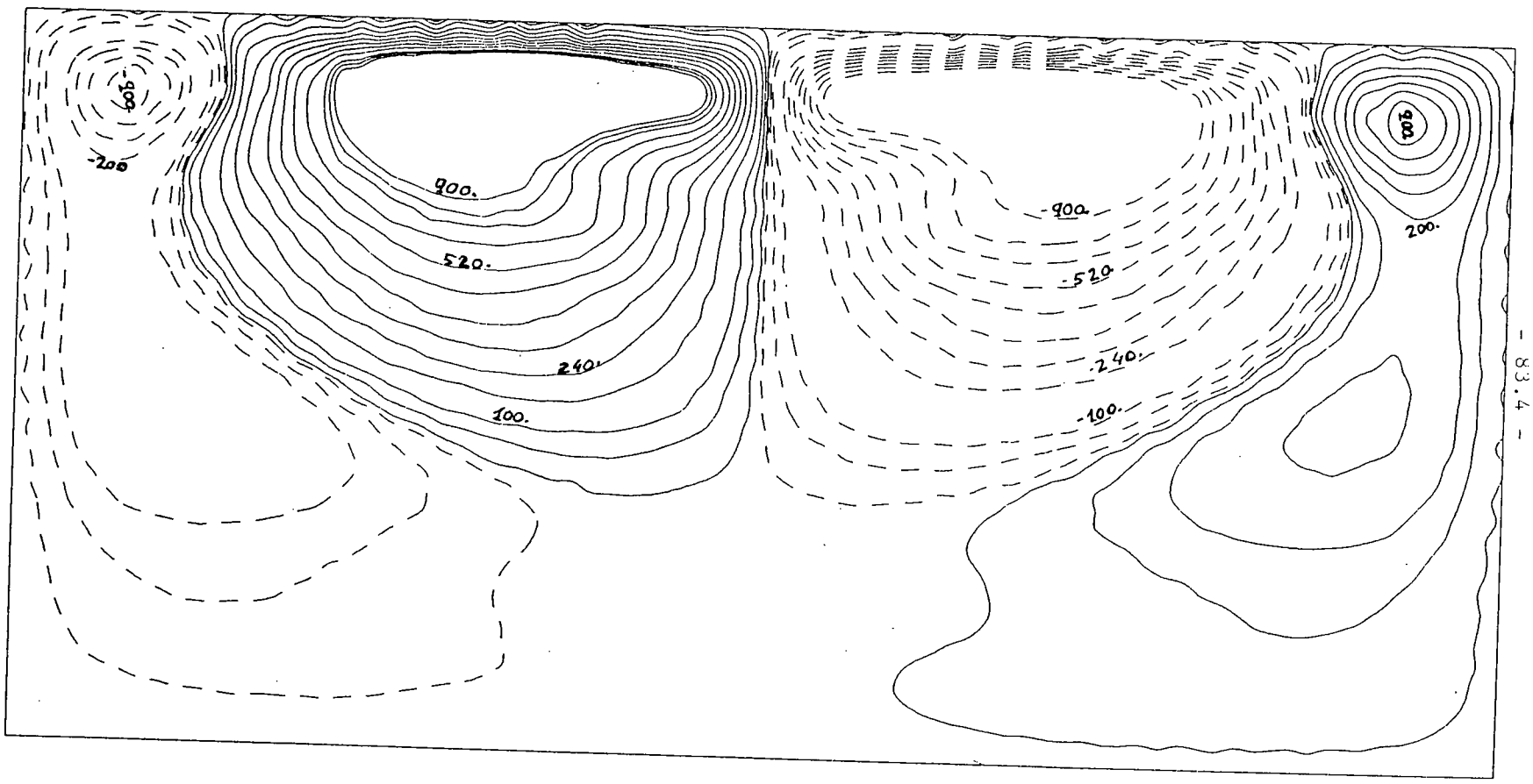

Stream Function Distribution 2nd Layer
(C.I. 70 m^2 s^{-1}) T = 300 days

Fig. 10b

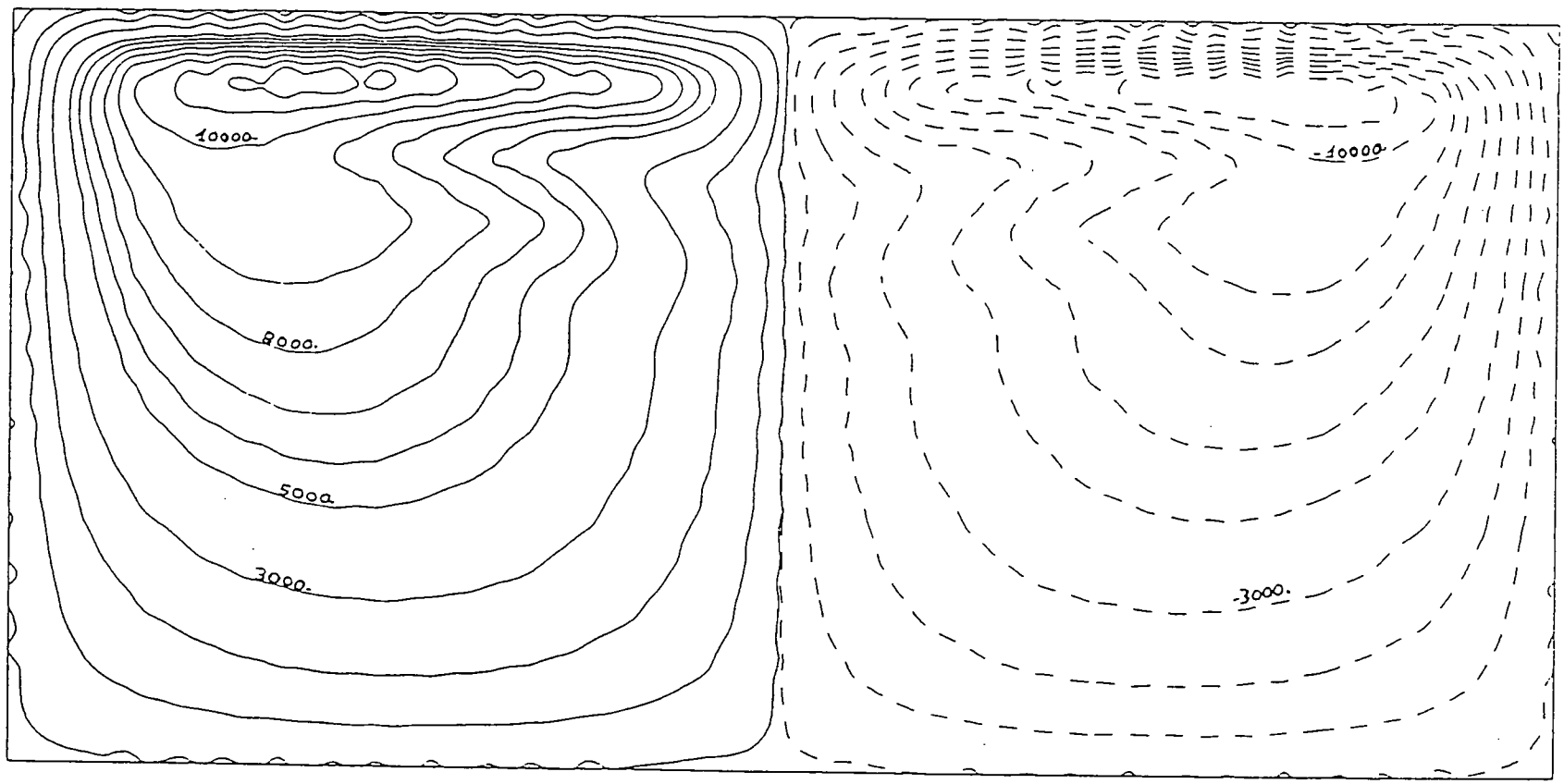

Stream Function Distribution 1st Layer
(C.I. 1000 $m^3 s^{-1}$) T = 400 days

Fig. 11a

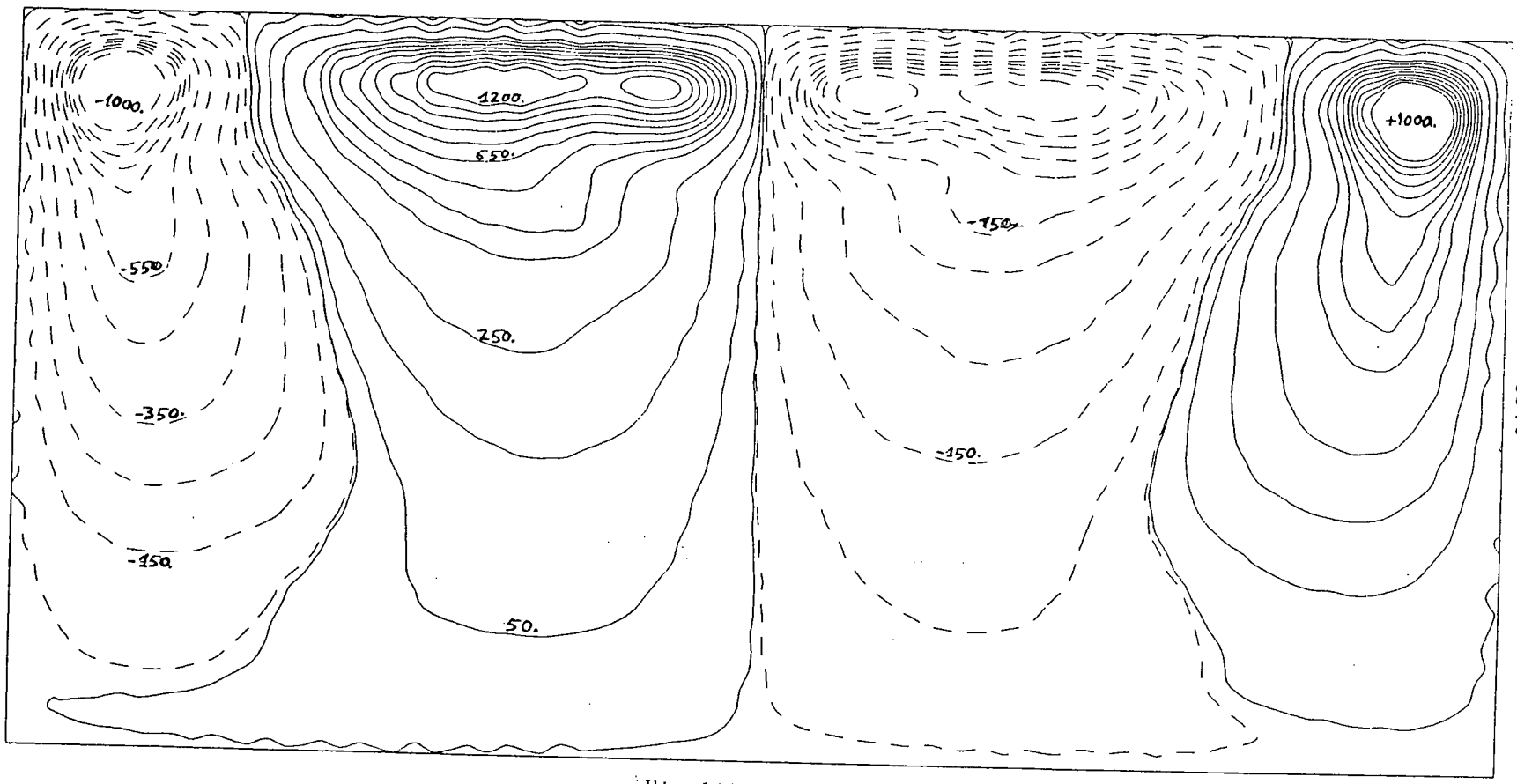

Fig.11b

Stream Function Distribution 2nd Layer
(C.I. 100 m^2 s^{-1}) T = 400 days

The numerical results for both upper and lower layers can be conceptually explained by Stewart's (1964) arguments. In the western boundary layer the relative vorticity is zero before the current reaches the separation point; but the wind stress inputs clockwise relative vorticity and the fluid has no relative vorticity when it enters in the boundary layer. Thus, the only possibility is for counter-clockwise vorticity to form at the boundaries and to diffuse into the current laterally. Further north of the separation point, and as long as the interior circulation is in Sverdrup balance, the stream lines turn seaward, but the relative vorticity in the interior of the ocean is negligible, so the water which leaves the boundary to re-enter the interior has to cancel its relative vorticity by a new mechanism. This new mechanism is the undulations of the stream functions which dissipate either positive or negative relative vorticity coming out from the boundary layer. Thus, the role of the undulations is to allow time for the excess of the relative vorticity to be dissipated before the boundary flow matches the interior one. Figures 12 to 14 show the adjustment of the relative vorticity. If the flow is such that the dissipative terms are larger than the inertial ones, then the cancellation of boundary vorticity will be faster and, hence, the undulating re-entry will be less conspicuous, or, in the absence of non-linearities, there will not be such a re-entry at all (Munk's dynamics). Now, upon comparing the pattern

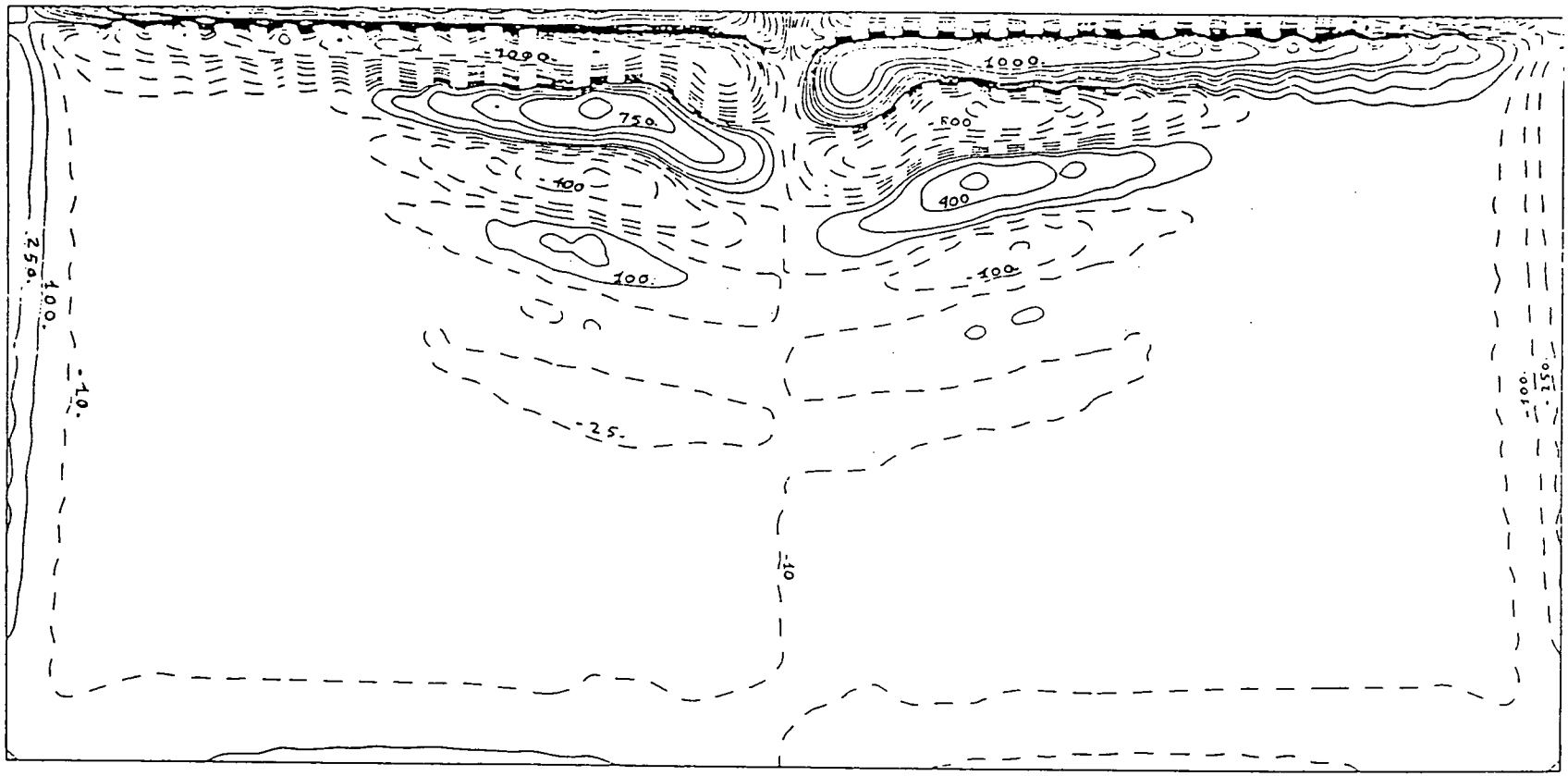

Fig. 12

Vorticity Distribution 1st Layer

T = 130 day (CI = $10^{-8} s^{-1}$)

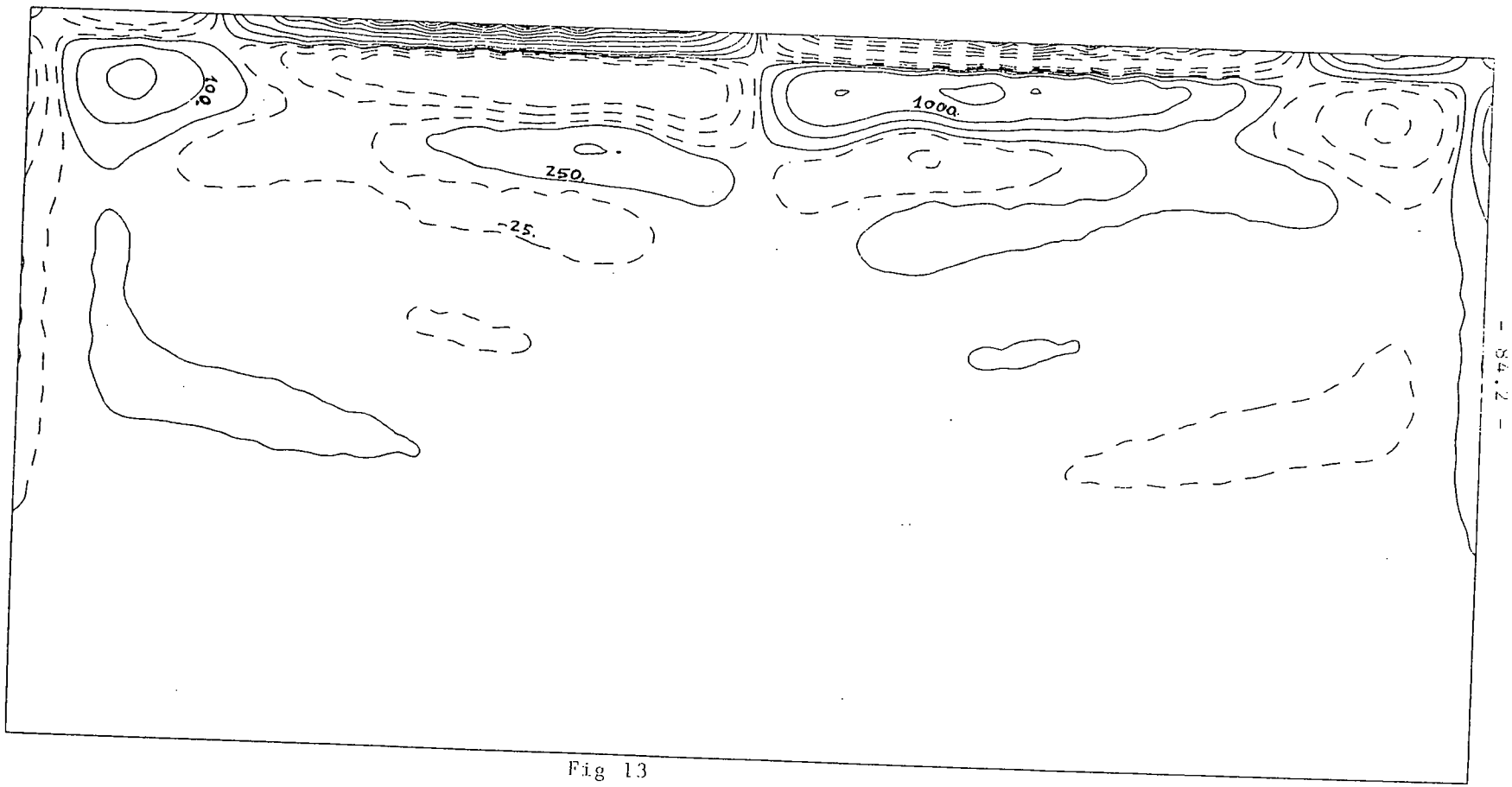

Fig 13

Vorticity Distribution 1st Layer
T = 300 days (CI x 10^{-6} S^{-1})

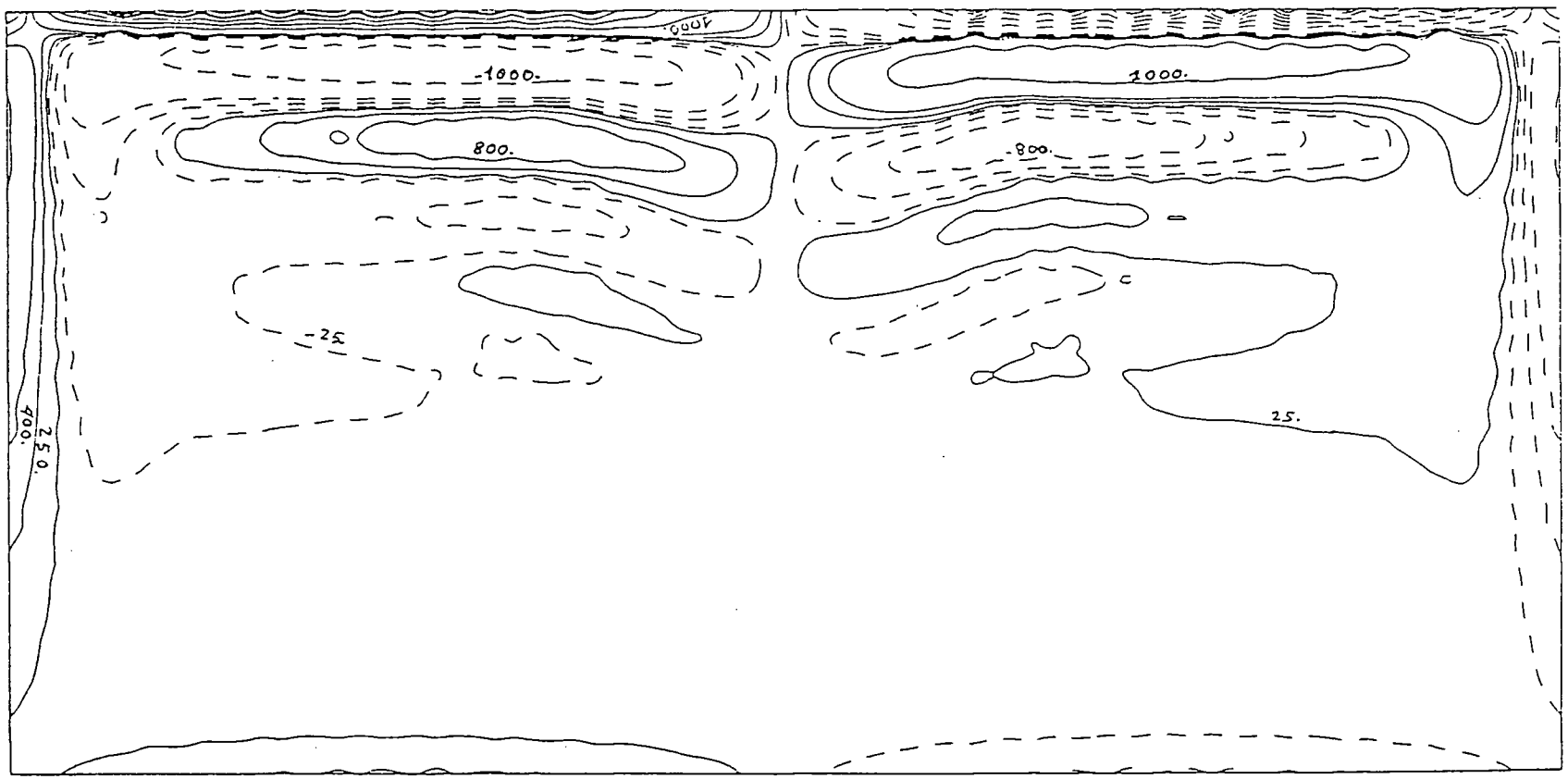

Fig.14

Vorticity Distribution 1st Layer
T = 400 days (CI x 10^{-8} S^{-1})

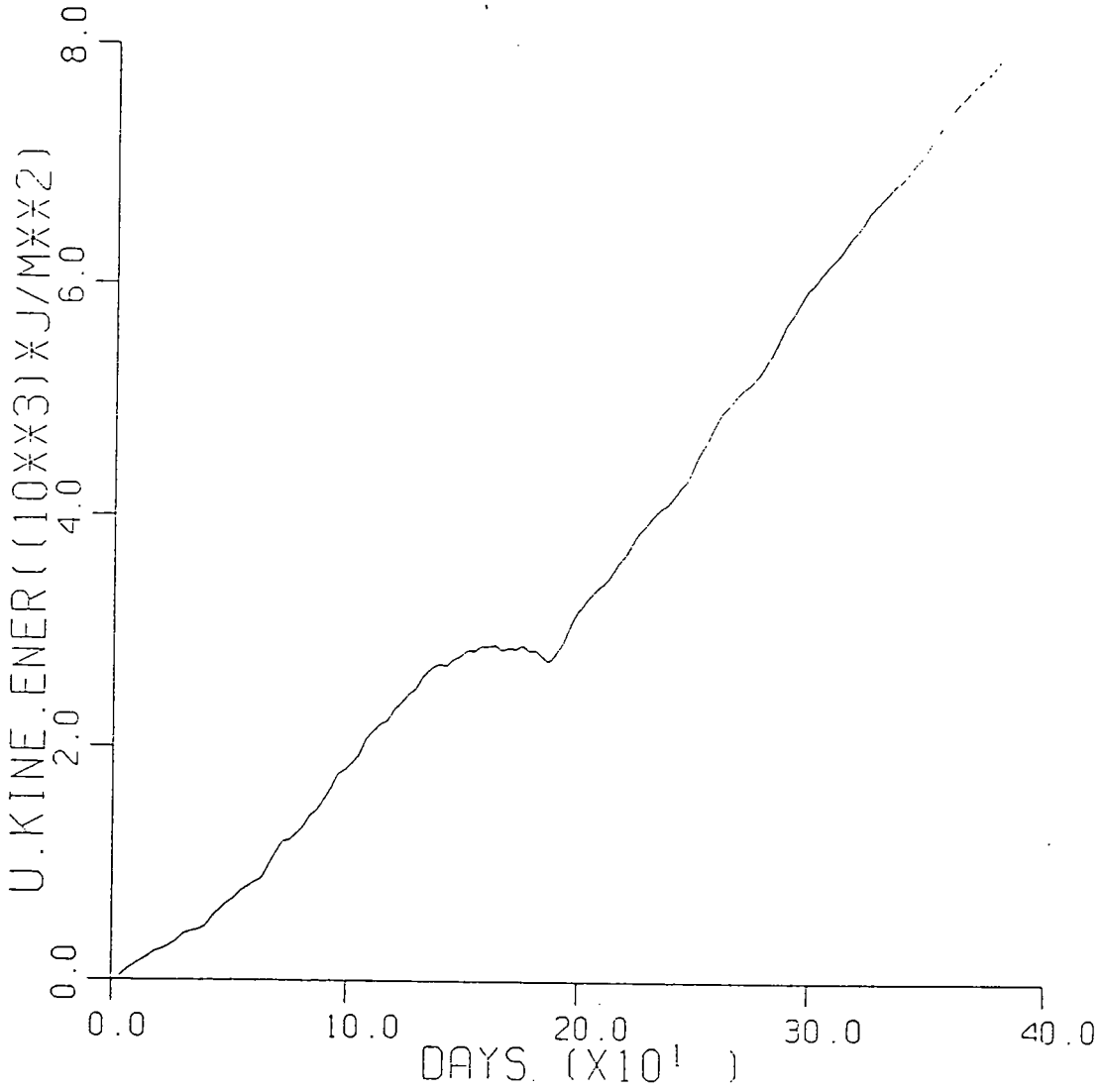

Fig.15.

Kinetic Energy per unit of area of the upper layer. Exp.3.

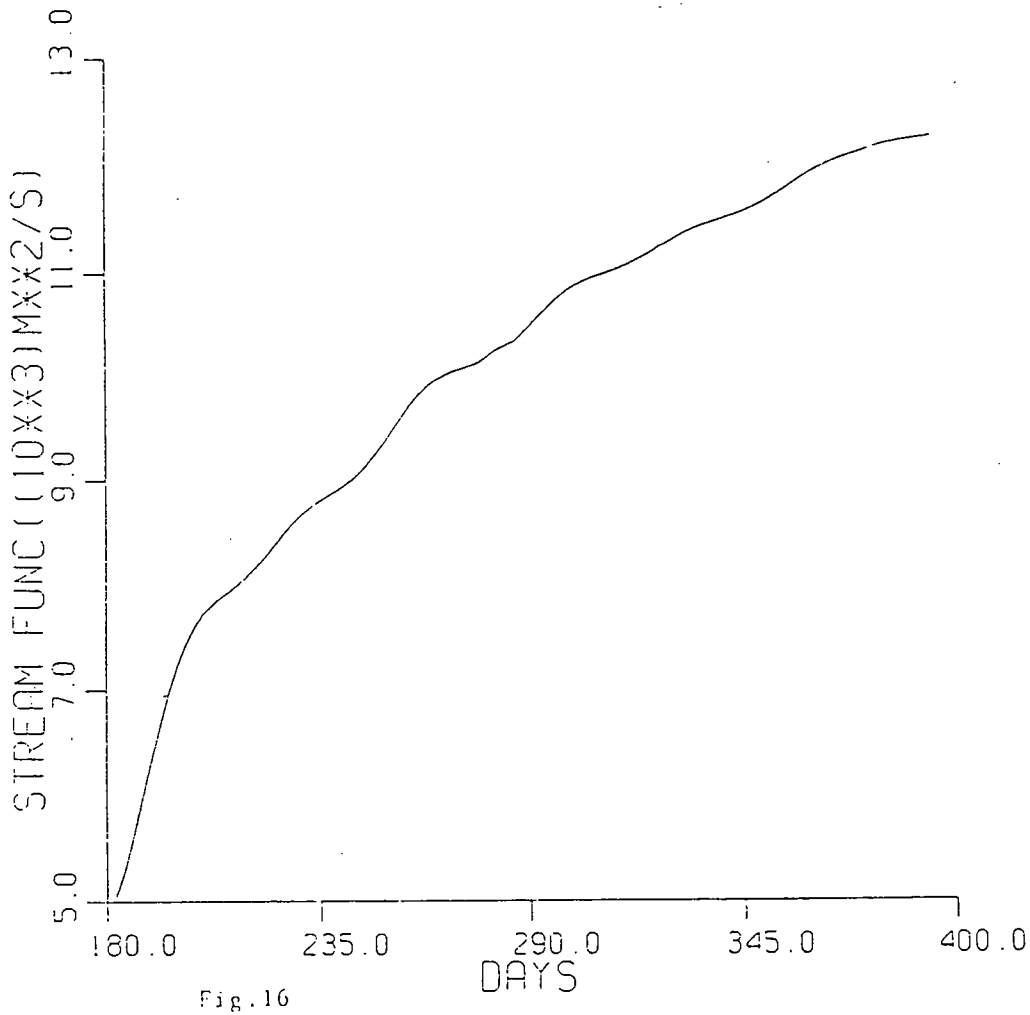

Fig.16

Plot of the Time Series of the Upper Stream Function at (x=100 Km,y=390 Km)

of the lower layer with that of the first layer (Figs. 10-11) we see that the former has more of a dissipative character; this is so because the driven mechanism of the second layer is the weak vortex stretching term while the coefficient A_H is the same at both layers. On the other hand, the circulation pattern of the first layer resembles the eddy-free patterns reached by barotropic models which have the same Re and Ro. Bryan (1963) and Ierley and Young ((1986), private communication). In the next section, we describe an analytical model to interpret the numerical results.

4.3 Theoretical Analysis

In the last section we have discussed the results of our experiments, emphasizing those results of Exp. 3. Our purpose now is to describe an analytical method to explain the main features of Exp. 3 and to isolate the mechanisms that control the dynamics when the no-slip boundary condition is imposed. Specifically, we wish to clarify the roles played by the western boundry layer and the stratification.

Let us write the continuum equations of the first and second layers in terms of the potential vorticities, q_1, q_2 as

$$q_{1t} = J(q_1, \psi_1) + A_H \nabla_H^2 \zeta_1 + \frac{\text{curl } \tau}{H_1}$$

$$q_{2t} = J(q_2, \psi_2) + A_H \nabla_H^2 \zeta_2 - \varepsilon \nabla_H^2 \psi_2, \qquad (4.1a,b)$$

where

$$q_1 = \nabla_H^2 \psi_1 + f + F_1 (\psi_2 - \psi_1),$$

$$q_2 = \nabla_H^2 \psi_2 + f + F_2 (\psi_1 - \psi_2), \qquad (4.2a,b)$$

$$F_1 = \frac{f_0^2}{g'H_1}, \qquad F_1 = \frac{f_0^2}{g'H_2}, \qquad (4.3)$$

We form the equation for the barotropic mode, viz.,

$$\psi_B = \frac{H_1 \psi_1 + H_2 \psi_2}{H},$$

by adding $\frac{H_1}{H}$ (4.1a) to $\frac{H_2}{H}$ (4.2b). Thus,

$$\frac{\partial \zeta_B}{\partial t} = \frac{1}{H} \{H_1 J(\zeta_1, \psi_1) + H_2 J(\zeta_2, \psi_2)\} - \beta \frac{\partial \psi_B}{\partial x}$$

$$- A_H \nabla_H^2 \zeta_B - \frac{H_2}{H} \varepsilon \nabla_H^2 \psi_2 + \frac{\text{Curl } \tau}{H}, \qquad (4.4a)$$

$$\zeta_B = \frac{H_1 \zeta_1 + H_2 \zeta_2}{H}. \qquad (4.4b)$$

Note that the vortex stretching terms, $\pm F_i(\psi_1 - \psi_2)$ have cancelled. In the Sverdrup interior, outside the frictional western boundary layer, the Jacobian and fractional terms can be neglected. Although the ocean is still spinning up, Figs. 9-11 show that there is a balance between planetry vorticity and the curl of wind stress in the interior of the ocean

so we can neglect $\frac{\partial \zeta_B}{\partial t}$ there. Hence, the equation in the interior is

$$\beta \frac{\partial \psi_B}{\partial x} = \frac{\text{curl } \tau}{H}, \quad \delta \leq x \leq L_x, \tag{4.5}$$

where δ denotes the width of the western boundary layer.

The solution of (4.5) is

$$\psi_B = \Phi_B \, f(y) \, (1 - \frac{x}{L_x}), \tag{4.6}$$

where

$$\Phi_B = - \frac{L_x \, \pi \, \tau_0}{H \, \beta \, L_y},$$

$$f(y) = \sin (\frac{\pi y}{L_y}), \tag{4.7}$$

The potential vorticity of the second layer in the Sverdrup interior is written in terms of ψ_B and ψ_2 as

$$q_{2,I} = f + F^* \, (\psi_B - \psi_2),$$

$$F^* = \frac{H}{H_1} F_2 \, . \tag{4.8}$$

Using (4.8) one can write (4.1b) in the Sverdrup interior as

$$J(q, \psi_2) + O(A_H, \varepsilon) = 0, \tag{4.9a}$$

where

$$q = f + F^* \psi_B \tag{4.9b}$$

represents the geostrophic contours of the second layer. Use has been made of the identity $J(\psi_2, \psi_2) = 0$ to obtain (4.9a) upon substituting (4.8) into (4.1a).

The solution of (4.9) up to zero order is

$$\psi_2 = G(q). \tag{4.10}$$

The geostrophic contours q will close in the northwest part of the basin if

$$\beta y - \frac{F^* \pi \tau_0}{H\beta} < 0,$$

or

$$\gamma = \frac{F^* \pi \tau_0}{H \beta^2 L_y} > 1 \tag{4.11}$$

In our experiments: $\tau_0 = 10^{-4}$, $F^* = 6.25 \times 10^{-10}$, $Ly = 10^6$ m, $H = 10^5$ m and hence $\gamma = 0.2$. Thus the geostrophic contours should not close. However, there exist closed streamlines $\psi 2$ that go through a western boundary layer and other ones that exhibit eddy nature. Rhines and Young (1982) and Young and Rhines (1982) show, by application of the Batchelor-

Prandtl theorem, that inside the closed geostrophy contours the potential vorticity is homogenized whereas outside such contours the whole region is threaded by geostrophic contours that hit the eastern boundary where $\psi_2 = 0$. It is this boundary condition that forces the function G of (4.10) to be identically zero. The parameter γ is greater than 1.0 if either the forcing τ_0 is strong enough or $F^* \ll 1$ or both together. Homogenization of potential vorticity arguments require the existence of frictional forces, no matter how weak they are, with no additional hypothesis on the existence of western boundary layers. Indeed, Young and Rhines (1982) close their theory by appending a western boundary layer in the classic sense. Ierley and Young (1983) show, however, that the presence of a Stommel frictional boundary layer type prevents the homogeneization of the potential vorticity inside the closed geostrophic contours of the second layer.

In our numerical experiments, the value of F^* is so small that we can consider $q = \beta y + 0(F^*)$ in the interior while the existence of a weak lower layer flow ($\psi_2 \neq 0$) must be due to the action of the weak vortex stretching terms and the eddies that have just started setting up in the lower left corner of the second layer. However small this flow is, the presence of a western boundary layer, where relative vorticity is generated, is so influential on the overall circulation that there are closed stream functions ψ_2 going

through the boundary layer and returning well into the interior, in contraposition to RY theory. This feature will be dominant on the lower layer dynamics (at least in the range of parameters we use and with the non-slip boundary condition) even in the presence of eddies.

To proceed further in our analysis, let us write the equation for the baroclinic mode Ψ. Since $\Psi = \psi_1 - \psi_2$, substracting (4.1b) from (4.1a) yields

$$F_1 J(\psi_1, \psi_2) - F_2 J(\psi_1, \psi_2) + \beta \frac{\partial}{\partial x}(\psi_1 - \psi_2)$$
$$= A_H \nabla_H^2 (\zeta_1 - \zeta_2) + \varepsilon \nabla_H^2 \psi_2^2 + \frac{\text{curl } \tau}{H_1}, \qquad (4.12)$$

where the $\frac{\partial}{\partial t}$ terms have been ignored.

To study the Sverdrupean dynamics of (4.12), we again assume that the relative vorticity is very small in the interior. The dimensional arguments such as

$$\psi_1 = U_1 L \psi_1^*$$

$$\psi_2 = U_2 L \psi_2^*$$

where $U_2 < 0$ $(\frac{H_1}{H} U_1)$ and parameter values

$$F_2 = 1.25 \times 10^{-10}, \quad F_1 = 5 \times 10^{-10}$$

lead to

$$F_1 U_1 \frac{\partial \Psi}{\partial x} + \beta \frac{\partial \Psi}{\partial x} \approx \frac{\text{curl } \tau}{H_1} + O(F_2 J(\psi_1, \psi_2)) + O(A_H, \varepsilon). \qquad (4.13)$$

Hence, the interior dynamics of the baroclinic mode is similar to the first layer dynamics. We should point out that for larger values of F_1 and F_2 (that is, increasing the strength of the vortex stretching terms by improving the vertical resolution of the model), the character of the interior dynamics of the few first baroclinic modes as well as of the upper layers would be less of Sverdrup type and more non-linear. The solution of (4.13) up to first order in $(\frac{F_1 U_1}{\beta})$ is:

$$\Psi = \Omega \left(1 - \frac{x}{L_x}\right) f(y) \tag{4.14}$$

$$\text{where } \Omega = - \frac{L_x \pi \tau_0}{H_1 \beta L_y} \left(1 - \frac{F_1 U_1}{\beta}\right) + 0 \left(\frac{F_1 U_2}{\beta}\right) + 0 (A_H, \varepsilon) \tag{4.15}$$

and $f(y)$ is given by (4.7b).

Since ψ_2 is given in terms of the baroclinic and barotropic modes as

$$\psi_2 = \psi_B - \frac{H_1}{H} \Psi$$

$$\psi_1 = \psi_B + \frac{H_2}{H} \Psi \tag{4.16}$$

then from (4.15), (4.6), and (4.16) one obtains the following expression of ψ_2 in the interior.

$$\psi_{2,I} = - \frac{F_1 U_1}{\beta} \frac{L_x \pi \tau_0}{H\beta L y} (1 - \frac{x}{L_x}) \sin (\frac{\pi y}{L_y}). \qquad (4.17a)$$

Analogously,

$$\psi_{1,I} = -\frac{L_x \pi \tau_0}{H_1 \beta L y} (1 - \frac{x}{L_x}) \sin(\frac{\pi y}{L_y}). \qquad (4.17b)$$

This expression yields a circulation in the second layer that is, at least, 1/13 times weaker than that in the first layer and with the same sinusoidal pattern. Both features are qualitatively confirmed by the numerical experiments except in the left lower/upper corners where eddies are setting up with intensity greater than $\psi_{2,I}$. See Figs. 10b and 11b.

4.3.1 Boundary Layer Equations

In this subsection, we confirm analytically the features exhibited by the upper and lower flows in the western boundary layer. As pointed out previously, we believe that Stewart's arguments about the role of the relative vorticity in the western boundary are able to explain conceptually the features of the numerical experiments. Our approach to examining the behaviour of the non-linear terms of the equations (4.1a,b) in the presence of lateral friction will

be in the line of Moore's (1963) heuristic model of a damped stationary Rossby wave supported by the eastward efflux from the western boundry. Although such a model is asymptotically correct at the outer edge of the boundary layer and agrees with Munk's model when the boundary layer Reynolds number tends to zero, it has the deficiency of replacing the tangential and normal advection of relative vorticity by the normal advection of relative vorticity at the outer edge of the layer. This shortcoming can be explained by the main hypothesis of the boundary layer theory, i.e.,

$$\frac{\partial}{\partial x} \gg \frac{\partial}{\partial y}$$

and by the lack of knowledge of the structure of the u-component of the velocity within the boundary layer. Similar criticism can be made of the inertial theories of the western boundary dynamics.

As we have already pointed out in Section 4.1, the structure of the western boundary in our experiments is a blend of inertial and Munk's boundary layer types. The Stommel layer is relatively unimportant so we neglect in the sequel the bottom friction terms. Our analysis assumes that the time dependence of the variables is inconsequential for the structure of the boundary layer because the eddy viscosity coefficient A_H is so large that we allow enough

time for the existence of a balance among the generation, advection and dissipation of relative vorticity in the boundary layer at any instant. Taking for granted that $\frac{\partial}{\partial x} \gg \frac{\partial}{\partial y}$ within the boundary layer we write (4.1) as

$$\frac{U_1}{\beta}\left(\frac{\partial^3 \psi_1}{\partial x^3}\right) + \frac{\partial \psi_1}{\partial x} + \frac{U_1 F_1}{\beta} \frac{\partial \psi_2}{\partial x} = \frac{A_H}{\beta} \frac{\partial^4 \psi_1}{\partial x^4} + \left\langle \frac{\text{curl } \tau}{\beta H_1} \right\rangle,$$

$$\frac{U_2}{\beta}\left(\frac{\partial^3 \psi_2}{\partial x^3}\right) + \frac{\partial \psi_2}{\partial x} + \frac{U_2 F_2}{\beta} \frac{\partial \psi_1}{\partial x} = \frac{A_H}{\beta} \frac{\partial^4 \psi_2}{\partial x^4}, \qquad (4.18a,b)$$

where we have replaced $\frac{\partial \psi_i}{\partial y}$ by $- U_i(x,y)$, $(i = 1,2)$, which are the interior velocities in the upper and lower layers. It is consistent with the interior field flow to assume also that in the boundary layer $\psi_1 > \psi_2$.

Since $\frac{U_1 F_1}{\beta} \approx 0(10^{-1})$ and $\frac{U_2 F_2}{\beta} \approx 0(10^{-2})$, in our experiments, then we can approximate (4.18a,b) as

$$\frac{U_1}{\beta}\left(\frac{\partial^3 \psi_1}{\partial x^3}\right) + \frac{\partial \psi_1}{\partial x} = \frac{A_H}{\beta} \frac{\partial^4 \psi_1}{\partial x^4} + \left\langle \frac{\text{curl } \tau}{\beta H_1} \right\rangle$$

$$+ \frac{U_1 F_1}{\beta} \frac{\partial \psi_2}{\partial x} = 0 \quad \left(\frac{U_1 F_1}{\beta} \frac{\partial \psi_2}{\partial x}\right),$$

$$\frac{U_2}{\beta}\left(\frac{\partial^3 \psi_2}{\partial x^3}\right) + \frac{\partial \psi_2}{\partial x} + \frac{U_2 F_2}{\beta} \frac{\partial \psi_1}{\partial x} = \frac{A_H}{\beta} \frac{\partial^4 \psi_2}{\partial x^4}. \qquad (4.19a,b)$$

The symbol $\langle\ \rangle$ means that the curl τ is not an active term of (4.19a).

The above equations show that up to order $0\ (\frac{U_1 F_1}{\beta} \frac{\partial \psi_2}{\partial x})$ the upper layer is uncoupled from the lower one, but it is not obvious that the lower layer be independent of the upper one because we do not know yet the relative magnitude of the term $\frac{U_2 F_2}{\beta} \frac{\partial \psi_1}{\partial x}$ with respect to the terms of (4.19b). Thus, let us consider as tentative the following scaling scheme:

Upper Layer

$$L_{1B} = (U_1/\beta)^{1/2} ,$$

$$x = L_{1B} X,$$

$$\psi_1 = U_1 L_{1B} \psi_1^*, \qquad (4.20a)$$

Lower Layer

$$L_{2B} = (U_2/\beta)^{1/2},$$

$$x = L_{2B} X,$$

$$\psi_2 = U_2 L_{2B} \psi_2^* \qquad (4.20b)$$

L_{1B} and L_{2B} are the inertial boundry layer widths of the upper and lower layers, respectively. Typical values of L_{1B} in our experiments are L_{1B} = 28 km, L_{2B} = 14 km. The non-dimensional equations are (dropping asterisks)

$$\frac{\partial^2 \psi_1}{\partial X^3} + \frac{\partial \psi_1}{\partial X} = \frac{1}{Re_1} \frac{\partial^4 \psi_1}{\partial X^4} + O(\ ),$$

$$\frac{\partial^3 \psi_2}{\partial X^3} + \frac{\partial \psi_2}{\partial X} + \frac{F_2\ U_1\ L_{1B}}{\beta\ L_2 B} = \frac{1}{Re_2} \frac{\partial^4 \psi_2}{\partial X^4} + O(\ ), \qquad (4.21a,b)$$

where

$$Re_1 = \frac{U_1^{3/2}}{A_H\ \beta^{1/2}},$$

and $$Re_2 = \frac{U_2^{3/2}}{A_H\ \beta^{1/2}}, \qquad (4.22a,b)$$

are the boundary layer Reynolds numbers in the first and second layers, respectively. In order to know whether the scaling scheme (4.20a,b) yields a system of uncoupled equations, we have to verify that the third term of the left-hand side of (4.21b) is much smaller than the other terms of the equation; this is true in our experiments because

$$\frac{F_2 U_1}{\beta} \frac{L_{1B}}{L_{2B}} \frac{\|\psi_1\|}{\|\psi_2\|} \approx O(10^{-1})$$

The boundary conditions associated with (4.21a,b) are

$$\psi_1,\ \psi_2 = C_{1,2}(t)$$

$$\frac{\partial \psi_1}{\partial x} = \frac{\partial \psi_2}{\partial x} = 0 \qquad \text{at } X = 0, \tag{4.23}$$

and

$$\psi_1 = \psi_{1,I}$$

$$\psi_2 = \psi_{2,I} \qquad \text{at } X \to \infty,\ x \to 0. \tag{4.24}$$

Notice that (4.23) includes the non-slip condition at the western boundary of the basin, whereas (4.24) represents the typical matching conditions between the boundary layer solutions and the interior solutions.

The difference between (4.21a,b) and Munk's model lies in the term $\frac{\partial^3 \psi_i}{\partial X^3}$ which arises from the Jacobian of the relative vorticity terms. The greater Re_1 (Re_2) is, the more inertial the flow becomes, eventually as Re_1 (Re_2) $\to \infty$ the flow becomes Fofonoff's inertial flow. On the contrary, the smaller Re_1 (Re_2) becomes, the more frictional the flow is; thus, as Re_1 (Re_2) $\to 0$, the flow reduces to Munk's solution because the only non-trivial combination of (4.21) is, for this case, between the right-hand side and the second term of the left-hand side.

Solutions to (4.21a,b) are of the form

$$\psi_{1,B}(x,y) = Ae^{\omega X},$$

$$\psi_{2,B}(x,y) = Be^{\alpha X}, \tag{4.25a,b}$$

Substituting (4.25) into (4.21) yields

$$\omega^3 - Re_1 (\omega^2 + 1) = 0, \quad \omega_0 = 0,$$

$$\alpha^3 - Re_2 (\alpha^2 + 1) = 0, \quad \alpha_0 = 0. \qquad (4.26a,b)$$

The above equations are two cubic equations. The nature of their roots depends on the values of the coefficients (Abramowitz and Stegun, 1964). In our experiments, when the values of $U_1(y)$ and $U_2(y)$ are

$$U_1(y), \; U_2(y) \geq 0$$

or if negative,

$$|U_1(y)|, \; |U_2(y)| < (\tfrac{27}{4})^{1/3} \beta^{1/3} A_H^{2/3}$$

the roots of (4.26) are

$$\omega_1 = p_1 + ib_1, \quad \omega_2 = p_2 + ib_2, \; \omega_3 > 0,$$

$$\alpha_1 = p_2 + ib_2, \quad \alpha_2 = p_2 + ib_2, \; \alpha_3 > 0, \qquad (4.27a,b)$$

where

$$p_i = -\{\tfrac{1}{2} [(a_i + c_i)^{1/3} + (a_i - c_i)^{1/3}] - \frac{Re_i}{3}\},$$

$$b_i = \sqrt{\tfrac{3}{2}} \; [(a_i + c_i)^{1/3} - (a_i - c_i)^{1/3}], \; (i=1,2).$$

For positive velocities $U_1(y)$ and $U_2(y)$

$$a_i = Re_i \left(\frac{1}{2} + \frac{Re_i^2}{27}\right),$$

$$c_i = Re_i \left(\frac{1}{4} + \frac{Re_i^2}{27}\right)^{1/2}, \qquad (i=1,2). \qquad (4.29)$$

If $U_1(y)$ and $U_2(y)$ are negative

$$a_i = Re_i \left(\frac{1}{2} - \frac{Re_i^2}{27}\right),$$

$$c_i = Re_i \left(\frac{1}{4} - \frac{Re_i^2}{27}\right)^{1/2}, \qquad (i=1,2). \qquad (4.30)$$

The solutions $\psi_{1,B}$ and $\psi_{2,B}$ are, then, of the form

$$\psi_{1,B} = A_0 + A_1 e^{\frac{\omega_1}{L_{1B}} x} + A_2 e^{\frac{\omega_2}{L_{1B}} x} + A_3 e^{\omega_3 \frac{x}{L_{1B}}},$$

$$\psi_{2,B} = B_0 + B_1 e^{\frac{\alpha_1}{L_{2B}} x} + B_2 e^{\frac{\alpha_2}{L_{2B}} x} + B_3 e^{\alpha_3 \frac{x}{L_{2B}}}. \qquad (4.31)$$

By imposing the boundary conditions (4.23) and (4.24) and taking into account that the uniform solution valid for the whole domain is given as

$$\psi(x,y) = \psi(\text{interior}) + \psi(\text{boundary}) - \psi(\text{matching})$$

yields

$$\psi_j = \psi_{j,I} - \psi_{j,I}\,(x=0)\,\frac{1}{2}\sqrt{1+\left(\frac{p_j}{b_j}\right)^2}\,e^{-p_j\,\frac{x}{L_{jB}}}\,[e^{i\nu_j} + e^{i\nu_j}],$$

$$(j=1,2), \qquad (4.32)$$

where

$$\nu_j = b_j\,\frac{x}{L_{jB}} + \theta_j,\quad \theta_j = \tan^{-1}\,(p_j/b_j)$$

$\psi_{j,I}\,(x,y)$ are given by (4.17).

When the velocities $U_1(y)$ and $U_2(y)$ are positive the solutions (4.32) are valid for the northwest region of the basin where the flow leaves the boundary and re-enters the interior. The wavy nature of (4.32) in this region increases with the value taken by Re_i and represents a damped standing wave whose role, as we have already mentioned, is to contribute to the dissipation of the positive relative vorticity that the flow owns when it leaves the boundary. A way to verify qualitatively the numerical results is to computing the damping scale LD_i, the wave-length λ_i and the number of the undulations that the standing wave undergoes before being completely damped.

In our experiment, we have the following values:

Upper Layer	Lower Layer
$Re_1 = 1.333$	$Re_2 = 0.167$
$L_{D1} \approx 130$ km	$L_{D2} \approx 63$ km
$\lambda_1 \approx 208.6$ km	$\lambda_2 = 186.3$ km

Notice that the wavelengths of the standing waves in the upper and lower layers are comparable; however, $L_{D1} \approx 2\ L_{D2}$, so the damping of the lower standing wave will be much stronger than that of the upper layer, a fact that the numerical results confirm. If the wavelength is greater than the damping scale, the number of undulations will depend on the ratio $\frac{\lambda}{L_D}$. Thus, we have,

$$\frac{\lambda_1}{L_{D1}} = 1.6,\ e^{-1.6} \approx 20\%$$

so it will be possible to observe a second crest of the standing wave; this means that $Nu_1 = 2$ as we can see in Figures 9-11.

For the lower layer

$$\frac{\lambda_2}{L_{D1}} = 2.96,\ e^{-2.96} \approx 5\%,$$

so a second crest of the wave will be drastically damped (Figs. 9-11).

We should point out that for asympototic values of Re_i, i.e., $Re_i \gg 1$ and $Re_i \ll 1$, the results of eqn. (4.32) accord with those given by Pedlosky (1979), sections 5.7 and 5.8.

We have just shown that a simple analytical approach based on the boundary layer theory and the Sverdrup regime in the interior is able to explain, at least qualitatively, the dynamics of our numerical experiments with the no-slip condition at the solid boundaries. The main point of our analysis lies in the fact that weak vortex stretching terms and local boundary scale analysis permits us to uncouple the dynamics of both layers and, therefore, to study the motion of each layer using the boundary layer theory for a homogeneous ocean. In the case where the vortex stretching terms were large enough to yield a strong coupling between the layers, we still can perform a local boundary scale analysis to isolate the boundary layer dynamics of each layer and then to solve a system of fourth order partial differential equations in one variable that would replace (4.21a,b). In this case, equation (4.11) also predicts the existence of closed geostrophic contours in the northwest region of the second layer and according to YR (1982) the homogenization of potential vorticity within those contours; however, with base on our method to obtain the analytical solutions of the potential vorticity equations, we feel that

the function G(q) in (4.10) is so dependent on the western boundary dynamics that it prevents the homogenization of the potential voriticity. In this respect, we can consider our method as a generalization of that of Ierley and Young's (1983) which was used to study the influence of the boundary layer on the distribution of potential vorticity in the interior. They choose a Stommel boundary layer closure in a linearized problem (their non-linearities are strong vortex stretching terms which they linearized by using an "ansatz" such as $\psi_2 = k\ \psi_B$, k a constant) and neglect the relative vorticity all over the whole domain.

However, the homogenization of potential vorticity has recently been observed by McDowell et al. (1982), Coats (1981), etc., so any reliable numerical model has to be able to reproduce this feature (Holland, 1985). We believe that a possible way to obtain that in our model is: (1) by increasing the vertical resolution, particularly in the upper thermocline, in order to force the existence of closed geostrophic contours which herald the onset of baroclinic instability; (2) by decreasing the value of A_H, say A_H = 50 $m^2\ s^{-1}$ instead of A_H = 200-300 $m^2\ s^{-1}$, and increasing the forcing term up to a more realistic value. The consequences of (2) are a reduction in the dissipation time and an increase in the amount of positive relative vorticity generated at the boundary, so the standing waves might become

unstable and shed eddies to dissipate the relative vorticity coming from the boundary. It is possible that disturbances amplify in this region and eventually equilibrate by inducing a mean flow in the lower layer which removes the reversal in sign of the mean potential vorticity. Analytical details of weakly non-linear instability in the presence of friction can be seen in Pedlosky (1970, 1971 and 1972) and Newell (1972). To accomplish this equilibration, a large fraction of the total transport must migrate down to the lower layer. This process may make the potential vorticity gradient equal to zero; if this is so, then the baroclinic instability, localized in the northwest, produces a source region of uniform potential vorticity.

In order to confirm these somewhat speculative arguments, new numerical experiments are underway. The first group of such experiments deals with the increase of vertical resolution in the upper thermocline, with the rest of parameters (i.e., Δx, Δy, A_H. Curl τ, etc.) being similar to those we have used so far, and it is intended to extend the computations up to at least five years. The main purpose these first experiments is to compare their results with the present ones and to validate our analysis. The second group of experiments will include (1) and (2) together. This experiments are computationally very demanding because, in addition being strongly non-linear, a very narrow boundary

layer develops at the western side that requires $\Delta x \approx 5$ km in a strip adjacent to that side and, therefore, $\Delta t \leq 30$ minutes if an explicit scheme is to be used. The only rational way of overcoming such a severe problem is by using a time implicit scheme, which allows a $\Delta t \approx 6$ to 8 hours, in conjunction with a least squares-conjugate gradient method to reduce the full non-linear problem to a sequence of Poisson problems at every time step. In order to solve as efficiently and economically as possible this sequence, we are present implementing a more powerful version of the conjugate gradient method.

CONCLUSIONS

The numerical model constructed here is the first step of a longer series of numerical studies on ocean circulation using higher accuracy models. We have shown that a finite element formulation with lumping and variable grid spacing of the dissipative quasi-geostrophic equations is able to deliver reliable solutions. To take advantage of the implicitness of the method and its higher accuracy to represent a wave, a time implicit scheme has to be used.

If one considers that the ocean water is a real fluid then the imposition of the no-slip constraint on the solid boundaries removes the incompatibilities between certain physical processes and the quasi-geostrophic equations which arise when free-slip constraints are used (McWillians 1977). However, for a given range of parameters such as A_H, Δx, Δy, F_1 and F_2, which is eddy generating as the latter constraint is imposed, the flow becomes quasi-laminar in both upper and lower layers with the no-slip condition. Thus, it is concluded that the generation of eddies with this constraint requires a much lower A_H and higher F_1 and F_2.

The western boundary layer is active in controlling the dynamics of the second layer, as is seen in the analytical model, and it is expected that even at higher F_1 and F_2

such that the lower geostrophic contours are closed the western boundary layer will prevent the homogenization of the potential vorticity in the second layer unless A_H is small enough to allow the appearance of instabilities in the northwestern meanders.

REFERENCES

Abramowitz, M. and Stegun, I.A. 1964. Handbook of Mathematical Functions. National Bureau of Standards.

Adams, R.A. 1975. Sobolev Spaces. Academic Press, New York.

Barret, K.E. 1978. A variational principle for the stream function-vorticity formulation of the Navier-States equations incorporating no-slips conditions. J. Comp. Physics, 153-161.

Basdevant, C., M. Lesieur, and R. Sadoury. 1978. Subgrid-scale modeling of enstrophy transfer in two-dimensional turbulence. J. Atm. Sci. 35, 1028-1042.

Basdevant, C., and R. Sadourny. 1975. Ergodic properties of inviscid truncated models of two-dimensional incompressible fluids. J. Fluid Mech., 69: 673-688.

Bennett, A.F., and P.E. Kloeden. 1981. The dissipative quasigeostrophic equations. Mathematika. 28, 265-285.

Blanford, R. 1971. Boundary conditions in homogeneous ocean models. Deep-Sea, Res. 18, 739-751.

Briggs, W.L., Newell, A.C. and Sarie, T. 1983. Focusing: A mechanism for instability of non-linear finite difference equations. J. Comp. Physics, 51, 83-106.

Bryan, K. 1963. A numerical investigation of a non-linear model of a wind driven ocean. J. Atmos. Sci. 20, 594-606.

Coats, D.A. 1981. An estime of absolute geostrophic velocity from the density field in the northeastern Pacific Ocean. J. Geophy. Res., 86, 8031-8036.

Charney, J.G. 1971. Geostrophic turbulence. J. Atm. Sci. 28: 1087-1095.

deSzoeke, R.A. 1985. Wind-driven mid-ocean baroclinic gyres over topography: A circulation equation extending the Sverdrup relation. J. Mar. Res. 43, 793-824.

Fix, G.J. 1975. Finite element models for ocean circulation problems. SIAM J. Appl. Math. 29, 371-387.

Fofonoff, N.P. 1954. Steady flow in a frictionless homogeneous ocean. J. Marine Res. 13, 254-262.

Glowinski, R. and Pironneau, O. 1979. Numerical methods for the first biharmonic equation and for the two-dimensional Stokes problem. SIAM Re. 2121, 2, 167-212.

Glowinski, R., Keller, H.B. and Reinhart, L. 1985. Continuation-Conjugate gradient methods for the least squares solution of non-linear boundary value prolems. SIAM J. Sci. Stat. Comput. 6,4, 793-832.

Gresho, P.M. and R.L. Lee. 1981. Don't suppress the wiggles--they are telling you something! Comp. and Fluids. 9, 223-253.

Haidvogel, D.B., et al. 1980. The accuracy, efficiency, and stability of three numerical models with application to open ocean problems. J. Comp. Phys. 34, 1-53.

Holland, W.R. 1985. Simulation of mesoscale ocean variability in mid-latitude gyres. In Adv in Geophy. Vol. 28A, 439-523.

Holland, W.R. 1978. The role of mesoscale eddies in the general circulation of the ocean numerical experiments using a wind driven quasi-geostrophic model. J. Phys. Oceanog. 8, 363-392.

Holland, W.R., and L.B. Lin. 1975a. On the origin of mesoscale eddies and their contribution to the general circulation of the ocean. I. A preliminary numerical experiment. J. Phys. Oceanogr. 5, 642-657.

Holland, W.R., and L.B. Lin. 1975a. On the origin of mesoscale eddies and their contribution to the general circulation of the ocean. II. A parameter study. J. Phys. Oceanogr. 5, 658-669.

Ierley, G.R. and Young, W.R. 1983. Can the western boundary layer affect the potential vorticity distribution in the Sverdrup interior of a wind gyre? J. Phys. Oceanog. 13, 1753-1763.

Jespersen, D.C. 1974. Arakawa's method is a finite element method. J. Comput. Phys. 16, 383-390.

Killworth, P.D. 1985. A note on smoothing techniques for leapfrog time-integration schemes. Ocean Model 60, 5-8.

Krauss, W. 1973. Dynamics of the Homogeneous and the Quasi-homogeneous Ocean. Gerbrüder Borntraeger, Berlin.

Kreiss, H.O. 1978. Numerical Methods for Solving Time-Depending Problems for Partial Differential Equations. Les Presses de L'Universite de Montreal.

Luyten, J.R., J. Pedlosky, and H. Stommel. 1983. The ventilated thermocline. J. Phys. Oceanogr. 13, 292-309.

Marshall, J.C. 1982. On the treatment of the lateral boundaries in quasi-geostrophic ocean models. Unpublished Manuscript.

Marshall, J.C. 1984. Eddy-mean flow interaction in a barotropic ocean model. Quart. J.R. Met. Soc. 110, 573-590.

McDowell, S., Rhines, P. and Keffer, T. 1982. North-Atlantic potential vorticity and its relation to the general circulation. J. Phys. Oceaog. 12, 1417-1436.

McWilliams, J.C. 1977. A note on a consistent quasi-geostrophic model in a multiple connected domain. Dyn. Atmos. Ocean, 1, 427-441.

Mijailov, P.V. 1978. Partial Differential Equations (English Translation), Mir. Moscow.

Moore, D.W. 1963. Rossby waves in ocean circulation. Deep-Sea Res. 10, 735-747.

Munk, W.H. 1950. On the wind driven circulation. J. Meteor. 7, 79-93.

Newell, A.C. 1972. The post bifurcation stage of a baroclinic instability. J. Atm. Sci. 29, 69-76.

Pedlosky, J. 1979. Geophysical Fluid Dynamics. springer-Verlag, N.Y.

Pedlosky, J. 1972. Limit cycles and unstable baroclinic waves. J. Atm. Sci. 29, 53-63.

Pedlosky, 1971. Finite-amplitude baroclinic waves with small dissipation. J. Atm. Sci. 28, 587-597.

Pedlosky, J. 1970. Finite-amplitude baroclinic waves. J. Atm. Sci. 27, 15-30.

Phillips, N.A. 1959. An example of non-linear computational instability. The Atmosphere and the Sea in Motion, Rossby Memorial Volume. Rockefeller Institute Press, 501-504.

Rhines, P.B. and W.R. Young, 1982. Mid-Ocean Gyres. J. Mar. Res. 40 (supp.), 559-596.

Richtmyer, R.D. and K.W. Morton. 1967. Different methods for initial value problems. Interscience Publishers.

Roache, P.J. 1972. Computational Fluid Dynamics. Hermosa Press, Alburquerque, N.M.

Robinson, A.R., D.E. Harrison., Y. Mintz, and A.J. Semtner. 1977. Eddies and the general circulation of an idealized oceanic gyre: A wind and thermally driven primitive equation numerical experiment. J. Phys. Oceanogr. 7, 182-207.

Sadourny, R. and C. Basdevant. 1981. Une classe d'operateurs adaptés a la modelisation de la diffusion turbulente en dimension deux. C.R. Acad. Sci. Paris. 292 II, 1061-1064.

Sadourny, R. 1975. The dynamics of finite difference models of the shallow water equations. J. Atmos. Sci. 32, 680-689.

Semtner, A.J., and Y. Mintz. 1977. Numerical simulation of the Gulf Stream and mid-ocean eddies. J. Phys. Oceanogr. 7, 208-230.

Semtner, A.J. and W.R. Holland. 1978. Inter-comparison of quasi-geostrophic simulations of the western North Atlantic circulation with primitive equation results. J. Phys. Oceanogr. 8, 735-754.

Staniforth, A.N. and H.L. Mitchell. 1977. A semi-implicit finite element barotropic model. Month Weath. Rev. 105, 154-169.

Stewart, R.W. 1964. Influence of friction on inertial models in oceanic circulation. In: Studies on Oceanography: Papers dedicated to Professor Hidaka in commemoration of his 60th birthday, K. Yoshida, editor. Tokyo University, Geophysical Institute.

Stommel, H. 1948. The westward intensification of wind-driven ocean currents. Trans. Amer. Geophys. Union. 99, 202-206.

Thomee, V. 1985. Galerkin Finite Element Methods for Parabolic Problems. Lecture Notes in Math. No. 1054. Spring Verlag, Belin.

Young, W.R. and P.B. Rhines. 1982. A theory of the wind-driven circulation T I gyres with western boundary layers. J. Mar. Res. 40, 849-872.

APPENDIX A

Equation of The Relative Vorticity in a Stratified Mid-Ocean Gyre

Consider a restricted oceanic domain D. The dynamical variables usually required to describe the motion in such a system are the density ρ, the pressure p, the vector velocity $\vec{u} = (u,v,w)$, and certain further thermodynamic variables as the temperature T, the internal energy per unit of mass e and the specific entropy s. In certain situations, depending on the physical nature of the fluid, additional variables such as salinity may be required, or in cases when the thermodynamic relations can be simplified, some state variables can be dispensed.

In an Eulerian description of the motion, the dynamical variables are functions of the vector position $\vec{x} = (x,y,z)$ and of time t. The equations of motion of a Boussinesq fluid in a rotating coordinate system are:

Conservation of mass

$$\frac{D\rho}{Dt} + \nabla \cdot \rho \vec{u} = 0 \text{ or } \frac{D\rho}{Dt} + \rho \nabla \cdot \vec{u} = 0 \qquad (A.1)$$

Momentum equation

$$\frac{D\vec{u}}{Dt} + 2\vec{\Omega}\Lambda\vec{u} = -\frac{1}{\rho}\nabla p + \nabla\Phi + \frac{\vec{\mathcal{F}}}{\rho} \qquad (A.2)$$

Heat equation

$$\frac{DT}{Dt} = \kappa \nabla^2 T + \frac{Q}{C_p} \qquad (A.3)$$

where $\frac{D}{Dt} = \frac{\partial}{\partial t} + \vec{u} \cdot \nabla$ is the material derivative

$\vec{\Omega}$ is the speed of rotation of the earth $= 7.2910^{-5}\ s^{-1}$

κ is the coefficient of thermal diffusivity

C_p is the specific heat at constant pressure

Q is the rate of heat addition per unit of mass by heat sources.

To complete the system, further thermodynamic state relations expressing the physics nature of the flid are required. For salt water

$$\rho = \rho(p,T,S) \qquad (A.4)$$

If the effects of compressibility are minor, then (A.4) can be written as

$$\rho = \rho_0[1 - \alpha(T - T_0)] \qquad (A.5)$$

Hence, equation (2.3) can be written entirely in terms of the density as

$$\frac{D\rho}{Dt} = \kappa \nabla^2 \rho - \frac{\alpha \rho_0}{C_p} Q. \qquad (A.6)$$

It is worth noting that equations (A.1) and (A.6), although both given in terms of density, are related to different physical principles; the former expresses mass conservation and the latter, for a liquid, expresses energy conservation.

If we assume that the ocean water is an incompressible liquid, or very nearly so, density differences are so slight that their effects on the mass balance can be neglected, so that

$$\nabla \cdot \vec{u} = 0 \tag{A.7}$$

Equation (A.7) does not mean $\frac{D\rho}{Dt} = 0$. Indeed, $\frac{D\rho}{Dt}$ is given by (A.6) in terms of internal heating and heat diffusion. $\frac{D\rho}{Dt}$ is identically zero if the fluid is incompressible and the motion is adiabatic.

The terms, $\nabla\Phi$ and $\vec{\mathcal{F}}$, in equation (2.2) represent the body force and the non-conservative forces respectively. Φ is the potential of the conservative forces and is, in this study, the frictional force acting on the fluid which is given in terms of the vector velocity as

$$\vec{\mathcal{F}} = A_H \nabla_H^2 \vec{u} + A_V \frac{\partial^2 \vec{u}}{\partial z^2} \tag{A.8}$$

A_H and A_V are the horizontal and vertical eddy viscosity coefficients, respectively, which are taken as constant.

The large-scale gyre ocean motions are primarily characterized by the following non-dimensional parameters:

$$\text{Rossby Number } \varepsilon = \frac{U}{2\Omega L} \ll 1 \qquad \text{(A.9a)}$$

$$\text{Burger's Number } S = g\frac{\Delta\rho}{\rho}\frac{D}{4\Omega^2 L^2} = \left(\frac{L_D}{L}\right)^2 \ll 1 \qquad \text{(A.9b)}$$

$$\text{Vertical Ratio Number } \delta = \frac{D}{L} \ll 1 \qquad \text{(A.9c)}$$

where U,L,D denote typical scales of velocity, horizontal length and depth of the motion, respectively. The small value of the Rossby Number ε implies that the Coriolis force will be dominant over most part of the ocean gyres except in narrow areas where the inertial and the frictional terms of the momentum equations can become important. On the other hand, the strong stratification of the ocean leads to large-scale oceanic motions which are nearly horizontal. The hydrostatic balance of the motion is guaranteed by $\delta \ll 1$. So as a first approximation the dynamics of the large-scale oceanic motions can be described by the geostrophic and hydrostatic equations (Pedlosky, 1979). Naturally, as is evident from the parametrization involved, the geostrophic

approximation breaks down in the vicinity of the equator and in high latitudes; in the latter area, there is no way with the geostrophic relations only to calculate the pressure field. As a diagnostic tool, the geostrophic equations inform us that if the velocity field slowly varies in time, then the Coriolis force will be balanced by the evolving pressure gradient; however, no information about the pressure field is conveyed by such an approximation. In fact, any pressure field with a small Rossby number is acceptable because the continuity equation (A.7) is always satisfied up to $0(\varepsilon)$. This indeterminancy of the geostrophic approximation can be removed by taking into account the effects of small departures from geostrophy, in other words, by introducing higher order dynamics. In doing so, we should notice that by applying the curl operator to the geostrophic equations the contribution of the Coriolis and pressure gradient forces to the vorticity balance vanish, so that it is in terms of the higher dynamics that the vorticity balance can be achieved. The forces which determine such a dynamics are usually the small non-geostrophic forces as:

a. the inertial forces which yield to non-geostrophic velocities of order $0(\varepsilon)$;

b. the vortex tube stretching by the Ekman suction/pumping velocities at the bottom/surface,

acting on the planetary vorticity filaments, will produce a variation of the relative vorticity proportional to $O(E_v^{1/2})$. ($E_v = 2A_v/2\Omega D^2$). These non-geostrophic effects arise from the vertical friction and give place both to an Ekman bottom layer which acts as a sink of vorticity and a surface Ekman layer at the basis of which the external mechanical forces input relative vorticity;

c. horizontal diffusion of momentum which is proportional to $O(E_H)$. ($E_H = \frac{2A_H}{2\Omega L^2}$, $\frac{E_H}{\varepsilon} = 2R_e^{-1}$);

d. sources, sinks and diffusion of heat.

The absolute vorticity in our rotating ocean system is $\vec{\zeta} + 2\vec{\Omega}$, $\vec{\zeta} = \nabla \Lambda \vec{u}$ is the relative vorticity and $2\vec{\Omega}$ is the planetary vorticity which dominates $\vec{\zeta}$ because $\varepsilon << 1$. The dominancy of the planetary vorticity introduces some distinctive peculiarities into the vorticity dynamics of a rotating system. Thus, for instance, the classic effect of vortex line stretching of three dimensional non-rotating fluids is absent here. It is not useful now to take $\vec{\zeta}$ as a tracer of the motion because the production $|\vec{\zeta}|^2$ and the accelerated dissipation of kinetic energy cannot occur at planetary scales at which R_e is large. Instead, the potential vorticity q will be a good tracelike scalar on surfaces of constant potential density. Deformation of

contours of q leads to dissipation of q^2 itself. The equation of the potential vorticity q as a conserved property is given by Ertel's theorem.

Following Pedlosky (1979) we take the curl of (A.2) and obtain

$$\frac{D\vec{\zeta}_a}{Dt} = \vec{\zeta}_a \cdot \nabla\vec{u} - \vec{\zeta}_a \nabla \cdot \vec{u} + \frac{\nabla\rho \wedge \nabla p}{\rho^2} + \nabla\Lambda \frac{\vec{\mathcal{F}}}{\rho} . \qquad (A.10)$$

From (2.1)

$$\nabla \cdot \vec{u} = \frac{1}{\rho} \frac{D\rho}{Dt} .$$

Hence, $\nabla \cdot \vec{u}$ can be eliminated from (2.10) and then

$$\frac{D}{Dt} \left(\frac{\vec{\zeta}_a}{\rho}\right) = \left(\frac{\vec{\zeta}_a}{\rho} \cdot \nabla\right) \vec{u} + \frac{1}{\rho^3} (\nabla\rho \wedge \nabla p) + \frac{1}{\rho} (\nabla\Lambda \frac{\vec{\mathcal{F}}}{\rho}), \qquad (A.11)$$

where $\vec{\zeta}_a = \vec{\zeta} + 2\vec{\Omega}$

In the absence of frictional effects and for adiabatic motions the conserved magnitude λ which leads to the conservation of potential vorticity in the ocean is the density ρ. In a more general context, where dissipative effects are to be taken into account to remove the indeterminancy of the motion, it is still convenient to keep ρ as a valid choice of a scalar property of the fluid that together with $\vec{\zeta}_a$ can yield to a useful version of Ertel's

theorem applied to the ocean circulation.

Let us write equation (A.6) as

$$\frac{D\rho}{Dt} = G = \kappa \nabla^2 \rho - \frac{\alpha \rho_0}{C_p} Q, \tag{A.12}$$

and consider the following identities:

$$\frac{\vec{\zeta}_a}{\rho} \cdot \frac{D\nabla\rho}{Dt} = \left(\frac{\vec{\zeta}_a}{\rho} \cdot \nabla\right) \frac{D\rho}{Dt} - \nabla\rho \cdot \left(\frac{\vec{\zeta}_a}{\rho} \cdot \nabla \vec{u}\right),$$

$$\nabla\rho \cdot \frac{D}{Dt}\left(\frac{\vec{\zeta}_a}{\rho}\right) = \nabla\rho \cdot \left[\left(\frac{\vec{\zeta}_a}{\rho} \cdot \nabla\right) \vec{u}\right] + \nabla\rho \cdot \left[\frac{\nabla\rho \wedge \nabla p}{\rho^3}\right] \tag{A.13a,b}$$

The sum of (A.13a) and (A.13b) then yields with (A.12)

$$\frac{D}{Dt}\left\{\frac{\vec{\zeta} + 2\vec{\Omega}}{\rho} \cdot \nabla\rho\right\} = \nabla G \cdot \frac{\vec{\zeta} + 2\vec{\Omega}}{\rho} + \frac{\nabla\rho}{\rho} \cdot \left[\frac{\nabla \wedge \vec{F}}{\rho}\right]. \tag{A.14}$$

Equation (A.14) is the most general equation of the potential vorticity $q = \frac{\vec{\zeta} + 2\vec{\Omega}}{\rho} \cdot \nabla\rho$; but it is not in this form as this equation is used in oceanography. Further manipulations in (A.14) using the relations of the geostrophy dynamics and Boussinesq approximation yield a more suitable form of the equation of potential vorticity. Thus, the horizontal components of relative vorticity which are produced mainly by the buoyancy twisting term, $\nabla p \wedge \nabla\rho$, are computed from the thermal wind relation (Pedlosky, 1979); whereas, the vertical

components of the absolute vorticity and of the gradient of density are the components which actually are used in (2.14). Therefore, this equation can be written as

$$\frac{D'}{D't}\left[(f+\zeta)\frac{\rho_z}{\rho}\right] = \frac{\partial G}{\partial z}\left(\frac{f+\zeta}{\rho}\right) + \frac{\rho_z}{\rho} A_H \nabla^2 \zeta + \frac{\rho_z}{\rho}\frac{\partial}{\partial z}\left((\nabla\Lambda)_z \vec{\tau}\right), \qquad (A.15)$$

where

$$\frac{D'}{D't} = \frac{\partial}{\partial t} + \vec{u}_H \cdot \nabla_H,\ \vec{u}_H = (u,v),\ \nabla_H = \left(\frac{\partial}{\partial x}, \frac{\partial}{\partial y}\right),$$

$\vec{\tau}$ are the stresses which act on the water column,

ζ is the vertical component of the relative vorticity,

$f = 2\left|\vec{\Omega}\right|\sin\theta$.

It is convenient to write equation (A.12) in terms of the operator $\frac{D'\rho}{D't}$ as

$$\frac{D'\rho}{D't} = -w\frac{\partial\rho}{\partial z} + G. \qquad (A.16)$$

The equations (A.15) and (A.16) form the basis for the study of oceanic motions which extend from the synoptic scales to the planetary scales. However, in order to facilitate the theoretical and numerical analysis of any dynamical state, it is necessary to isolate the relevant mechanism of such a state at a given scale. A detailed description of such

mechanisms as well as of their interactions with other scales of the global dynamical state requires the introduction of complementary and physically and mathematically consistent approximations to the equations (A.15) and (A.16). Since our main interest is the description of motions which take place at mid-latitudes and such that their metric can be accurately described by the tangent plane approximation, we now introduce the standard scaling variables for a mid-latitude β-plane.

The scaling parameters are (Pedlosky, 1979):

$$\rho = \rho_s(z)\ (1 + \varepsilon F \rho'),$$

$$\varepsilon = \frac{U}{f_0 L},$$

$$S = \frac{g}{\rho_s} \frac{\partial \rho_s}{\partial z} \frac{D^2}{f_0^2 L^2} = \left(\frac{L_D}{L}\right)^2, \qquad \text{(A.17)}$$

$$N^2 = \frac{S f_0 L^2}{D^2} \text{ Brunt-Värsala frequency},$$

$$f = f_0\ \left(1 + \frac{\beta_0}{f_0}\, y\right), \quad \frac{\beta_0}{f_0} \ll 1,$$

$$\beta = \frac{\beta_0 L}{\varepsilon f_0} = \frac{\beta_0 L^2}{U},$$

where $F = \frac{f_0^2 L^2}{gD}$, $f_0 = 2|\vec{\Omega}|\sin\theta_0$, θ_0 is a reference latitude. Notice that the buoyancy frequency is taken to vary only with depth. Although this is an unrealistic assumption for the real ocean we take it as valid because in our computations we exclude any dynamical change caused by horizontal variations of the density.

It is easy to obtain from (A.15) and (A.16) the equation for the relative vorticity:

$$\frac{D'\zeta}{D't} + \vec{u} \cdot \nabla_H f = f w_z + A_H \nabla_H^2 \zeta + \frac{\partial}{\partial z} (\nabla \Lambda \vec{\tau}). \qquad (A.18)$$

APPENDIX B

Consider that the magnitude ζ obeys the equation

$$\frac{\partial \zeta}{\partial t} + \vec{u} \cdot \nabla \zeta = 0, \quad \nabla \cdot \vec{u} = 0.$$

We classify a numerical scheme as:

(i) Semi-Conservative

If neglecting errors in time differencing

$$\frac{\partial}{\partial t} \int_D \zeta \, dx = 0.$$

The integral has been represented by a summation formula of the same order as the discretization method.

(ii) Conservative

If the values of ζ given by the numerical solution obey

$$\int_D \zeta \, dx = \text{const.}$$

(iii) Quadratically Semi-conservative

If neglecting errors in the time differencing

$$\frac{\partial}{\partial t} \int_D \zeta^2 \, dx = 0.$$

(iv) Quadratically Conservative

If the values of ζ^2 given by the numerical solution satisfy

$$\int_\Omega \zeta^2 \, dx = \text{Const.}$$

APPENDIX C

We prove here that the approximation (3.31) is dissipative of second order for either a consistent mass matrix formulation or a lumping mass matrix formulation.

We use Kreiss' definition of disspativeness (see Kreiss (1978). Thus, the approximation (3.31) is dissipative of order 2r if there exists an α_s such that

$$\left|\kappa(S_h)\right| \leq e^{\alpha_s \Delta t}\ (1 - \delta\left|\xi\right|^{2r}),\ \left|\xi\right| \leq M,$$

where

$\left|\kappa\right|$ is the modulus of the largest eigen-value of the discrete operator S_h of the approximation. In our case $\left|\kappa\right|$ is the modulus of the amplification factor. $\delta > 0$ is some constant independent of h and Δt. $\varepsilon = (\frac{k\Delta x}{2}, \frac{\ell\Delta y}{2})$.

Let us consider, for example, the equation (3.36); that is

$$\left|\lambda_1\right|^2 = 1 - \frac{48A_H\Delta t}{\Delta x\Delta y}\ (\frac{4 - (x + y - 2xy}{(2 + x)\ (2 + y)}), \qquad (C.1)$$

where

$$x = \cos k\Delta x,\ y = \cos \ell\Delta y.$$

For $k\Delta x$ and $\ell\Delta y$ small,

$$4 - (x + y) - 2xy = (1 - x) + (1 - y) + 2(1 - xy)$$

becomes

$$(1 - \cos 2\varepsilon_1) + (1 - \cos 2\varepsilon_2) + 2(1 - \cos 2\varepsilon_1 \cos 2\varepsilon_2) =$$

$$2\sin^2\varepsilon_1 + 2\sin^2\varepsilon_2 + 2(1 - \cos 2\varepsilon, \cos 2\varepsilon_2), \qquad (C.2)$$

where

$$\varepsilon_1 = \frac{k\Delta x}{2}, \quad \varepsilon_2 = \frac{\ell\Delta y}{2}$$

By expanding in Taylor series the right hand side of (C.2) and retaining up to 2nd order terms yields

$$4 - (x + y) - 2xy \simeq 6(\varepsilon_1^2 + \varepsilon_2^2) = 6|\varepsilon|^2 \qquad (C.3)$$

Likewise, the numerator $(2 + x)(2 + y)$ is equivalent to 4 for $k\Delta x$ and $\ell\Delta y$ very small. Therefore, we can write (C.1) as

$$|\lambda_1|^2 \simeq 1 - 72 \frac{A_H \Delta t}{\Delta x \Delta y} |\varepsilon|^2 \qquad (C.4)$$

since $\frac{A_H \Delta t}{\Delta x \Delta y} \leq \frac{1}{192}$ according to (3.38b),

then

$$|\lambda_1|^2 \lesssim 1 - \delta|\varepsilon|^2, \qquad (C.5)$$

where $\delta = 72/192$.

Similarly, we can show that for the lumped mass matrix formulation

$$|\lambda_1|^2 \leq 1 - \delta|\varepsilon|^2, \quad \delta = \frac{288}{18}$$